ACTA PHYSIOLOGICA

Acta Physiol 2015, **213**, 107–144

REVIEW

Quantification of skeletal muscle mitochondrial function by ^{31}P magnetic resonance spectroscopy techniques: a quantitative review

G. J. Kemp,[1] R. E. Ahmad,[1] K. Nicolay[2] and J. J. Prompers[2]

1 Department of Musculoskeletal Biology, and Magnetic Resonance and Image Analysis Research Centre, University of Liverpool, Liverpool, UK

2 Biomedical NMR, Department of Biomedical Engineering, Eindhoven University of Technology, Eindhoven, the Netherlands

Received 3 November 2013, revision requested 30 December 2013, revision received 1 April 2014, accepted 23 April 2014

Correspondence: G. Kemp, Department of Musculoskeletal Biology, University of Liverpool, Duncan Building, Daulby Street, Liverpool L69 3GA, UK.
E-mail: gkemp@liv.ac.uk

Present address: R. E. Ahmad[1], Department of Physiology, Faculty of Medicine, University of Malaya, Kuala Lumpur, Malaysia

Abstract

Magnetic resonance spectroscopy (MRS) can give information about cellular metabolism *in vivo* which is difficult to obtain in other ways. In skeletal muscle, non-invasive ^{31}P MRS measurements of the post-exercise recovery kinetics of pH, [PCr], [Pi] and [ADP] contain valuable information about muscle mitochondrial function and cellular pH homeostasis *in vivo*, but quantitative interpretation depends on understanding the underlying physiology. Here, by giving examples of the analysis of ^{31}P MRS recovery data, by some simple computational simulation, and by extensively comparing data from published studies using both ^{31}P MRS and invasive direct measurements of muscle O_2 consumption in a common analytical framework, we consider what can be learnt quantitatively about mitochondrial metabolism in skeletal muscle using MRS-based methodology. We explore some technical and conceptual limitations of current methods, and point out some aspects of the physiology which are still incompletely understood.

Keywords metabolism, mitochondria, non-invasive methods, oxygen consumption, ^{31}P magnetic resonance spectroscopy, skeletal muscle.

Magnetic resonance spectroscopy methods for measuring metabolic flux

Magnetic resonance spectroscopy (MRS) methods can give quantitative information about cellular metabolism *in vivo* which is difficult to obtain in any other way, but interpretation must take account of the technical characteristics of the methods and their relationship to the underlying biochemistry and physiology.

Approaches to measuring mitochondrial 'function'

MRS methods *in vivo* depend on measuring signals from cellular metabolites, and there are basically three ways in which they can be used to measure cellular metabolic fluxes: using exogenous tracers, by magnetic labelling and net-flux methods based on concentration change kinetics.

^{13}C MRS with exogenous tracers. An application of this methodology to study muscle mitochondrial metabolism is the use of [2-^{13}C]acetate infusion to measure tricarboxylic acid (TCA) cycle rate (V_{TCA}) in resting muscle (Befroy *et al.* 2009): some published results have been reviewed elsewhere (Kemp 2008a, Kemp & Brindle 2012).

^{31}P MRS magnetization transfer. Measurements of exchange flux between inorganic phosphate (Pi) and ATP have been used to probe muscle mitochondrial metabolism in resting muscle (Befroy *et al.* 2009), although this presents some serious technical and

© 2014 Scandinavian Physiological Society. Published by John Wiley & Sons Ltd, doi: 10.1111/apha.12307

interpretative difficulties, discussed elsewhere (Kemp & Brindle 2012).

^{31}P MRS concentration kinetics. The metabolic capability of skeletal muscle for large changes of ATP turnover in support of changing mechanical work output presents a key opportunity for estimation of net fluxes (Kemp & Radda 1994). Of particular relevance here, ^{31}P MRS measurements of the post-exercise recovery kinetics of cytosolic pH and the cytosolic concentrations of phosphocreatine (PCr), orthophosphate (Pi) and ADP contain much information about two main areas of metabolism. One is cellular pH homeostasis, which involves the processes of what might be termed H^+ production, consumption, buffering and efflux (Kemp *et al.* 1994b, 2001b, 2009). The other is muscle mitochondrial function, in the sense of oxidative ATP synthesis, its regulation in relation to ATP demand, and its pathophysiology. This is the subject of this review.

Mitochondrial capacity

What we will call muscle 'mitochondrial capacity', also known as muscle 'oxidative' or 'aerobic' capacity (Kemp *et al.* 1993b), is a concept distinct from metabolic flux (Befroy *et al.* 2009), but can be thought of as a maximum rate of mitochondrial ATP synthesis under some actual or notional maximal activation. There are basically three ways to assess mitochondrial capacity:

^{31}P MRS measures of mitochondrial capacity. Several different approaches will be discussed in this review, but it is often convenient to lump these together as '^{31}P MRS-based Measures of Mitochondrial Function' (MMMF). Given the physical constraints of MR scanning, MMMF are usually based on inferences from measured responses to submaximal exercise, and the key issue is therefore the validity of the inference. In what follows we will review some key technical and physiological aspects of these approaches, illustrated in Figures 2–7, before analysing in Figures 8 and 9 the published ^{31}P MRS studies of normal adult human muscle which are reliably interpretable in these terms.

Oxygen consumption (V_{O2}) during maximal exercise. Non-invasive measurements of whole-body V_{O2} using expired-gas spirometry test the integrated response of the whole cardiorespiratory/vascular/muscular system; this allows not only measurement of whole-body V_{O2} at peak exercise but also studies of whole-body V_{O2} kinetics, to which the contribution of the exercising muscle can be reconstructed by analysis and modelling (Rossiter 2011). Measurement of absolute V_{O2} in specific muscles or muscle groups requires invasive arteriovenous difference (AVD) methods; these can be used in exercise, including maximal single- or two-limb exercise. Published AVD V_{O2} data, including studies with suitably interpretable measurements of muscle biochemistry, will be analysed in Figures 10–12.

Oxidative ATP synthesis ex vivo. Relationships between MMMF and *ex vivo* measurements of, for example, muscle mitochondrial numbers and content of oxidative enzymes and respiratory chain components will be reviewed below [in the section entitled 'Validation of MRS-based measures of mitochondrial function (MMMF)']. Published data from experiments in which maximal rates of mitochondrial ATP production or O_2 consumption under optimum near-physiological conditions *ex vivo* are extrapolated to maximum rates *in vivo* will be presented for comparative purposes later (in Fig. 10d).

Thus, in this review we will compare for the first time in a common quantitative framework published AVD V_{O2} measurements with comparable ^{31}P MRS data,[1] and data derived *ex vivo*. These comparisons will reveal some technical and conceptual limitations of all these methods, and some areas of physiology which are still incompletely understood.

^{31}P MRS approaches to muscle energy metabolism

An outline of muscle energy metabolism and its regulation

The utility and limitations of ^{31}P MRS are illustrated in the simplified view of muscle energy metabolism in Figure 1. The main processes involved can be summarized as follows:

ATP supply and demand. ATP is produced either by glycolysis to lactate, or by oxidation of acetyl coenzyme A in the TCA cycle and subsequent oxidation of NADH via the mitochondrial electron transport chain; the acetyl coenzyme A supplied to the TCA cycle can be derived either from muscle glycolysis or β-oxidation of fatty acids. ATP is used by various ion pumps including the sarcolemmal Na^+/K^+-ATPase and the sarcoplasmic Ca^{2+}-ATPase, and by the myosin ATPase whose force-generating role dominates ATP use during exercise. Creatine kinase (CK) is sufficiently near equilibrium that its kinetics can usually by ignored (Kemp *et al.* 1998), and operates such that any temporary mismatch between ATP demand and supply is met by change in [PCr], with very little change in [ATP]; this

[1]The authors' experimental work described here was performed in conformity with Persson (2013).

 © 2014 Scandinavian Physiological Society. Published by John Wiley & Sons Ltd, doi: 10.1111/apha.12307

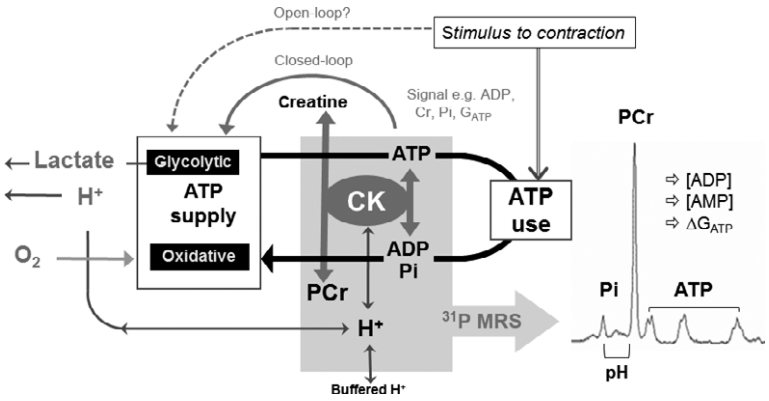

Figure 1 Muscle metabolism as seen by ^{31}P magnetic resonance spectroscopy (^{31}P MRS). Muscle 'energy metabolism' is simplified to ATP supply and demand, buffered by the creatine kinase (CK) reaction which equilibrates phosphocreatine (PCr), creatine (Cr), ATP and ADP. ADP and Pi are the products of ATP hydrolysis and the substrates for ATP synthesis. ATP turnover is largely demand-driven, regulated by closed-loop feedback mediated by metabolites related to CK, and perhaps also by direct open-loop signals (parallel activation). The shaded block represents what is 'visible' to ^{31}P MRS: the resting muscle ^{31}P MRS spectrum shows the peaks of Pi and PCr and the three peaks of ATP; indirect calculations yield cytosolic pH, the free concentrations of ADP and ADP, and the free energy of ATP hydrolysis (ΔG_{ATP}). See main text for a detailed explanation.

is the 'temporal buffering' role of CK (Meyer *et al.* 1984, Kemp 1994, Kemp *et al.* 1998). Consequent changes in [PCr] are exactly matched by opposite changes in the concentration of creatine (Cr), such that total creatine ([TCr] = [Cr] + [PCr]) remains constant, and approximately matched by changes in [Pi], such that [PCr] + [Pi] remains approximately constant. Free [ADP] is held much lower than [ATP], and tends to increase when [PCr] falls or pH rises according to the CK equilibrium expression, which can most straightforwardly be written as

$$\begin{aligned}\text{CK equilibrium}: [\text{ADP}] &= ([\text{Cr}]/[\text{PCr}])[\text{ATP}]K_{\text{eq}}/[\text{H}^+] \\ &= \{([\text{TCr}]/[\text{PCr}]) - 1\} \\ &\quad [\text{ATP}]K_{\text{eq}}/[\text{H}^+]\end{aligned} \quad (1)$$

A related quantity is the free energy of ATP hydrolysis, which can be most simply defined as

$$\begin{aligned}&\text{Free energy of ATP hydrolysis}: \Delta G_{\text{ATP}} \\ &= \Delta G^0_{\text{ATP}} + \text{RT In}([\text{ADP}][\text{Pi}]/[\text{ATP}])\end{aligned} \quad (2)$$

where the standard free energy $\Delta G^0_{\text{ATP}} = -32$ kJ mol^{-1} and RT = 8.31 J mol^{-1} K^{-1} × 310 K ≈ 2.57 kJ mol^{-1}. More complicated versions of Eqns 1 and 2 take more precise account of binding of relevant species by Mg^{2+} and K^+ (Lawson & Veech 1979, Harkema & Meyer 1997, Kushmerick 1997, Iotti *et al.* 2005, Vinnakota *et al.* 2009).

O_2 supply and demand. For present purposes, we need not say much about cardiac and pulmonary function, vascular and microvascular physiology, and intramuscular O_2 diffusion. However, it is an important principle that O_2 usage by muscle requires an appropriate [O_2] gradient profile from lungs to the mitochondrion (Kemp *et al.* 2002a, Kemp 2004): in particular myocyte $[O_2]_{\text{cytosolic}}$ must be low enough to support O_2 diffusion from the capillary, but high enough to drive mitochondrial cytochrome oxidase (Richardson *et al.* 1999). We return to some relationships between ^{31}P MRS recovery measurements and non-invasive measures of muscle tissue oxygenation below (in the sections entitled 'Approaches to measurement of O_2 transport and consumption *in vivo*. *Combining NIRS and ^{31}P MRS*' and 'Published data on patients with abnormalities in MMMF. *Diseases impairing O_2 delivery*').

Cellular pH homeostasis. Lactate production by glycolytic ATP synthesis can be thought of as accompanied by 1 : 1 generation of H^+ which tends to lower cell pH, while the pH-dependent stoichiometry of H^+ in the CK reaction tends to raise cell pH when [PCr] falls and *vice versa* (Kemp *et al.* 1993a, 2001b, 2006, Kemp 2005b). When pH falls, various processes that amount to net H^+ efflux (Kemp *et al.* 1994b, 1997) tend to restore it. The resulting net changes in cell pH depend on the net H^+ load to the cytosol (H^+ production less H^+ consumption and H^+ efflux), and are inversely proportional to the cytosolic buffer capacity (Kemp 2005b, Vinnakota *et al.* 2009). During recovery from exercise, ATP synthesis is overwhelmingly oxidative, and net H^+ efflux restores pH to resting values (Kemp *et al.* 1994b, 1997).

Metabolic regulation of ATP turnover. For much of the dynamic range of ATP turnover, until fatigue

© 2014 Scandinavian Physiological Society. Published by John Wiley & Sons Ltd, doi: 10.1111/apha.12307

supervenes, control is dominated by ATP demand (Jeneson *et al.* 2000). Important in the present context is how ATP supply is matched to demand. Attention has long been focused on the role of closed-loop negative-feedback regulation, particularly with reference to CK-related metabolites (ADP, Cr, Pi), in the control of mitochondrial ATP synthesis. Some details will be discussed later in relation to estimation of maximal rates, but the general idea (Kemp 1994) is that the rate of oxidative ATP synthesis (Q) is some function of a signal (X), which itself is some function of the mismatch between ATP supply and ATP demand:

$$\text{General feedback regulation of oxidative ATP synthesis}: Q = f(X) \quad (3)$$

This works such that any tendency of ATP supply to fall short of demand will result in a change in X sufficient to restore the balance. As we will see, there are several candidate negative-feedback signals which are related to the CK-equilibrium. In engineering terms, this is integral feedback control, because the CK system is a time-integrating comparator of ATP supply and demand, where any mismatch leads to a signal which increases with time; there can be no true steady-state error (Kemp 1994, Cloutier & Wellstead 2010). The possibility of a direct ('open loop', 'feed-forward' or 'parallel') activation of ATP synthesis by the signal to contraction (Korzeniewski 1998), independent of closed-loop feedback, is discussed later (in the sections entitled 'Regulation of oxidative ATP synthesis: open vs. closed-loop mechanisms' and 'Parallel activation revisited').

Resting muscle. In what follows, we are mainly concerned with perturbations from the resting steady state. We discuss what 'resting' means below (in the section entitled 'What is the relevant 'basal' rate of ATP synthesis?'). For present purposes, we simply note that muscle's dynamic responses are conditioned by biochemical characteristics of the resting state. We must therefore consider how concentrations are regulated in resting muscle, where ATP is supplied almost exclusively by oxidative phosphorylation, oxidizing mainly fatty acids in the fasting state, and glucose postprandially (Kemp & Brindle 2012). Any metabolite that functions as a mitochondrial feedback signal must be at a value appropriate to resting ATP demand: in resting muscle (denoted by the subscript R), Eqn 3 becomes

$$\text{Feedback regulation of resting ATP synthesis}: Q_R = f(X_R) \quad (4)$$

This logic probably applies both to [ADP], which defines [Cr]/[PCr] (Eqn 1), and to [Pi] (Kemp 1994), both of which contribute to ΔG_{ATP} (Eqn 2). Resting cell [Pi] is additionally dependent by pump-and-leak principles on sarcolemmal Na^+-dependent Pi uptake (Kemp & Bevington 1993, Polgreen *et al.* 1994), and total cell creatine ([TCr]) similarly on sarcolemmal Na^+-dependent Cr uptake (Odoom *et al.* 1996). Resting cell pH is set by processes of H^+ efflux, dominated by the Na^+/H^+-antiporter, such that resting pH is, approximately, the pH at which net H^+ efflux is zero (Kemp *et al.* 1994b). Lastly, the total adenine nucleotide pool size, the overwhelmingly largest part of which is ATP, is set by the balance of net adenine nucleotide synthesis and breakdown, not by ATP supply and demand.

The view through 'the ^{31}P MRS window'

Figure 1 also illustrates how key components of this system can be quantified by ^{31}P MRS. PCr, Pi and ATP are directly detectable. Although absolute quantitation methods exist, a literature value of [ATP] is commonly used as an internal standard to quantify [Pi] and [PCr] (Kemp *et al.* 2007). Cytosolic pH is estimated from the chemical shift (i.e. MR resonance frequency) difference between Pi and PCr. Other quantities can be calculated indirectly: free [ADP] from [PCr] and pH using the CK equilibrium [Eqn 1, usually assuming a literature value of [TCr] (Kemp *et al.* 2007)], free [AMP] from [ATP] and [ADP] using the adenylate kinase equilibrium, and ΔG_{ATP} from [Pi], [ADP] and [ATP] (Eqn 2). Published mean pH and concentrations[2] in normal resting muscle (indicated by subscript R) are summarized elsewhere (Kemp *et al.* 2007): roughly $[PCr]_R \approx 33$ mmol (l cytosolic water)$^{-1}$ more economically expressed as 33 mM, $[Pi]_R \approx 4$ mM, $pH_R \approx 7.0$, $[ADP]_R \approx 14$ μM and $\Delta G_{ATP,\,R} \approx -63$ kJ mol^{-1}; the 'parametric' concentration [TCr] ≈ 43 mM can be taken as constant across the dynamic range of ATP turnover, and the same is true of [ATP] ≈ 8 mM under most of the conditions relevant here.

Quantitative analysis of ^{31}P MRS data from skeletal muscle

In the light of the outline of muscle energy metabolism presented above, two general principles of analysis of dynamic ^{31}P MRS data can be summarized as follows:

[2]These mean values are used in the recalculation of published data presented in Figures 8, 9, 11 and 12 where study-specific values are not available, or where departures from consensus means would skew the comparisons.

 © 2014 Scandinavian Physiological Society. Published by John Wiley & Sons Ltd, doi: 10.1111/apha.12307

$$\begin{aligned}\text{ATP turnover: basal ATP use} &+ (\text{force} \times \text{contractile cost}) \\ &\approx \text{glycolytic ATP synthesis} \\ &+ \text{oxidative ATP synthesis} \\ &+ \text{net PCr breakdown}\end{aligned} \quad (5)$$

$$\begin{aligned}\text{pH homeostasis: glycolytic } H^+ \text{ production} &\approx \\ H^+ \text{ buffering} + H^+ &\text{consumption by PCr breakdown} \\ + H^+ &\text{efflux}\end{aligned} \quad (6)$$

Equations 5 and 6 are generally valid, but it is convenient to rewrite them for the special case of recovery from exercise: here no ATP is being used to generate contractile force; glycolytic ATP synthesis has fallen to zero at the end of exercise;[3] rather than H^+ being 'buffered' by cytosolic buffers as pH falls, pH is rising back to basal as a result of processes amounting to H^+ efflux, and while this is happening H^+ is being released from cytosolic buffers (there is no agreed term for this, so if H^+ is buffered when pH falls, we will say that H^+ is 'unbuffered' when pH rises); finally, the term 'H^+ consumption accompanying PCr breakdown' in Eqn 6 is now negative, i.e. there is H^+ generation as a consequence of PCr resynthesis, and this is part of the H^+ load which must be removed by H^+ efflux. Thus,

$$\begin{aligned}\text{ATP turnover in recovery: oxidative ATP synthesis} &\approx \text{PCr resynthesis} \\ &+ \text{basal ATP use}\end{aligned} \quad (7)$$

$$\begin{aligned}\text{pH homeostasis in recovery: } H^+ &\text{efflux} \\ \approx H^+ &\text{from PCr resynthesis} + H^{+\prime} \text{unbuffering}'\end{aligned} \quad (8)$$

Thus, ^{31}P MRS gives access to a limited set of cytosolic metabolite concentrations, which nevertheless occupy a central place in the structure of muscle metabolism which allows some useful inferences about metabolic fluxes (Kemp & Radda 1994).

^{31}P MRS approaches to muscle mitochondrial function

Mitochondrial function in largely oxidative exercise and recovery

The subject of this review is the use of ^{31}P MRS to assess mitochondrial metabolism, in the sense of the oxidative generation of ATP (Kemp *et al.* 2002b, Kemp 2004). The simplest case to analyse is 'pure aerobic' exercise (i.e. exercise beneath the lactate threshold, where the contribution of glycolytic ATP synthesis is relatively small) and recovery following its cessation. In exercise of this kind PCr kinetics are monoexponential (Meyer 1988), and at least in the early phase so are the kinetics of pulmonary V_{O2} (Rossiter 2011). Monoexponential kinetics of [PCr] imply a linear steady-state relationship of oxidative ATP synthesis to the fall in [PCr], and *vice versa* (Mahler 1985, Funk *et al.* 1990, Kemp 1994, Kemp *et al.* 1998). Similar arguments apply to the relationship between oxidative ATP synthesis rate and ΔG_{ATP} (Meyer 1988, Kemp 1994). This analysis also predicts that post-exercise PCr recovery kinetics will be 'first order', i.e. exponential (Meyer 1988), and that the absolute PCr resynthesis rate measures suprabasal oxidative ATP synthesis rate.

Some experimental data to illustrate the analyses

An example of data from an experiment using largely oxidative exercise and recovery is given in Figures 2 and 3. These show time-course data from isometric exercise at two intensities; even at the high-intensity pH changes are fairly small, and the PCr recovery rate constants (k_{PCr}) are the same for both, consistent with simple models of mitochondrial regulation (Meyer 1988) which we will discuss in the next section. Figure 4 uses this data set to illustrate three approaches to analysing PCr recovery data. The three panels show either the rate of PCr resynthesis (V_{PCr}) (Fig. 4a) or the estimated oxidative production rate (Q) derived from it by adding an assumed basal rate (Q_B) (Fig. 4b,c), plotted against one of three other variables throughout the period of recovery, beginning at the end-exercise/initial-recovery point and ending when concentrations have returned to their resting level. These plots illustrate the extrapolation used either explicitly or implicitly in the three approaches. The legend to Figure 4 gives details of the calculations used.

The aim of this analysis was to use recovery data to derive an MMMF, as defined above. While any such measure will correlate with other relevant measurements, we can usefully define an *absolute* MMMF as one which is intended to correspond to a maximal rate of mitochondrial ATP synthesis, and so has units of metabolic flux, here mmol (l cytosolic water)$^{-1}$ min^{-1} i.e. mM min^{-1}. A *relative* MMMF is one for which this is not so. Here, we use the symbol Q_{MAX} for the absolute MMMF calculated from PCr recovery kinetic data. The general argument follows from Eqn 3: assuming a relationship between Q and some feedback signal X, we calculate

[3]Subject to some qualifications which we discuss below (in the section entitled 'Is PCr resynthesis fuelled entirely by oxidative ATP synthesis?').

© 2014 Scandinavian Physiological Society. Published by John Wiley & Sons Ltd, doi: 10.1111/apha.12307

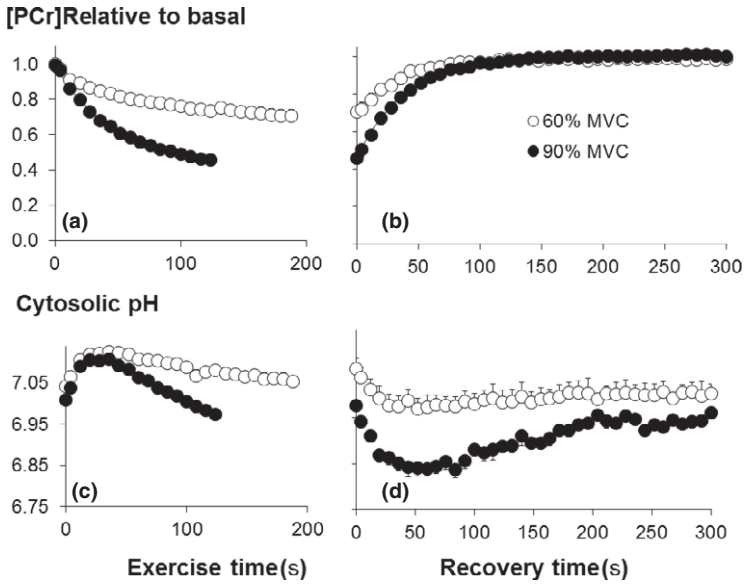

Figure 2 Example ^{31}P MRS data: exercise and recovery time-course data. ^{31}P MRS data (Ahmad 2010, Ahmad et al. 2010) were obtained from 11 healthy subjects aged 20–26 years using a 3T Trio scanner (Siemens, Munich, Germany), an 18 cm dual-tuned surface coil (Rapid Biomedical, Rimpar, Germany) and a purpose-built rig for isometric knee extension. Local research ethics committee approval was obtained, and all subjects gave written informed consent. After resting acquisition (TR = 10 s), data were acquired with TR = 2 s during 1 min rest, 3 min exercise at 60% maximal voluntary contraction force (MVC) (0.25 Hz, 50% duty cycle), 5 min recovery, 2 min exercise at 90% MVC and 5 min recovery. The upper panels show [PCr] expressed relative to the basal (resting) value during (a) exercise at 60 and 90% MVC (see key) and (b) subsequent recovery; there was no significant difference in the recovery rate constant k_{PCr} (mean 1.7 ± 0.2 min^{-1}) at the two exercise intensities, measured by least-squares fit. The lower panels show cytosolic pH in the same format during (c) exercise and (d) recovery. Standard error bars are included, but largely obscured by the symbols.

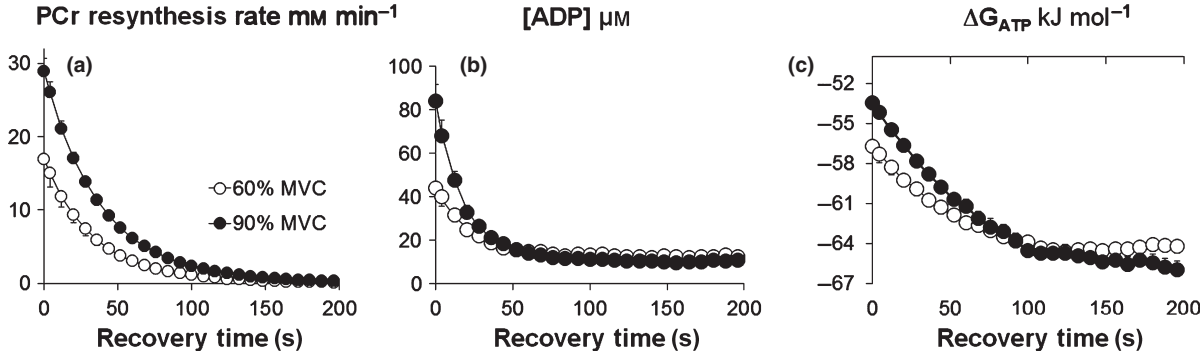

Figure 3 Example ^{31}P MRS data: recovery time-course data and analysis. The figure shows time-course data from the recovery phase of the experiments in Figure 2. (a) shows the point-by-point rate of PCr resynthesis throughout recovery calculated from the exponential fit to the [PCr] time-course in Figure 2(b), (b) shows the cytosolic free [ADP], and (c) the free energy of ATP hydrolysis (ΔG_{ATP}). Standard error bars are included, but often obscured by the symbols.

$$\text{General estimate of maximal oxidative ATP synthesis rate: } Q_{MAX} = f(X_{MAX}) \quad (9)$$

where X_{MAX} is the value of X in some suitable state of 'maximal' stimulation and/or output. We will now consider three main approaches which we can describe in terms of three 'models': the 'linear-model', the 'ADP-model', and the 'non-equilibrium thermodynamic (NET) model', differing according to the choice of f and X in Eqn 9.

Linear-model approaches to muscle mitochondrial function

Figure 4(a) plots V_{PCr} against the relative fall in [PCr] below resting values (i.e. the absolute fall in [PCr],

 © 2014 Scandinavian Physiological Society. Published by John Wiley & Sons Ltd, doi: 10.1111/apha.12307

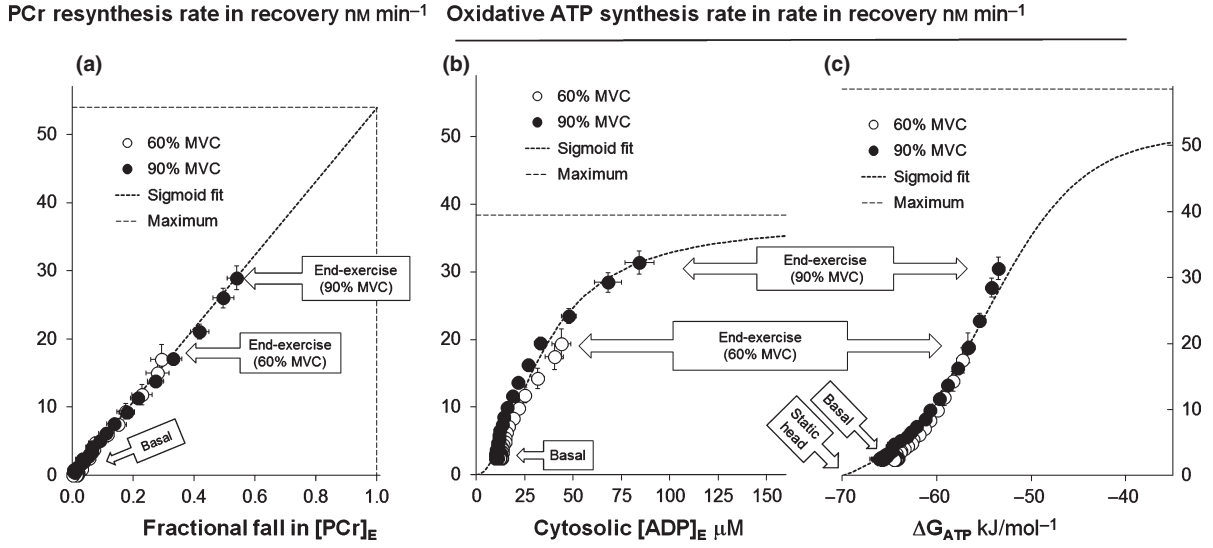

Figure 4 Example data: analysis of recovery data. The figure shows, for the data in Figures 2 and 3, the point-by-point rate of PCr resynthesis throughout recovery (whose time-course is shown in Fig. 3a) plotted against three variables: (a) the relative fall in [PCr] below resting (which is 1 minus the relative [PCr], whose time-course is shown in Fig. 2b), (b) free [ADP] and (c) ΔG_{ATP} (whose time courses are shown in Fig. 3b,c respectively). The labelled arrows indicate the end-exercise (initial-recovery) starting points for the two exercise intensities (see key), and the basal value reached again at the end of the recovery period. The inset panels shows notional extrapolation (for clarity, of just the 90% MVC data plots) to 'complete' PCr depletion in panel (a) (mean 'linear model' Q_{MAX} = 56 ± 4 mM min^{-1}), and the corresponding 'infinite' [ADP] in panel (b) ('ADP-model' Q_{MAX} = 34 ± 2 mM min^{-1}) and ΔG_{ATP} in panel (c) ('NET-model' Q_{MAX} = 55 ± 4 mM min^{-1}). These estimates are derived from the initial-recovery PCr resynthesis rate (V) and end-exercise concentration measurements, assuming the relevant models described in the main text. We have used a published value for n = 1.9 (Jeneson et al. 2009), and assumed a compromise value of Q_B = 2.4 mM min^{-1} (Jeneson et al. 2009), larger than true resting ATP turnover, but arguably reasonable given the likelihood of extra demands, for example, ion pumping in muscle immediately post-exercise (see text for further discussion of this point). We used Km = 35 μM based on the fit to the data shown here, which is about halfway between values of 22 μM (Jeneson et al. 2009) and 44 μM (Jeneson et al. 1996) used in earlier studies. None of these values can be considered firmly established, but they are not critical to any of the points discussed here.

which we will call Δ[PCr], divided by the resting value, $[PCr]_R$). The slope from the origin to the end-exercise (initial-recovery) point is an apparent rate constant; if PCr kinetics are monoexponential the data will lie on a straight line whose slope is the exponential rate constant k_{PCr}, and the initial rate is then $V_{PCr} = k_{PCr}\Delta[PCr]_E$, where the subscript E refers to the end-exercise value. A popular approach is to use k_{PCr} as a relative MMMF, or else the time constant τ_{PCr} (=1/k_{PCr}) or half-time $t_{1/2}$ (=$\log_e$2/k_{PCr}) as inverse MMMFs. An extension of this approach (Conley *et al.* 2000a, Jubrias *et al.* 2003) is to define V_{PCr} notionally extrapolated to maximal PCr depletion as an absolute MMMF (Fig. 4a): this yields a 'linear model' estimate of the maximum rate of oxidative ATP synthesis:

$$\text{Linear extrapolation to maximal oxidative ATP synthesis rate: } Q_{MAX} = k_{PCr}[PCr]_R \quad (10)$$

in which the maximal 'signal' (X_{MAX} in Eqn 9) is the theoretically maximum rise in [Cr] and fall in [PCr]. Note that the extrapolation implicit in Eqn 10 is not literally possible: when exercise is intense enough for substantial PCr depletion, pH will fall, which is associated with slowing of PCr recovery, as we discuss below (see Figs 5 and 6a). Despite the complex effects of [Cr] and [PCr] on mitochondrial respiration mentioned later, Eqn 10 is usually taken as an empirical index rather than a formal extrapolation of a causal feedback relationship which holds across the full dynamic range. Furthermore, this approach does not claim to account for the resting rate of ATP turnover: the origin in Figure 4(a) is the normal resting state where $V = 0$ (because [PCr] is stable), but $Q = Q_R$; there is no suggestion that the linear relationship observed in recovery holds 'below' the normal resting state (which would imply, unrealistically (Kemp & Brindle 2012), that $Q_R = k[Cr]_R$)

'ADP-model' approaches to muscle mitochondrial function

Figure 4(b) illustrates an alternative approach based on the hyperbolic (Michaelis–Menten) dependence *in vitro* of mitochondrial respiration rate on experimentally

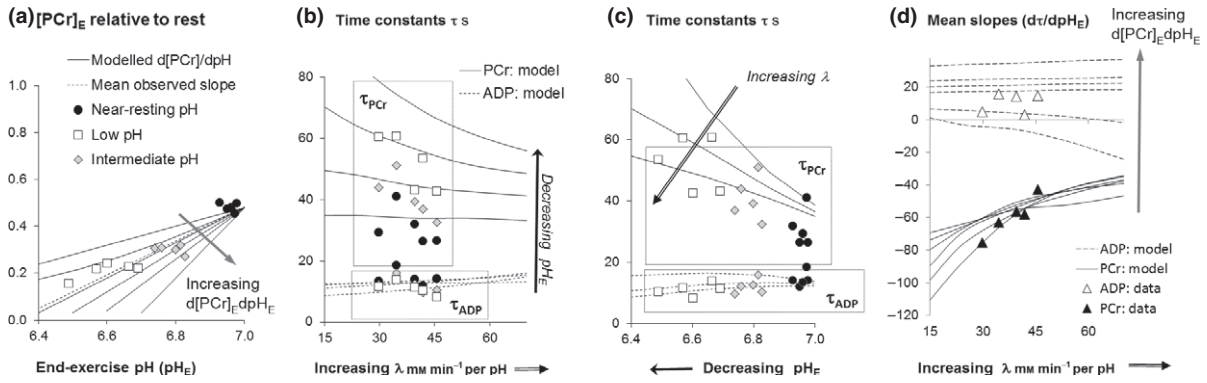

Figure 5 Example: observed and simulated effects of H^+ handling and pH on recovery. The figure shows the results of a minimal simulation (see main text) applied to published data from five subjects each studied several times each under different exercise conditions to achieve a range of pH_E (van den Broek et al. 2007). (a) shows relationships of $[PCr]_E$ and pH_E, the starting point for recovery; in the simulations shown later in (d) $[PCr]_E$ is varied incrementally and pH_E is obtained for various values of $d[PCr]_E/dpH_E$, increasing as the arrows show: a mean $d[PCr]_E/dpH_E$ line is also shown. Data points (1 per subject) are shown in three pH-groups, taking together studies where pH change during exercise was small (the 'near-rest pH' group), moderate ('intermediate pH') and large ('low pH'). (b) shows the simulated time constants τ_{PCr} (solid lines) and τ_{ADP} (dashed lines) as a function of the H^+ efflux pH-sensitivity parameter λ for various values of pH_E, which is varied holding $[ADP]_E$ constant. (c) shows the same data in a different way, τ_{PCr} and τ_{ADP} as a function of pH_E for various H^+ efflux settings λ. The data points (key as (a)) show reasonably similar behaviour to the simulated lines. In (b) and (c) $d[PCr]_E/dpH_E$ was chosen to keep $[ADP]_E$ constant, but different assumptions better match the initial conditions in (a), where $[ADP]_E$ (not shown) rises modestly with decreasing pH_E. (d) is a summary figure in which each pair of lines (solid = τ_{PCr}, dashed = τ_{ADP}) makes a different assumption about $d[PCr]_E/dpH_E$ (corresponding to the lines in (a)) and each data point (see key) is the mean of all studies for a single subject.

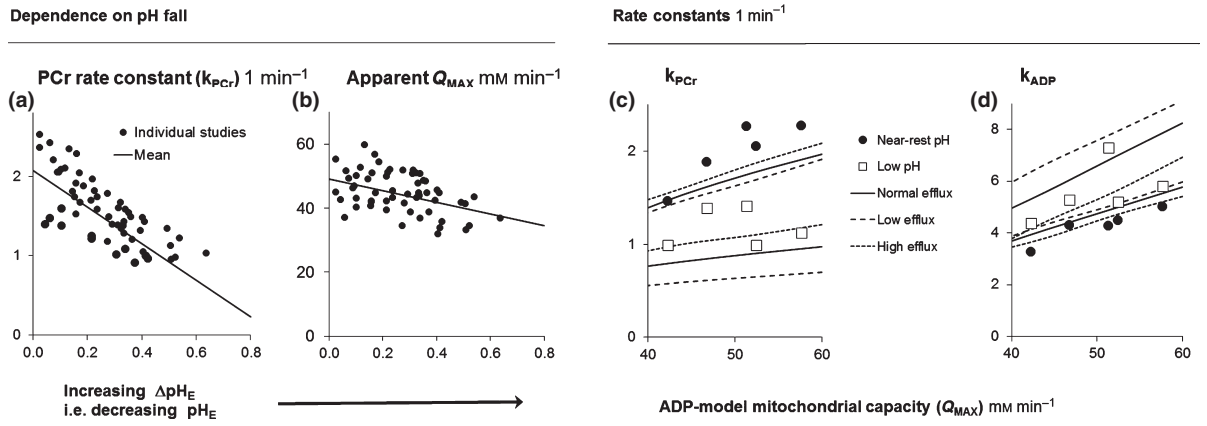

Figure 6 Example: further observed and simulated effects of H^+ handling and pH on recovery. This figure continues the analysis and simulation of Figure 5, based on the published data set from five subjects (van den Broek et al. 2007). The leftmost pair of panels (a) and (b) show data from all studies of each subject (not distinguished in these plots), to show the marked pH-dependence of k_{PCr} ($=1/\tau_{PCr}$) (a) and the small but statistically significant ($P = 0.03$) pH-dependence of apparent Q_{MAX} (b), along with overall regression lines. The rightmost pair of panels (c) and (d) show the simulated recovery rate constants k_{PCr} (c) and k_{ADP} ($=1/\tau_{ADP}$) (right-hand panel) as a function of Q_{MAX} for three assumptions about H^+ efflux (see key); data points (1 per study) are the 'near-rest' and 'low' pH subgroups. These simulations assume the same pH-dependence of Q_{MAX} as the regression line in panel (b), although this assumption does not have much effect on the results.

manipulated [ADP] (Chance & Williams 1955). A similar relationship was first described in exercising muscle *in vivo* using power output as a surrogate for oxidative ATP synthesis (Chance *et al.* 1985), and it has since been often noted that the initial-recovery V_{PCr} has such a relationship to end-exercise [ADP] ($[ADP]_E$) across experiments in which this varies (Kemp *et al.* 1993a,b, 2002b, Boska 1994, Jeneson *et al.* 1995, 1996, 2009, Thompson *et al.* 1995, Combs *et al.* 1999). (We present a comprehensive literature summary of this relationship below in Figs 8a and 9a). A similar relationship holds when V_{PCr} is followed through

 © 2014 Scandinavian Physiological Society. Published by John Wiley & Sons Ltd, doi: 10.1111/apha.12307

recovery to baseline[4] (Kemp *et al.* 1996, Layec *et al.* 2013a): we present an example in Figure 4(b). Unlike the linear model considered above, in principle the ADP-model, and the NET-model considered in the next two sections, can explain the basal state according to Eq 4. This is why the *y*-axis in Figure 4(b,c) is the absolute rate of oxidative ATP synthesis $Q = V + Q_B$, where V is the measured rate of PCr resynthesis and Q_B the relevant basal rate of ATP turnover, which is discussed further below (in the section entitled 'What is the relevant 'basal' rate of ATP synthesis?').

For any candidate model of feedback control of mitochondrial ATP synthesis, the question must be asked whether a single relationship plausibly holds across the whole dynamic range: in other words does the single function work in both Eqns 4 and 9? For the ADP-model, it was realized some while ago that a simple hyperbolic relationship to [ADP] cannot, given observed resting [ADP] ($[ADP]_R$), account for the whole dynamic range of rates without unrealistic assumptions about basal ATP turnover rate. A cooperative, sigmoid, relationship, corresponding to a Hill coefficient (n) of ~2 gives a better fit (Jeneson *et al.* 1996, 2009, Cieslar & Dobson 2000, Layec *et al.* 2013a). This is sometimes called a 'second-order' relationship, to distinguish it from the 'first order' case where $n = 1$. In this model, Eqn 3 takes the form

$$\text{ADP-model control of oxidative ATP synthesis: } Q = Q_{MAX}/\{1 + (Km/[ADP]_E)^n\} \quad (11)$$

It follows that Eqn 9 used to estimate maximal oxidative ATP synthesis rate takes this form:

$$\text{ADP-model extrapolation: } Q_{MAX} = (V_E + Q_B)\{1 + (Km/[ADP]_E)^n\} \quad (12)$$

where the maximal 'signal' (X_{MAX} in Eqn 9) corresponds to 'infinite' [ADP]. We return to this below.

An alternative relative MMMF in this approach is the ADP recovery halftime (or time constant) (Adatia *et al.* 1993, Taylor *et al.* 1994, Kemp *et al.* 1995, Argov *et al.* 1996, De Stefano *et al.* 1996). This is discussed further below (in Fig. 5).

Non-equilibrium thermodynamic approaches to muscle mitochondrial function

Figure 4(c) illustrates a third approach, which can be broadly thought of as based on NET. The simplest version focuses on quasi-linear relationships of oxidative ATP synthesis rate to ΔG_{ATP} (Meyer 1988, Jeneson *et al.* 1995); either the rate constants of PCr or ΔG_{ATP}, or, equivalently, the slope $dQ/d\Delta G_{ATP}$, which has been defined on an electrical analogy as mitochondrial conductance (Meyer 1988), are used as relative MMMF (Kemp 1994). However, this relationship is linear only over a middle range of ΔG_{ATP} (Westerhoff & van Dam 1987, Westerhoff *et al.* 1995), being more exactly sigmoid, as is observed for initial V_{PCr} and ΔG_{ATP} *in vivo* (Jeneson *et al.* 1995, 1996, 1997, 2009, Combs *et al.* 1999). More complex fits can be used to obtain an extrapolated NET-model maximum flux (Fig. 4c), for example, (Westerhoff & van Dam 1987, Westerhoff *et al.* 1995)

$$\text{NET extrapolation: } Q_{MAX} = (V_E + Q_B)\{A.\exp[(\Delta G_E - C)/(RT)] - 1\}/\{A.\exp[(\Delta G_E - C)/(RT)] + B\}, \quad (13)$$

where A is a constant which has the value =1 in a simple unimolecular substrate-to-product reaction (Van der Meer *et al.* 1980), but no particular expected value in more complex cases, B is a constant relating to thermodynamic reversibility and C is the 'static' head, the ΔG_{ATP} at which flux is zero, which can be given a physiological interpretation (Harkema & Meyer 1997). The maximal 'signal' (X_{MAX} in Eqn 9) is now at 'infinite' ΔG_{ATP}, although the Q-ΔG_{ATP} is usually taken to flatten out well before ΔG_{ATP} approaches positive values (Fig. 4c). A simple analysis based on the ADP-model shows that the mid-range slope $dQ/d\Delta G_{ATP}$, the 'mitochondrial conductance' (Meyer 1988), is $\sim 6Q_{MAX}/RT$ (Kemp *et al.* 1998, 2001b)). A purely empirical sigmoid function has also been used to fit Q-ΔG_{ATP} relationships, and so to estimate a maximum value of Q (Jeneson *et al.* 1997, 2009).

Some formal relationships between [ADP]- and ΔG-dependence, as well as some general properties of closed-loop feedback, are summarized elsewhere (Kemp 1994, 2008b, Kemp *et al.* 1998); we return to this in discussion of Figure 7 below.

Some technical and physiological issues in the analysis of PCr recovery kinetics

Different Q_{MAX} estimates in different models

Calculations based on these different models do not in general give numerically similar extrapolated estimates of Q_{MAX}. The ADP-model (Eqn 12) gives values lower than the 'linear' approach (Eqn 10): compare Figure 4(a,b). In general, this relationship depends on the shape of the [ADP]-dependence of Q: for submaximal exercise the two models predict

[4]A concave-downwards relationship between d[PCr]/dt and [ADP] is mathematically necessarily when – as is invariably observed – PCr and ADP recovery are both approximately exponential, the latter being faster.

© 2014 Scandinavian Physiological Society. Published by John Wiley & Sons Ltd, doi: 10.1111/apha.12307

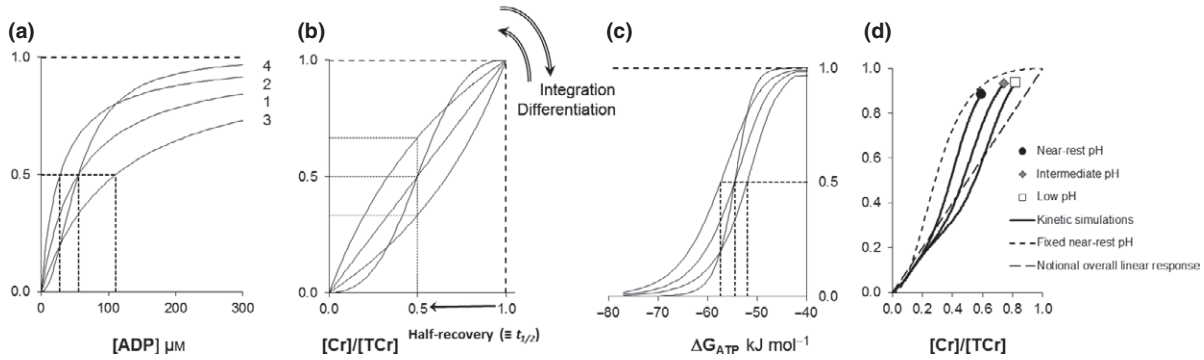

Figure 7 Other lessons from the simple computational simulation of recovery. The figure shows the oxidative ATP synthesis rate (expressed relative to the maximal value as Q/Q_{MAX}) as a function of [ADP] or free creatine (expressed relative to the total creatine pool size as [Cr]/[TCr]). (a) shows some different shapes of Q-[ADP] (taken as primary here), and (b) shows how the corresponding Q-[Cr]/[TCr] curves are related to the halftime (i.e. literally time for 50% recovery) from notional complete PCr depletion (Cr/TCr = 1). (c) Shows the corresponding Q-ΔG_{ATP} curves. Parameters: for n = 1, line 1 represents Km = 30 μM (corresponding to linear Q-[Cr]/[TCr]), line 2 is Km > 30 μM and line 3 is Km < 30 μM; case 4 is Km = 30 μM with n = 2. pH is assumed constant at resting value. (d) shows the three pH-grouped end-exercise data points from (van den Broek et al. 2007) and the simulated recovery time courses (thick lines), while the dotted lines represents the underlying relationship at constant pH, and the dashed line represents a notional monoexponential recovery from complete PCr depletion. See main text for a detailed discussion.

the same extrapolated maximal rate only (if pH changes are ignored) in what is now agreed to be the unrealistic case where $n = 1$, and then only if $Km = [ATP]K_{eq}/[H^+] \approx 50$ μM (Kemp 1994, Kemp *et al.* 1998). Of course for maximal exercise, in the literal sense where [PCr] is negligible and [ADP] is very high, the extrapolated Q_{MAX} is close to the observed initial V_{PCr} in all approaches.

Regulation of oxidative ATP synthesis: open- vs. closed-loop mechanisms

Setting aside these model-dependent technicalities of calculation, there is considerable empirical support for feedback-based regulation of oxidative ATP synthesis, including the observational studies cited above. In the simulation studies to be discussed below, this kind of model is also capable of explaining much of the observed relationship between PCr recovery kinetics and pH. Studies in model systems *ex vivo* (mitochondria, CK and its substrates, and a glucose + hexokinase ATP-splitting system) confirm the basic prediction of monoexponential ('linear') kinetics, with rate constant proportional to mitochondrial content and inversely proportional to [TCr] (Glancy *et al.* 2008). While these results were originally presented (Glancy *et al.* 2008) as confirmation of an electrical analogue of the linear thermodynamic model (Meyer 1988), they also reproduce a number of general properties of CK-mediated feedback-controlled supply-demand mechanisms (Kemp 2008b).

However, it might seem that standard feedback models take, by contemporary standards, a naïve view of metabolic causation, seeming to posit a single signal acting at a single step. Nevertheless, detailed computational modelling approaches have left this approach surprisingly unchanged, in the sense that V_{O2} continues to appear as a relatively invariant function of [ADP] (or other CK-related signals such as ΔG_{ATP}) (Wu *et al.* 2007, Jeneson *et al.* 2009, Schmitz *et al.* 2011, 2013).

Is PCr resynthesis fuelled entirely by oxidative ATP synthesis?

That post-exercise PCr recovery is overwhelmingly aerobic is shown by the common observation that PCr does not recover during cuff ischaemia (Harris *et al.* 1975, Dawson *et al.* 1980, Taylor *et al.* 1983, Blei *et al.* 1993, Quistorff *et al.* 1993, Wackerhage *et al.* 1998). Furthermore, the observation of higher order (i.e. non-monoexponential) PCr recovery kinetics following high-intensity exercise (Harris *et al.* 1976, Arnold *et al.* 1984, Walter *et al.* 1997) does not imply any glycolytic contribution: the usual explanation for a slow component of PCr recovery relates it to the interactions between pH and PCr in the CK equilibrium (Sahlin *et al.* 1979, Takahashi *et al.* 1995) that we discuss below (in Fig. 5).

However, whether there is never any glycolytic contribution to post-exercise PCr recovery cannot be answered definitively. *In vitro* and modelling studies show that glycolytic ATP production *could* drive PCr re-

 © 2014 Scandinavian Physiological Society. Published by John Wiley & Sons Ltd, doi: 10.1111/apha.12307

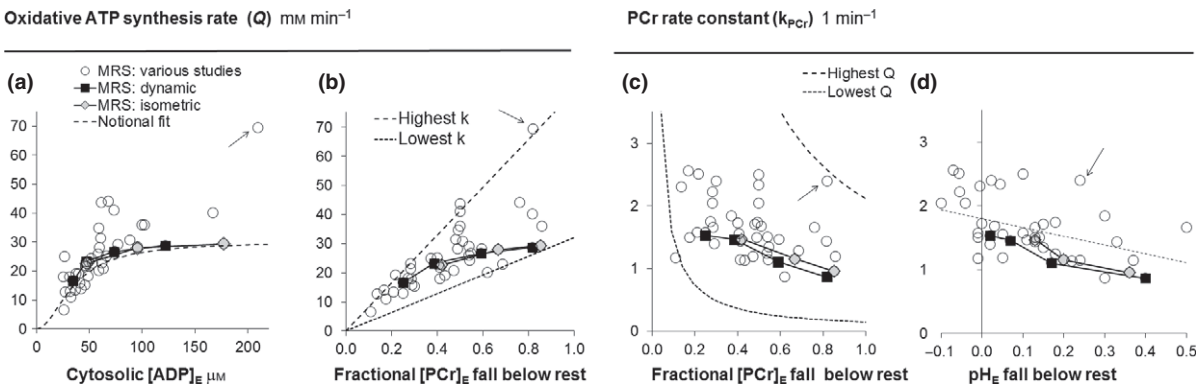

Figure 8 Published ^{31}P MRS data from quadriceps. This figure summarizes the results of a number of published ^{31}P MRS studies of human quadriceps muscle. Each point (or pair of linked points) shows the mean value(s) in a single study. Two studies yielding multiple data points are shown separately: 'MRS: dynamic' is (Takahashi et al. 1995), 'MRS: isometric' is (Vanderthommen et al. 2003). Other symbols shows single data points (or sometimes two) from Figure 2 and the following studies: (Marrades et al. 1996, Sala et al. 1999, Conley et al. 2000a, Rossiter et al. 2002a,b, Jeneson & Bruggeman 2004, Smith et al. 2004, Trenell et al. 2006, 2007, Schrauwen-Hinderling et al. 2007, 2008, Barker et al. 2008, De Feyter et al. 2008, Forbes et al. 2008, Jeneson et al. 2009, Jones et al. 2009, Larsen et al. 2009, 2012, 2013, Layec et al. 2009, 2011, 2013d, McCully et al. 2009, Kemps et al. 2010, Schmitz et al. 2010, Willcocks et al. 2010, Lanza et al. 2011, Makimura et al. 2011a,b, Sleigh et al. 2011, Chidnok et al. 2013, van Oorschot et al. 2013, Valkovic et al. 2013). (a) shows estimated oxidative ATP synthesis rate (Q i.e. initial V_{PCr} calculated as $k\Delta[PCr]_E$, plus assumed Q_B) as a function of $[ADP]_E$; the notional fit is the one given in Figure 4(b). (b) shows Q as a function of relative fall in [PCr] below resting (as in Fig. 4a); the slope from the origin to each point is the rate constant k_{PCr}, and the radiating lines correspond to the lowest and highest observed values of k_{PCr}. (c) Shows k_{PCr} as a function of the fractional fall in PCr; the product of the x and y coordinates is the initial V_{PCr}, and the two rectangular hyperbolae correspond to the lowest and highest observed values of V_{PCr}. (d) shows k_{PCr} plotted against the end-exercise fall in pH below basal. Note the congruence, particularly evident in the multipoint datasets, between the decline in k_{PCr} with increasing pH fall in panel (d) and with increasing [PCr] fall in panel (c), and the progressive decline in the slope of PCr resynthesis rate against [PCr] in panel (b); all these are absorbed into the notionally pH- and [PCr]-independent relationship between PCr resynthesis rate and [ADP] in panel (a). A possible explanation is considered later (see Fig. 12) for the apparently anomalous data point arrowed in panel (a), which is from a two-leg in-magnet cycle exercise study at unusually high power output for an MRS study (Jeneson & Bruggeman 2004); the very high rate of PCr resynthesis in this study (arrowed in panel b) corresponds mathematically to a high recovery rate constant at relatively high PCr depletion (arrowed, which defines the 'highest Q' line in panel c).

synthesis (Vinnakota *et al.* 2006). PCr recovery kinetics after high-intensity exercise contain a small fast component which might reflect a glycolytic component in early recovery (Forbes *et al.* 2009a). Furthermore, despite the general consensus that cuff ischaemia prevents PCr recovery (Harris *et al.* 1975, Dawson *et al.* 1980, Taylor *et al.* 1983, Blei *et al.* 1993, Quistorff *et al.* 1993, Wackerhage *et al.* 1998), there are two reports of partial PCr recovery in the early phase after cessation of exercise while ischaemia was maintained (Crowther *et al.* 2002, Lanza *et al.* 2006); given the absence of vascular O_2 supply, this must be the result of glycolytic ATP production: by analogy with Eqn 7 above:

$$\begin{aligned}&\text{ATP turnover in ischaemic recovery:}\\&\quad\text{glycolytic ATP synthesis} \approx \text{PCr resynthesis}\\&\quad + \text{basal ATP use}\end{aligned} \tag{14}$$

It might be thought that buffering calculations could detect glycolytic ATP synthesis in early recovery, but unfortunately they depend on relatively uncertain matters of H^+ buffering and efflux (Kemp 2005b, Kemp *et al.* 2006). Although such calculations are difficult, given their sensitivity to, e.g. spectrum-to-spectrum errors in pH and uncertainties about appropriate values of buffer capacity, there is general agreement that H^+ efflux (Eqn 8) is non-zero even in relatively non-acidifying exercise (Kemp *et al.* 1994a, 1996, 1997, 2001a, van den Broek *et al.* 2007, Layec *et al.* 2013d, Walter *et al.* 1999, Trenell *et al.* 2006, Tonson *et al.* 2010, Meyerspeer *et al.* 2012), at rates which are at least not obviously different from invasive AVD estimates of H^+ efflux (Bangsbo *et al.* 1992a, 1993). If glycolytic ATP synthesis were still active in recovery, Eqn 8 would underestimate the true H^+ efflux rate

$$\begin{aligned}&\text{pH homeostasis in recovery: True } H^+\text{efflux}\\&\quad\approx H^+\text{unbuffering} + H^+\text{from PCr resynthesis}\\&\quad\quad + \text{glycolytic } H^+ \text{ production}\end{aligned} \tag{15}$$

but this cannot settle the question of a glycolytic contribution, as there are no reports of parallel H^+ efflux measurements by both methods, or even close

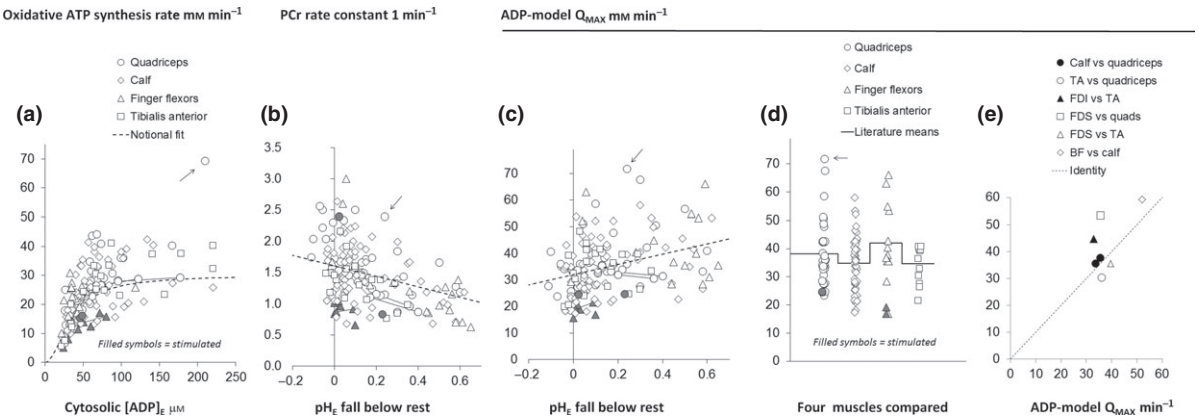

Figure 9 Published ^{31}P MRS data from several muscles compared. This figure adds to published quadriceps data (as in Fig. 8) the results of published studies of other human muscles than quadriceps (see key). (a) shows (as in Fig. 8a) initial V_{PCr} as a function of $[ADP]_E$; the notional fit is as in Fig. 4(b). (b) Shows (as in Fig. 6c) the corresponding values of k_{PCr} as a function of the end-exercise fall in pH. (c) Shows, similarly, the pH-dependence of the apparent mitochondrial capacity Q_{MAX}, calculated on the ADP-model from the data in (a). (d) collects these apparent Q_{MAX} values by muscle, and the solid line shows the overall means. In panels (a–d), the quadriceps data are the same as in Figure 8 [again the arrow indicates a two-leg ^{31}P MRS study at unusually high power output (Jeneson & Bruggeman 2004)]; the other muscles from which published data are shown are tibialis anterior (Ryschon et al. 1997, Kent-Braun & Ng 2000, Crowther & Gronka 2002, Crowther et al. 2003, Jubrias et al. 2003, Ljungberg et al. 2003, Lanza et al. 2005, 2006, Brons et al. 2008, Larsen et al. 2009, 2012, Gam et al. 2011), calf muscle (gastrocnemius/soleus) (Mancini et al. 1992, McCully et al. 1993, 1994, Boska 1994, Taylor et al. 1994, Kemp et al. 1995, 1997, 2004, Mannix et al. 1995, Argov et al. 1996, Barnes et al. 1997, Cooke et al. 1997, Walter et al. 1997, 1999, Wackerhage et al. 1998, Lodi et al. 1999, Vandenberghe et al. 1999, Larson-Meyer et al. 2000, 2001, Pipinos et al. 2000, Yquel et al. 2002, Bendahan et al. 2003, Brons et al. 2008, Scheuermann-Freestone et al. 2003, Haseler et al. 2004, 2007, Kornblum et al. 2005, Forbes et al. 2007, Greiner et al. 2007, Martinuzzi et al. 2007, Ko et al. 2008, Trenell et al. 2008, Wray et al. 2009, Khushu et al. 2010, Meyerspeer et al. 2011, 2012, Edwards et al. 2012, Schmid et al. 2012, Layec et al. 2013a,c,d, 2014, Nachbauer et al. 2013, Ryan et al. 2013, Sinha et al. 2013, 2014, Yoshida et al. 2013) and finger flexor muscle (Dudley et al. 1990, Adamopoulos et al. 1993, Blei et al. 1993, Thompson et al. 1993, Kemp et al. 1994a, McCully et al. 1994, Taylor et al. 1994, Barnes et al. 1997, Roussel et al. 2000, Layec et al. 2013d, Tonson et al. 2010). Data from muscle using nerve/muscle stimulation rather than voluntary exercise are shown with grey symbols (Blei et al. 1993, Conley et al. 2000b, Jeneson et al. 2000, Vanderthommen et al. 2003). (d) collects data from the few studies in which more than one muscle is studied, plotting ADP-model Q_{MAX} estimates of one muscle against the other (see key): tibialis anterior vs. quadriceps (Larsen et al. 2009); calf vs. quadriceps (Ahmad 2010, Ahmad et al. 2010, Layec et al. 2013d), finger flexors vs. quadriceps (Layec et al. 2013d), first dorsal interosseus vs. tibialis anterior (Jubrias et al. 2003), finger flexors vs. tibialis anterior (Brons et al. 2008) and calf vs. biceps femoris (Yoshida et al. 2013). Data are not shown for a gated study of PCr recovery whose design precludes measurement of end-exercise pH and [PCr], which finds a significantly lower k_{PCr} in tibialis anterior than in the calf muscle (Forbes et al. 2009b). There are not enough suitable published studies of biceps femoris (Yoshida & Watari 1993, Yoshida 2002, Yoshida et al. 2013) or first dorsal interosseus (Jubrias et al. 2003) for meaningful display in panels (a–d).

comparisons between different experiments achieving comparable end-exercise pH. In the special case of partial PCr recovery in early post-exercise ischaemia, where H^+ efflux must be zero, one report (Crowther *et al.* 2002) finds evidence of very transient glycolytic ATP synthesis in a buffering analysis

$$\begin{aligned}&\text{pH homeostasis in ischaemic recovery:}\\&\quad\text{glycolytic } H^+ \text{ production}\\&\approx H^+ \text{ buffering} - H^+\\&\text{from PCr resynthesis}\end{aligned} \qquad (16)$$

which is reasonably consistent with that inferred from PCr changes alone by Eqn 14 (Crowther *et al.* 2002).

Overall, a reasonable conclusion is that a glycolytic contribution to PCr recovery cannot be excluded, but it is always small. It is worth noting that this rapid deactivation of glycolytic ATP synthesis at the end of exercise implies that, whatever the role of closed-loop feedback mechanisms involving, e.g. Pi, ADP and AMP (Vinnakota *et al.* 2006), the control of glycolytic ATP synthesis *in vivo* during exercise/recovery must be dominated by open-loop mechanisms (Crowther *et al.* 2002). A computational study suggests that this may be mediated by inactivation of phosphofructokinase and pyruvate kinase (Schmitz *et al.* 2010).

What is the relevant 'basal' rate of ATP synthesis?

The basal needs of the muscle for ATP synthesis rate (Q_B in Eqns 11–13) also contribute to ATP demand during recovery from exercise, and this complicates

 © 2014 Scandinavian Physiological Society. Published by John Wiley & Sons Ltd, doi: 10.1111/apha.12307

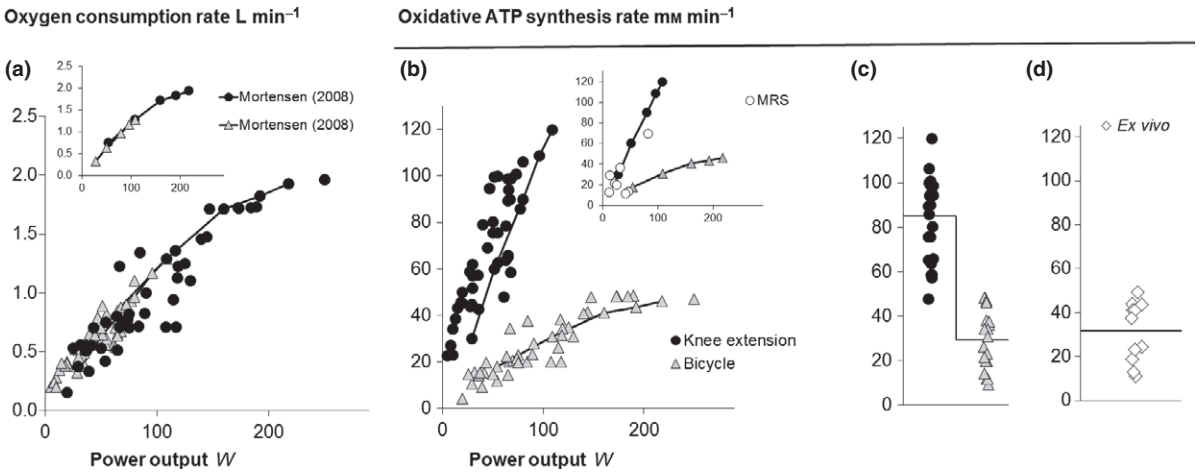

Figure 10 O_2 consumption rates in quadriceps in cycle exercise (CE) and single-leg knee extension (KE). This figure summarizes the results of a number of published arteriovenous difference (AVD) measurements of O_2 consumption rate (V_{O2}) of human quadriceps muscle. In (a) and (b), one study yielding multiple data points in a direct comparison between CE and KE (Mortensen et al. 2008) is shown separately (linked points) and in the insets; other symbols shows single data points (or sometime two) from the following studies: CE (Welch et al. 1977, Bender et al. 1988, Ahlborg & Jensen-Urstad 1991b, Poole et al. 1991, 1992, Jensen-Urstad & Ahlborg 1992, Knight et al. 1992, 1993, Roca et al. 1992, Jensen-Urstad et al. 1993, Schaffartzik et al. 1993, Marrades et al. 1996, Sala et al. 1999, Stellingwerff et al. 2006, Mortensen et al. 2008, Esposito et al. 2011, Barrett-O'Keefe et al. 2012, Rud et al. 2012), and KE (Andersen & Saltin 1985, Andersen et al. 1985, Bangsbo et al. 1990, 1992a,b, 2001, 2002, Blomstrand et al. 1997, Gibala et al. 1998, Pedersen et al. 1999, Radegran & Saltin 2000, Rasmussen & Rasmussen 2000, Ferguson et al. 2001, Krustrup et al. 2001, 2003, 2004, 2009, Rasmussen et al. 2001, Richardson et al. 2002, Lawrenson et al. 2003, Mourtzakis et al. 2004, Amann et al. 2011, Esposito et al. 2011, Jones et al. 2012). (a) Shows whole-muscle V_{O2} as a function of power output. (b) shows, in the same studies, inferred rates of oxidative ATP synthesis: these are calculated from V_{O2} rates in (a) using the following assumptions: P:O = 2.16 on the basis of mouse experiments combining NIRS and ^{31}P MRS during resting ischaemia (Marcinek et al. 2004), multiplied by 1.19 (Brand 2005) to account for the oxidation of predominantly pyruvate (from glycogen) in short-duration exercise rather than fatty acids as at rest; muscle mass is as given in the cited papers, or else taken as relevant means of those: 10 kg for resting leg muscle and for each leg in CE, 2.5 kg for KE; muscle density = 1.049 kg l^{-1} and muscle cell water = 0.67 l kg^{-1} wet wt (Brindle et al. 1989); 1 mol O_2 = 25.5 l (Blomstrand et al. 1997). (c) collects the maximal-exercise rates of oxidative ATP synthesis (a subset of the data points in b), and the solid line shows the overall means. (d) shows, for comparison, values from *ex vivo* experiments (Tonkonogi & Sahlin 1997, Starritt et al. 1999, Tonkonogi et al. 1999, Rasmussen & Rasmussen 2000, Rasmussen et al. 2001, 2003, 2004, Hou et al. 2002, Williams et al. 2004, Boushel et al. 2011) in which data are back-calculated to physiological temperature and mitochondrial density to estimate the *in vivo* maximal V_{O2}; the solid line shows the overall means. For comparison with (c), the equivalent mean value of five studies of two-arm ergometer exercise is 35 mM min^{-1} (Ahlborg & Jensen-Urstad 1991a, Jensen-Urstad et al. 1993, Volianitis & Secher 2002, Volianitis et al. 2004, Boushel et al. 2011). The inset to panel (b) also shows data from the few quadriceps ^{31}P MRS studies in which power output data from dynamic exercise is reported (references listed later in legend to Fig. 12c).

the interpretation of PCr recovery data. There are several related issues.

ATP turnover in resting muscle. Consider first the rate of ATP turnover in resting muscle (Q_R in Eqn 4), i.e. in muscle which is not only mechanically inactive, but long enough after prior exercise for PCr and pH to have recovered back to pre-exercise values. This equates to steady-state basal ATP turnover, in which special case Eqn 5 becomes the following:

$$\text{Resting ATP turnover: oxidative ATP synthesis} = \text{basal ATP demand} = Q_R \quad (17)$$

and in Eqn 6 glycolytic H^+ production $\approx$ H^+ efflux $\approx$ 0. Note that resting muscle responding, e.g. to acutely increased circulating insulin is 'basal' in the sense that ATP turnover is not being increased to sustain contraction, but not in all senses: compared to the non-insulin-stimulated state both glucose uptake and glycogen synthesis are increased, so perhaps are V_{O2} and oxidative synthesis rate, and so are both pH and [Pi] (reviewed in (Kemp & Brindle 2012)). We can ignore this distinction in the present context.

One approach to estimating Q_R is to use cuff ischaemia to inhibit oxidative ATP synthesis and H^+ efflux; once muscle O_2 has fallen to near-zero, basal ATP demand, which is assumed not to change during this manipulation (Befroy *et al.* 2009), is met first by PCr breakdown, then increasingly also by glycogenolysis:

© 2014 Scandinavian Physiological Society. Published by John Wiley & Sons Ltd, doi: 10.1111/apha.12307

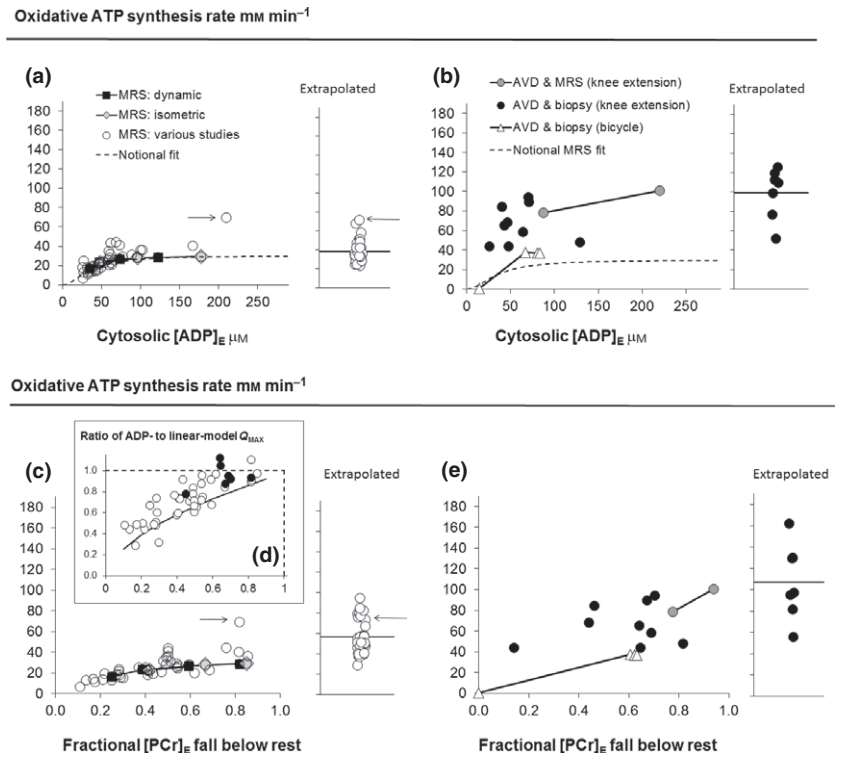

Figure 11 Measured O_2 consumption and inferred oxidative ATP synthesis rates in exercising quadriceps. This figure summarizes the results of a number of published ^{31}P MRS and AVD studies of human quadriceps muscle, showing inferred rates of oxidative ATP synthesis as a function of some metabolite concentration changes. Panel (a) shows rates inferred from published ^{31}P MRS studies as a function of $[ADP]_E$ (cf Fig. 8a). (b) Shows rates inferred from published AVD studies (a subset of those in Fig. 8a–c) as a function of $[ADP]_E$: standard assumptions are made for resting metabolites (Kemp et al. 2007), using relative changes in PCr measured by freeze-clamp biopsy [to minimize possible artefacts (Kemp et al. 2007)]; for some studies pH was measured (Bangsbo et al. 1992a,b, Krustrup et al. 2003), in others this is estimated from lactate measurements assuming a normal 'apparent buffer capacity' ($-\Delta$[lactate]/ΔpH) of 256 mmoL kg^{-1} dry weight (Spriet et al. 1987a,b). In each panel, the inferred maximal values are collected on the right. (c) and (e) show the same rates as (a) and (b), plotted against the relative fall in [PCr] below resting value (cf Fig. 8b). (a) and (c) show the same ^{31}P MRS data (with the same key) as Figure 8. As noted in the main text, the linear-model estimates of Q_{MAX} are generally larger than those of the ADP-model, and the inset panel (d) shows the ratio of the two estimates as a function of the end-exercise PCr change. In (b) and (d), two AVD studies yielding multiple data points are shown separately: 'AVD and MRS, knee extension' is (Richardson et al. 2002), 'AVD & biopsy: CE' is (Stellingwerff et al. 2006); other symbols shows single data points (or sometime two) from the following AVD KE studies: (Bangsbo et al. 1990, 1992a,b, 2001, 2002, Ferguson et al. 2001, Krustrup et al. 2003). As in Figures 8, 9 and 12, the arrow in (a) and (c) indicates a two-leg ^{31}P MRS study at unusually high power output (Jeneson & Bruggeman 2004).

$$\text{Ischaemic resting ATP turnover: basal ATP use} \approx \text{glycolytic ATP synthesis} + \text{PCr breakdown} \quad (18)$$

$$\text{Ischaemic resting pH homeostasis: glycolytic } H^+ \text{ production} \approx H^+ \text{ buffering} + H^+ \text{ consumption by PCr breakdown} \quad (19)$$

Data on ATP turnover in 'normal' resting muscle obtained by this method and others are summarized elsewhere (Kemp 2008a, Kemp & Brindle 2012), but little is known about how this might change with disease, age or training state. Resting V_{TCA} is increased in trained muscle (Befroy *et al.* 2008), in hereditary resistance to thyroid hormone (Mitchell *et al.* 2010) and by experimental treatment with T_3 (Jucker *et al.* 2000), whereas it is reduced in insulin resistance (Befroy *et al.* 2007) and with ageing (Petersen *et al.* 2003). However, it is not known how these changes in substrate oxidation are related to changes in resting ATP turnover, because Pi-ATP exchange measurements, which have been used to make inferences in such cases, largely reflects a glycolytic exchange component not causally related to ATP turnover (Kemp & Brindle 2012).

'Basal' ATP turnover in exercise and early recovery. However, the 'basal' rate of ATP turnover at the end of exercise (Q_B in Eqns 11–13), in the sense of that not available to drive the resynthesis of PCr, is not necessarily the same rate in resting muscle at

 © 2014 Scandinavian Physiological Society. Published by John Wiley & Sons Ltd, doi: 10.1111/apha.12307

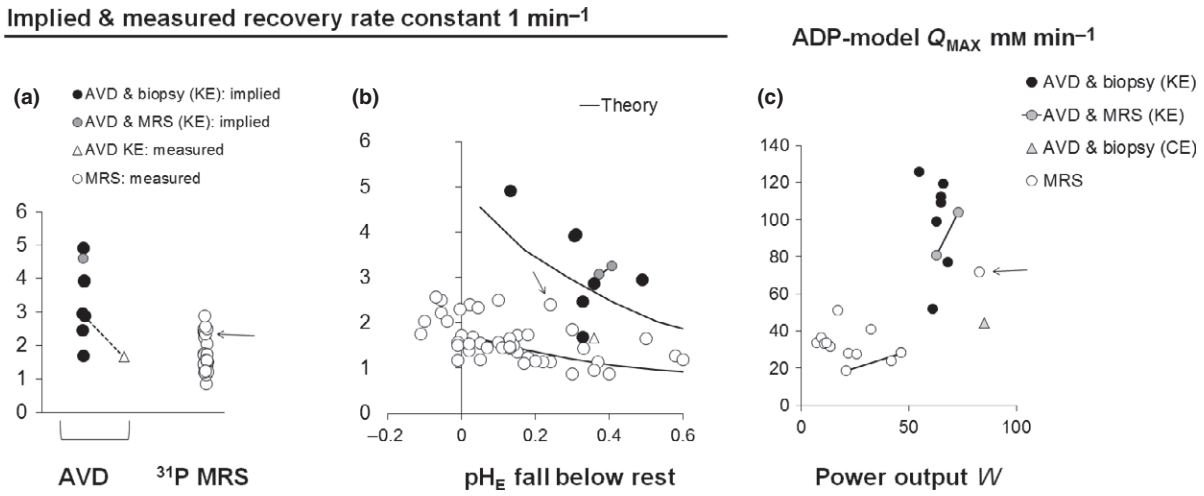

Figure 12 Apparent kinetic implications of AVD data. The first two panels show some apparent kinetic implications of AVD data. (a) Compares the measured PCr recovery rate constants k_{PCr} in published ^{31}P MRS studies ('MRS: measured' in key), with notional values from various AVD studies derived as the origin slopes of the data points in Figure 11(e) ('AVD and biopsy (KE)' in key), and the one published rate constant of the recovery of AVD V_{O2} to baseline ('AVD KE: measured') (Krustrup et al. 2003); for this study the dashed line links the measured k (triangle) to the inferred k (black circle). (b) Shows the same rate constants as a function of pH fall below basal (key same as (a)), together with a pair of simulated curves derived as in Figure 5, using mean Q_{MAX} values derived from the data sets. Panel (c) shows the relationship for studies of quadriceps between mechanical power output and the apparent Q_{MAX} calculated on the ADP-model for the few suitable ^{31}P MRS studies (taken from those analysed in Fig. 9) for which power output is reported ('MRS' in key) (Takahashi et al. 1995, Marrades et al. 1996, Sala et al. 1999, Rossiter et al. 2002a,b, Jeneson & Bruggeman 2004, Barker et al. 2008, Willcocks et al. 2010, Chidnok et al. 2013), the few maximal KE AVD studies for which biopsy data is available (analysed in panels (a) and (b): 'AVD and biopsy: KE' in key), the one AVD-biopsy study using CE and ^{31}P MRS data for maximal KE ('AVD and MRS') (Richardson et al. 2002). As in Figures 8, 9 and 11, the arrow in each panel indicates a two-leg ^{31}P MRS study at unusually high power output (Jeneson & Bruggeman 2004).

steady state, because, for example, ion transport might be much larger at the end of exercise. There are no independent measurements of this. All we can say is that Q_B is presumably not very large, otherwise its own intrinsic decay kinetics (whatever they might be) would dominate those of PCr recovery, making unlikely any reasonable fit to the simple models discussed here. Assumptions about Q_B vary in the literature, some using near-true resting values (Jeneson *et al.* 1996, 1997), others using larger values based on fits to the whole dynamic range such as 1.5 mM min^{-1} (Jeneson *et al.* 1996) and 2.4 mM min^{-1} (Jeneson *et al.* 2009): we have used the latter value here.

Resting ATP turnover and resting metabolite concentrations. A notable gap in our knowledge is whether pathological changes in resting ^{31}P MRS metabolite measurements are consistent with candidate models of mitochondrial regulation, in accordance with Eqn 4 (Kemp 1994). There is ample evidence that [Pi] and [ADP] are increased in, for example, mitochondrial myopathies (Taylor *et al.* 1994). However, we do not know whether particular disease states affect basal ATP turnover rate Q_R. Furthermore, we usually lack independent measurements of [TCr], which makes calculated [ADP] and ΔG_{ATP} potentially misleading (Kemp *et al.* 2007). Lastly, the pure ADP-model has nothing to say about [Pi], although it or course contributes to ΔG_{ATP}, and computational simulation finds it has an influence around resting concentrations (Schmitz *et al.* 2012); unlike [ADP], though, its basal value cannot be determined solely by a mitochondrial feedback loop, as cell [Pi] must eventually be at steady state with respect to plasma [Pi] consistent with the still poorly understood kinetic properties of trans-sarcolemmal Pi transport (Kemp & Bevington 1993).

Direct effects of creatine and the role of mitochondrial creatine kinase?

There is a large literature on mitochondrial CK, its structural and functional associations with other mitochondrial and cytoskeletal components (Saks *et al.* 2010), and many reports of physiological and experimental changes in the creatine-sensitivity of respiration *in vitro* (Perry *et al.* 2012, Smith *et al.* 2004, Walsh *et al.* 2006, 2002). It has proved difficult to bring insights from this work to bear on the interpretation of PCr recovery. We will not discuss this here, but simply reiterate a point made earlier (Kemp 2006a,b), that the impact *in vivo* of effects of creatine on e.g. the ADP-affinity of respiration which are demonstrable *in vitro*

is severely constrained by the cytosolic CK equilibrium, which makes [Cr]/[PCr] and [ADP] strongly correlated (Connett 1988).

Approaches to measurement of O_2 transport and consumption in vivo

Although the focus of this review is ^{31}P MRS methods, brief discussion of O_2 physiology is relevant, given its relevance to muscle mitochondrial function and the availability of non-invasive probes.

Measuring cellular PO_2. As well as the feedback mechanisms abstractly summarized in Eqn 3, oxidative ATP synthesis is also influenced by cytosolic [O_2] (sometimes expressed in terms of PO_2), which is a direct kinetic influence on cytochrome oxidase activity. Eqn 3 could be generalized to accommodate this

$$\text{General regulation of oxidative ATP synthesis: } Q = g(X, [O_2]_{cytosol}) \quad (20)$$

Non-invasive measurements of $[O_2]_{cytosol}$ would be useful in disentangling these effects. ^{1}H MRS measurements of deoxymyoglobin concentration, appropriately calibrated (Gussoni *et al.* 2010) and interpreted in terms of an O_2-dissociation curve, can estimate averaged $[O_2]_{cytosol}$ (Richardson *et al.* 1995, Vanderthommen *et al.* 2003, Carlier *et al.* 2006). A major contributor to the near-infrared spectroscopy (NIRS) signal is deoxyhaemoglobin (Tran *et al.* 1999), and a O_2-dissociation curve could be used to estimate mean $[O_2]_{capillary}$, the driving force for O_2 diffusion into the myocyte, although in practice calibration is very difficult. NIRS can be made to discriminate deoxyhaemoglobin and deoxymyoglobin (Marcinek *et al.* 2003, 2004), but practical difficulties have so far precluded using this to measure the capillary and myocyte [O_2] separately.

Measuring muscle O_2 content. Another way in which NIRS can probe contributions of O_2 transport to MMMF is by measurement of total muscle O_2 content ($[O_2]_{muscle}$, i.e. myocytes plus muscle vascular bed). By conservation of mass and the Fick principle, this is related to muscle O_2 usage (V_{O2}), blood flow and AVD (= $[O_2]_{arterial} - [O_2]_{venous}$) by

$$\text{General } O_2 \text{ balance: } V_{O2} = \text{AVD} \times \text{flow} - d[O_2]_{muscle}/dt \quad (21)$$

In the maximal exercise studies discussed later, the change in $[O_2]_{muscle}$ is negligible compared to the vascular and metabolic O_2 fluxes, and V_{O2} is directly calculable from AVD data by Eqn 21.

A different application of Eqn 21 is the use of cuff ischaemia to eliminate the contribution of O_2 inflow and outflow. Eventually, this abolishes oxidative ATP synthesis (as in Eqn 18), but in the early stages before muscle O_2 is fully depleted, Eqn 21 becomes:

$$\text{Ischaemic } O_2 \text{ balance: } V_{O_2} = -d[O_2]_{muscle}/dt \quad (22)$$

Equation 22 has been used to measure V_{O2} in resting muscle: estimates of Q_R derived from published measurements are reviewed elsewhere (Kemp & Brindle 2012). Furthermore, a combination of ^{31}P MRS (Eqns 18 and 19) and NIRS (Eqn 22) during arterial occlusion has been used to derive the P : O ratio estimate (Marcinek *et al.* 2004) which underpins our calculations of oxidative ATP turnover from published V_{O2} estimates (see legend to Fig. 10; Kemp & Brindle 2012).

The methodology of Eqn 22 can also be applied using transient arterial occlusion to measure V_{O2} during exercise and recovery (Hamaoka *et al.* 2007). Absolute quantitation of V_{O2} is technically difficult (Hamaoka *et al.* 2007), but the rate constant of V_{O2} measured by Eqn 22 using repeated transient arterial occlusion during recovery can be interpreted, like k_{PCr}, as an index of mitochondrial function (Brizendine *et al.* 2013, Ryan *et al.* 2013).

Combining NIRS and ^{31}P MRS. Intuitively, where defects in PCr recovery are mainly vascular in origin one might expect the fractional abnormality in NIRS reoxygenation kinetics to be larger than that in PCr recovery, and also the two abnormalities to correlate positively across individuals. (In contrast, a pure mitochondrial defect will slow O_2 consumption, which *if vascular flow remained unchanged*, would lead to faster post-exercise reoxygenation). Both these findings are observed in clinical vascular disease (Kemp *et al.* 2001a), and a slowing of NIRS recovery relative to PCr recovery is also reported in chronic heart failure (Kemps *et al.* 2010). A positive correlation between NIRS and PCr recovery kinetics is reported in type 2 diabetes (Schmid *et al.* 2012), which appears to suggest a major vascular component to impaired 'mitochondrial' function, interesting in view of the debate on mitochondrial dysfunction and insulin resistance discussed in (Kemp & Brindle 2012) and below (in the section entitled 'Published data on clinical abnormalities in MMMF. *Type 2 Diabetes*'). A similar correlation between deoxymyoglobin and PCr recovery kinetics (Duteil *et al.* 2004, Carlier *et al.* 2006, Ryan *et al.* 2013) appears to carry the same implication in normal controls. A simple model of this relationship has been proposed to distinguish contributions of impaired O_2 delivery and 'intrinsic' mitochondrial dysfunction to slow PCr recovery in chronic kidney disease (Kemp *et al.* 2004).

 © 2014 Scandinavian Physiological Society. Published by John Wiley & Sons Ltd, doi: 10.1111/apha.12307

Measuring muscle perfusion. Although post-exercise recovery kinetics of $[O_2]_{muscle}$ (Willcocks *et al.* 2010), easily studied by NIRS and relatively independent of calibration issues, are sensitive to abnormalities of vascular O_2 delivery (Pipinos *et al.* 2000, Kemp *et al.* 2001a), quantitative analysis is hampered by lack of knowledge of relevant variables. Furthermore, even big differences in absolute $[O_2]_{muscle}$ imply only small fractional imbalances between O_2 inflow and O_2 outflow-plus-usage (Kemp 2005a). The potential utility of simultaneous measurement of muscle perfusion is obvious, but this poses major technical problems. Although there are MR-based approaches, notably arterial spin labelling (ASL), movement artefacts make these almost impossible in exercising muscle, and post-exercise perfusion measurements are an uncertain guide to in-exercise perfusion rates. One interleaved ASL and ^{31}P MRS study reported a relation between PCr recovery and post-exercise tissue perfusion (Carlier *et al.* 2006), which is broadly consistent with the idea that vascular O_2 delivery exerts some influence on mitochondrial function during recovery in normal muscle.

MR spectroscopic localization

The ^{31}P MRS studies to be discussed here generally use simple surface-coil localization, and rely on a 'fair-sample' principle that necessarily neglects the important issue of heterogeneity (Cannon *et al.* 2013). Single voxel techniques have until recently (Meyerspeer *et al.* 2012) required an unacceptable trade-off with time resolution. This is even more true of chemical shift imaging methods (Pesta *et al.* 2013), although the problem can be partially avoided with a gated methodology using multiple repetition of a very small exercise perturbation (Slade *et al.* 2006, Forbes *et al.* 2009b). Recently, a specialized imaging sequence has been devised which gives good spatial and temporal resolution of changes in PCr, at the cost of the ability to measure pH (Parasoglou *et al.* 2013).

Validation of 'MRS-based measures of mitochondrial function'

Principles of validating MMMF

Magnetic resonance spectroscopy-based measures of mitochondrial function reflect a system property with a number of contributing factors: these include the number of mitochondria, the amount and activity per mitochondrion of all the respiratory chain components and the enzymes of fat and carbohydrate oxidation, the vascular supply of O_2 and its diffusion across the capillary wall and through the myocyte to the mitochondria (Kemp 2004). The empirical validity of any MMMF might be addressed in several ways. Most straightforwardly, in states where intrinsic mitochondrial function or mitochondrial numbers change (such as training, ageing, primary mitochondrial diseases and secondary causes of mitochondrial dysfunction), does an MMMF change detectably in the right direction? Further, does it correlate, across a range of such states, with other relevant measures? Correlations of MMMF with *ex vivo* measures (such as respiration rate in skinned fibres or isolated mitochondria) would be expected where much of the primary physiological variation or abnormality is mitochondrial, e.g. training, ageing and primary mitochondrial disease), but not in e.g. peripheral vascular disease, where the lesion is mainly extramitochondrial. MMMF would be in general be expected to correlate with *in vivo* measures such as whole body V_{O2max}, although whole body measurements can be limited by factors that do not necessarily affect skeletal muscle metabolism. In clinical conditions affecting muscle mitochondrial function, whatever the pathophysiology, correlations of MMMF with V_{O2max} would be expected where the muscle sampled by ^{31}P MRS is typical of a sufficiently large mass of muscle.

It is interesting to ask whether an observed x% decrease in an MMMF in some disease or physiological state can be quantitatively explained by an observed y% decrease in, e.g. mitochondrial content, or in activity of a particular mitochondrial component, or of some extramitochondrial parameter such as capillarity or capillary-myocyte diffusion parameters. However, this depends on metabolic control principles not yet worked out for any particular case. Moreover, data are very sparse.

The most stringent test of a claimed absolute MMMF is whether it gives values similar to other measures, such as V_{O2max} appropriately expressed for the same muscle volume, and *ex vivo* measures of mitochondrial maximal ATP synthesis fluxes appropriately extrapolated back to *in vivo* conditions (Rasmussen & Rasmussen 2000). We will do this in Figure 11. As we will discuss, this is made difficult by formidable technical issues, a consequent lack of directly comparable data, and gaps in our understanding of some pertinent physiology.

Published data on experimental changes and normal variation in MMMF

Animal models. Manipulation of mitochondrial content in rat by training and chemical thyroidectomy results in a linear correlation between MMMF (specifically, k_{PCr}) and muscle citrate synthase activity

(Paganini *et al.* 1997). Manipulation of intrinsic mitochondrial function with the complex I inhibitor diphenyleneiodonium reduces MMMF as well as maximal ADP-stimulated V_{O2} in isolated mitochondria (van den Broek *et al.* 2010).

Human training studies. In cross-sectional studies, MMMF correlate with training state and *in vitro* and whole-body measures (Takahashi *et al.* 1995, Larson-Meyer *et al.* 2000, 2001, Tartaglia *et al.* 2000, Hunter *et al.* 2005, Larsen *et al.* 2009, van Oorschot *et al.* 2013). MMMF respond to training in longitudinal studies in healthy subjects (Forbes *et al.* 2008, Larsen *et al.* 2013) and disease (Adamopoulos *et al.* 1993, Stratton *et al.* 1994, Sala *et al.* 1999, Taivassalo *et al.* 2001, van Tienen *et al.* 2012, Cordina *et al.* 2013). Things may be more complicated: a recent study reports that short-term training enhances apparent cooperativity before 'classical' MMMF respond (Layec *et al.* 2013a).

Ageing. In cross-sectional studies, MMMF are usually reported as declining with age (Taylor *et al.* 1997, Layec *et al.* 2013b). Across populations of differing age, MMMF correlate with measures of whole-body aerobic performance (McCully *et al.* 1993, Takahashi *et al.* 1995, Larson-Meyer *et al.* 2000, Hunter *et al.* 2001, 2002, Edwards *et al.* 2013), and with measurements *ex vivo* of mitochondrial numbers, mitochondrial enzyme and respiratory chain components (Meyer 1989, McCully *et al.* 1993, Conley *et al.* 2000b, Larson-Meyer *et al.* 2001, Hunter *et al.* 2002, Praet *et al.* 2006, Bajpeyi *et al.* 2011, Lanza *et al.* 2011, Johannsen *et al.* 2012).

Manipulations of inspired O_2. Here, correlations would only be expected, if at all, with whole-body (or whole-limb) measures: in trained subjects, hypoxia decreases, and hyperoxia increases, MMMF (Haseler *et al.* 1999) as it does limb V_{O2max} (Richardson *et al.* 1999); by contrast, in sedentary subjects, although hypoxia decreases MMMF, hyperoxia does not increase MMMF, indicating that O_2 supply is not limiting in normal untrained muscle (Haseler *et al.* 2004). These experiments have not enabled a quantitative evaluation of the contribution of cellular PO_2 to Eqn 20 above, although the observation of a relationship between PCr recovery kinetics and mean $[O_2]_{cytosol}$ measured by ^{1}H MRS of deoxymyoglobin (Haseler *et al.* 1999) illustrates how these influences play out.

Published data on patients with abnormalities in MMMF

In studies on patients (Kemp *et al.* 1993b), correlations might be expected with whole-body or *ex vivo* measures, depending on the pathophysiology. In any clinical condition reducing physical activity, detraining effects can contribute to reduced MMMF as well as whole-body fitness measures, making necessary careful selection of activity-matched controls in clinical ^{31}P MRS studies Here, we briefly discuss the findings in some important disease groups.

Primary mitochondrial disease. Magnetic resonance spectroscopy-based measures of mitochondrial function are abnormal as expected in mitochondrial myopathy (Arnold *et al.* 1985, Taylor *et al.* 1994, Argov *et al.* 1996, Taivassalo *et al.* 2001) and Friedreich Ataxia (Nachbauer *et al.* 2013). Abnormalities in complicated migraine (Lodi *et al.* 1997b) probably reflect mitochondrial involvement.

Diseases impairing O_2 delivery. Magnetic resonance spectroscopy-based measures of mitochondrial function are also abnormal in peripheral vascular disease (Kemp *et al.* 1995, 2001a, 2002a, Kemp 2004), where muscle perfusion is reduced, and in congenital heart disease (Adatia *et al.* 1993, Cordina *et al.* 2013), where blood O_2 content is reduced. In these conditions the abnormal PCr recovery kinetics could in principle be modelled in terms of Eqn 20 and the low cell $[O_2]_{cytosol}$ resulting from impaired O_2 delivery; what little evidence there is in peripheral vascular disease suggests that this plays out as a down-scaling of the Q-X relationship resembling that seen in intrinsic mitochondrial disease or defect (Kemp *et al.* 1995, 2001a, 2002a, Kemp 2004), and in experimental hypoxia (Haseler *et al.* 1999). Given a suitable measurement of exercising muscle PO_2 in, say, peripheral vascular disease, where a conventional calculation according to Eqn 9 will reveal a reduced Q_{MAX}, we might in principle measure a reduced $[O_2]_{cytosol}$ and use this to derive a Q_{MAX} 'corrected' for cellular hypoxia

$$Q_{MAX} = g(X_{MAX}, \text{corrected}\,[O_2]_{cytosol}) \quad (23)$$

which could reveal accompanying abnormalities in intrinsic mitochondrial function, or even partly-compensatory supranormal mitochondrial function. Even given relevant PO_2 measurements, however, we lack enough knowledge of the relevant relationships to make this assessment (Kemp 2004).

Type 2 diabetes. The possible role of abnormalities of muscle mitochondrial function and lipid metabolism in the pathophysiology of insulin resistance in general, and Type 2 diabetes specifically, is much-debated: two recent reviews examine the possible mechanisms in detail (Coen & Goodpaster 2012,

 © 2014 Scandinavian Physiological Society. Published by John Wiley & Sons Ltd, doi: 10.1111/apha.12307

Watt & Hoy 2012). In brief, studies using both *in vivo* and *ex vivo* measurements have provided evidence for and against a reduced muscle mitochondrial capacity in Type 2 diabetes. Reduced MMMF have been reported in type 2 diabetic patients, relative to appropriate controls, in some (Scheuermann-Freestone *et al.* 2003, Schrauwen-Hinderling *et al.* 2007, Meex *et al.* 2010, Bajpeyi *et al.* 2011) but not all (De Feyter *et al.* 2008, Trenell *et al.* 2008) studies, and even when group differences are observed correlation with insulin resistance is poor (Bajpeyi *et al.* 2011). Abnormal MMMF are also reported in to accompany insulin resistance in obese adolescent girls (Slattery *et al.* 2014), but not young men of low birthweight (Brons *et al.* 2008). Improvements in MMMF accompany the metabolic improvements induced in Type 2 diabetes by 12 weeks exercise training (Meex *et al.* 2010), but not by 8 weeks of increased daily walking (Trenell *et al.* 2008) or by rosiglitazone therapy (Schrauwen-Hinderling *et al.* 2008). Two rare diseases characterized by insulin resistance, primary congenital insulin resistance (Sleigh *et al.* 2011) and congenital lipodystrophy (Sleigh *et al.* 2012), show abnormal MMMF relative to controls matched for age, gender, BMI and fitness, which must be a consequence or an accompaniment of insulin resistance, since it cannot be its cause in these patients. For present purpose, the important point is that while muscle mitochondrial function assessed by localized ^{31}P MRS studies of post-exercise PCr recovery tests a component of the overall cardiovascular/respiratory/muscle system whose performance is assessed by conventional whole-body fitness testing, these are not identical concepts (Kemp 2004), or are they anywhere near 100% correlated across individuals (Edwards *et al.* 2013). ^{31}P MRS focusses on processes within the muscle.

Other diseases. Abnormal MMMF in chronic cardiac failure (Mancini *et al.* 1989, Adamopoulos *et al.* 1993, Stratton *et al.* 1994, Kemps *et al.* 2010), chronic pulmonary disease (Sala *et al.* 1999), chronic kidney disease (Marrades *et al.* 1996, Kemp *et al.* 2004), thyroid disease (Argov *et al.* 1988, Taylor *et al.* 1992, Khushu *et al.* 2010) and denervation (McCully *et al.* 2011) are likely multifactorial, with impaired O_2 delivery and O_2 diffusion and loss of mitochondria and mitochondrial components perhaps playing a role. Abnormalities in McArdle's disease (De Stefano *et al.* 1996, Kemp *et al.* 2009) presumably reflect impaired glycogenolytic supply of pyruvate for oxidation, illustrating clearly the need for caution in interpreting MMMF.

Computational insights into interactions between pH, ADP and PCr recovery

Relationships between end-exercise pH and metabolite concentrations

There has long been interest in the effect of end-exercise pH (pH_E) on PCr recovery kinetics (Figs 5–7). A low end-exercise pH_E is associated with slowing of PCr recovery, best expressed for present purposes as a decrease in k_{PCr} (Arnold *et al.* 1984, Bendahan *et al.* 1990, Iotti *et al.* 1993, Kemp *et al.* 1994a, Lodi *et al.* 1997a, Roussel *et al.* 2000, van den Broek *et al.* 2007, Layec *et al.* 2013d). This can be explained in terms of the interaction between oxidative ATP synthesis, cellular pH homeostasis and the CK equilibrium (Kemp 2004), without necessarily assuming any direct effects of low pH on mitochondrial function (Kemp *et al.* 1997, Lodi *et al.* 1997b). Whether there are nevertheless such effects is considered below (Figs 6a and 9c).

A technical limitation is that there are no *in vivo* 'pH-clamp' experiments in muscle physiology: we exercise the muscle in various ways and work with the end-exercise states achieved. Another limitation is that effects of pH_E on PCr recovery will depend on the accompanying $[ADP]_E$, that is, on the relationship between pH_E and $[PCr]_E$. This in turn depends on events in the preceding exercise period which are straightforward in principle: integrated over the whole course of exercise, the total glycolytic production of H^+, less H^+ lost from the cell, must equal the (pH-dependent) sum of the H^+ buffered in the cytosol and the H^+ 'consumed' by PCr breakdown (Kemp 2005b, Kemp *et al.* 2006). There are two special cases. In mainly oxidative exercise, the small glycolytic H^+ production roughly balances the consumption of H^+ by PCr breakdown (Eqn 6), pH therefore changes very little and there is negligible H^+ efflux. In ischaemic exercise, there is no H^+ efflux or oxidative ATP synthesis, and so there is a straightforward relationship (Eqns 18, 19) between changes in pH and PCr and the integrated glycolytic ATP production (which is $1.5 \times \Delta$[lactate]) (Kemp 2005b); however, the balance between the changes in pH and [PCr], and consequently [ADP] (by Eq 1), is a function of 'glycolytic setting' (Kemp *et al.* 2001b) in a sense which even given recent advances in computational modelling of glycolysis (Vinnakota *et al.* 2006) is not easy to define. In the more general case where both glycolytic and ATP synthesis are important there are no useful simplifications. In what follows, we simply regard end-exercise state as given.

© 2014 Scandinavian Physiological Society. Published by John Wiley & Sons Ltd, doi: 10.1111/apha.12307

We will elucidate some effects of end-exercise state and changes in mitochondrial function and pH homeostasis using a simple simulation to interpret (Kemp *et al.* 2010) data from ^{31}P MRS quadriceps exercise-recovery experiments which examine these relationships in detail (van den Broek *et al.* 2007). This is not intended to be a detailed computational model, or is it claimed to yield any kind of optimal fit. It will, however, illustrate some important interactions between these aspects of the physiology and their implications for the quantitative interpretation of ^{31}P MRS recovery data.

A simple model of recovery from exercise

The end-exercise/initial-recovery rate of H^+ efflux (E_E), which can be estimated from pH and PCr recovery data (Kemp *et al.* 1994b, 1997) (Eqn 8) lumps together several different processes of ion transport, and its pH-dependence likely reflects a fundamental cellular physiological setting. In van den Broek *et al.* (2007) a relationship was found, across individuals, between the individual pH-sensitivity of H^+ efflux measured as the apparent rate constant $\lambda = -(dE_E/dpH_E)_{mean}$, and the between-experiment slope of τ_{PCr} against end-exercise pH, $(d\tau_{PCr}/dpH_E)_{mean}$, suggesting that intersubject differences in the pH-dependence of τ_{PCr} are related to differences in cellular pH homeostasis. As we shall see, purely verbal argument about these interactions risks circularity. However, a simple modelling approach (with ADP-dependent oxidative PCr resynthesis and pH-dependent H^+ efflux), accounts qualitatively for the main ^{31}P MRS features of post-exercise recovery (Styles *et al.* 1992); for example, ADP recovers faster than PCr because only the initial phase of PCr resynthesis requires a substantial suprabasal oxidative ATP synthesis, the later phase being mainly an adjustment of PCr to the recovering pH (Arnold *et al.* 1984). It will emerge that this model provides a 'systems' perspective which avoids some conceptual problems, and indeed reproduces the experimental findings in some detail.

The simulation assumes ADP-controlled oxidative ATP synthesis driving PCr resynthesis: from Eqns 7 and 11

$$\text{ATP turnover: } d[PCr]/dt + Q_B = Q_{MAX}/\{1 + (Km/[ADP])^n\} \quad (24)$$

PCr resynthesis is accompanied by H^+ generation with a (negative) stoichiometric coefficient γ which depends (Kushmerick 1997, Kemp *et al.* 2006) on the pH-dependent difference in charge [more precisely, in 'bound' H^+ (Vinnakota *et al.* 2009)] between the accumulating PCr and the near-stoichiometrically declining Pi (Eqn 8). Cytosolic pH recovers back to resting values because this H^+ generation is opposed by net H^+ efflux, which we assume for simplicity to be linearly pH-dependent: H^+ efflux rate = λ (pH_R-pH). The resulting pH change is proportional (from Eqn 8) to the difference between these rates:

$$\begin{aligned}\text{pH homeostasis: } dpH/dt &= \{(H^+\text{efflux rate}) \\ &\quad - (H^+\text{ generation by PCr resynthesis})\}/\beta_T \\ &= \{\lambda(pH_R - pH) + \gamma d[PCr]/dt\}/\beta_T\end{aligned} \quad (25)$$

where β_T is the cytosolic buffer capacity (β_T) (Kemp *et al.* 2001b, Kemp 2005b). The simulation proceeds by incremental solution of Eqs 24 and 25. For comparison with the published data, parameters in the simulation follow those in the analysis (van den Broek *et al.* 2007).

Effects of end-exercise pH and H^+ efflux setting

Figure 5(a) compares relationships between $[PCr]_E$ and pH_E in the conditions which will be simulated here and in the data (van den Broek *et al.* 2007) with which the simulation will be compared. Figure 5(b) shows the effect of changing the setting of H^+ efflux. It is known that pH and PCr recovery kinetics correlate across individuals (Chen *et al.* 2001), which seems intuitive: high H^+ efflux causes faster pH recovery; for given [ADP], a higher pH requires a higher [PCr]; this means faster PCr recovery. The difficulty is that [ADP] recovery does not follow a fixed recovery time course to which [PCr] adjusts, and there are interactions outside the posited causal chain. If faster pH recovery speeds PCr recovery, faster PCr resynthesis would require increased mitochondrial drive by [ADP] (which would tend, via CK, to oppose the recovery of [PCr]), and entail increased H^+ generation (tending to oppose pH recovery). In the simulation, increasing λ does indeed accelerate recovery of both pH and PCr (Chen *et al.* 2001, van den Broek *et al.* 2007) with little effect on ADP recovery. The point is that these are all system co-responses, not causes and effects. Simulation shows, as intuition may not, that in the overall system response these countervailing effects are small. The kinetics of the error signal (τ_{ADP}) are therefore stable (Styles *et al.* 1992) against changes in a parameter (λ) not part of the mitochondrial transfer function.

Figure 5(c) shows the effects of changing pH_E in the case which most closely resembles the data (van den Broek *et al.* 2007), where $[ADP]_E$ rises with decreasing pH_E. The reason why decreasing pH_E slows PCr recovery (i.e. raises τPCr) with little effect on τ_{ADP}, is that feedback-signal kinetics are insensitive (Styles *et al.* 1992) to initial-state change not affecting initial d[PCr]/dt, while PCr recovery is slowed by the system properties of the CK equilibrium. Figure 5(d)

 © 2014 Scandinavian Physiological Society. Published by John Wiley & Sons Ltd, doi: 10.1111/apha.12307

summarizes these effects, showing that the pH_E-dependence of PCr recovery is sensitive to efflux setting, while ADP recovery is relatively insensitive. No more is claimed here than that the fit to the data in (van den Broek *et al.* 2007) is reasonably good. Detailed analysis shows that these predicted λ-dependences are fairly robust, being relatively insensitive to alternative assumptions about mitochondrial control (e.g. assuming NET-regulation rather than the ADP-model used here) or about the pH-dependence of H^+ efflux [e.g. assuming a degree of non-linearity or time dependence (Kemp *et al.* 1997)]. The predicted λ-dependences are also relatively independent of potential correlations between the model parameters; for example, in a subject with a higher proportion of glycolytic fibres, one might see higher λ in correlation with a less-acid pH_E [for which there is some evidence (Kemp *et al.* 1997)], or else with lower Q_{MAX} [which has not been noted (Kemp *et al.* 1997, Lodi *et al.* 1997a), although not much studied]. The range of potential relationships is constrained by realistically observable initial conditions as much as by metabolic constraints operating during recovery itself.

Effects of altered mitochondrial function

In the application of ^{31}P MRS to assess mitochondrial function, much attention has been given to how quantify this, and in particular how to correct for the effects of pH change. The normal-subject data set analysed here allows us to approach this. Figure 6(a) shows how the PCr recovery rate constant varies with pH fall in exercise, making no distinctions between different subjects and different work rates. Figure 6(b) shows that the inferred ADP-model values of Q_{MAX} show a small but significant decrease with end-exercise pH. We present the whole-literature equivalent of this plot later (in Fig. 9c).

Although we have no examples of clinical defect or experimental manipulation of mitochondrial capacity in this data set, the normal variation it contains (visible against the *y*-axis in Fig. 6b) allows us to test the quantitative relationship between some different MMMFs. Figure 6(c,d) shows some simulated effects of altered mitochondrial capacity (Q_{MAX}), comparing this with the variability of Q_{MAX} among the (normal) subjects studied. Figure 6(c) shows the rate constant of PCr ($k_{PCr} = 1/\tau_{PCr}$) (a relative MMMF) as a function of Q_{MAX} (an absolute MMMF, and on this model closer to the underlying physiology). Figure 6(d) shows the same relationship for the apparent rate constant of ADP recovery ($k_{ADP} = 1/\tau_{ADP}$): it is not usual to quantify ADP recovery in this way, but direct comparison with k_{PCr} is instructive. The theoretical lines (calculated for assumptions of 'normal', 'low' and 'high' efflux setting (see key to Fig. 6c) are compared with the data points from the individual subjects. The expected positive slopes are seen, although at low pH_E the Q_{MAX}-slope of k_{PCr} is lower, and that of k_{ADP} is slightly higher than predicted. As expected the efflux setting makes more difference at low pH_E.

The sensitivity of ADP recovery to mitochondrial function makes intuitive sense on the ADP-model. Any impairment of mitochondrial function results in higher [ADP] at any given V_{PCr}, and this must mean that ADP recovery is slowed (Styles *et al.* 1992). The workings of the feedback loop are modified by pH, which defines the [PCr] required for a particular [ADP] (by Eqn 1). Thus, an increase in the H^+ efflux setting, as in mitochondrial myopathy (Taylor *et al.* 1994), ameliorates the slowing of PCr recovery, as PCr adjusts to more rapidly recovering pH, the slightly higher rate of late-phase PCr recovery requiring a slightly higher [ADP] (Styles *et al.* 1993). Moreover, simulation of the effects of changing $[PCr]_E$, pH_E or Q_{MAX} suggest that variation in λ is the only plausible cause of the positive correlation between pH and PCr recovery (Chen *et al.* 2001); so when pH recovery is fast in mitochondrial myopathy (Arnold *et al.* 1985, Taylor *et al.* 1994) the reason must be increased H^+ efflux (Chen *et al.* 2001); conversely a slow PCr recovery could be compatible with normal mitochondrial function if accompanied by slow pH recovery (Chen *et al.* 2001).

In summary, these results support the traditional position: PCr kinetics reflect mitochondrial function, although their pH-dependence can complicate interpretation; ADP recovery kinetics are more robust in this respect, although less often reported (presumably because calculation of [ADP] requires pH data which is often unreliable in early recovery, when [Pi] falls very low).

Possible direct effects of pH on mitochondrial function

There has been some interest in the idea that cytosolic pH has a direct influence on mitochondrial function, independent of the CK equilibrium: in the present terms, this means a pH-dependent Q_{MAX} (Fig. 6b). In *ex vivo* arterially perfused cat soleus, experimental respiratory acidosis both 'left-shifts' and decreases the apparent maximum of the relationship of V_{O2} to both [ADP] and ΔG_{ATP} (Harkema & Meyer 1997). Acid pH also inhibits respiration in isolated skeletal muscle fibres (Walsh *et al.* 2002). The importance of this is difficult to establish *in vivo*, because it is difficult to define, e.g. a Q-[ADP] relationship and then the effect of pH upon it: a series of Q and [ADP] pairs at various pH values might

© 2014 Scandinavian Physiological Society. Published by John Wiley & Sons Ltd, doi: 10.1111/apha.12307

be seen as lying on one Q-[ADP] curve, or on a pH-dependent family of curves.

When we come later to discuss parallel activation, it will be useful to make this kind of argument more abstractly: suppose we have good reason to believe that the feedback system matching ATP supply to demand works via a signal X (Eqn 3), for example, a sigmoid function of [ADP] as in Figure 4(b); our confidence is based on experiments *in vitro* where an experimental rise in X increases Q, other things being equal, and data from a variety of experimental and physiological manipulations in which the relationship holds (in general, we cannot manipulate X directly *in vivo*). If we now find data *in vivo* where $Q \neq f(X)$, for example, because X has increased but Q has decreased relative to some control situation, then we are forced to assume some other factor, outside the X-feedback loop. If the pH is also lower in the new data point, this can reasonably be proposed as a direct effect of cellular acidosis. One such case (Forbes *et al.* 2009a) is calf muscle in (Walter *et al.* 1997), where extending a period of maximal exercise results in a higher [ADP] with a bigger pH fall, and a lower V_{PCr}: with the present assumptions (and in fact with any reasonable assumption about Km and n, since both $[ADP]_E$ values are very high in this study), this lower pH is therefore associated with a decreased Q_{MAX}. Another result cited in support of direct pH effects (Forbes *et al.* 2009a) is in tibialis anterior muscle (Jubrias *et al.* 2003), where 'burst' exercise is associated with a smaller pH fall than sustained exercise, a higher [ADP] and a higher V_{PCr}; on any reasonable assumptions this means a higher Q_{MAX} with the smaller pH change. The same effect is not seen in the parallel studies on first dorsal interosseous muscle in this paper (Jubrias *et al.* 2003), where [ADP] is very high and V_{PCr} very similar in both burst and sustaining exercise.

The data set of (van den Broek *et al.* 2007), interpreted as in Figure 6(b), show evidence of a slight decrease in Q_{MAX} with decreasing pH which is not sensitively dependent on the choice of parameters. (As we will see later in Fig. 9c, this is not apparent across the whole literature, but it may be that subtle effects have gone unnoticed).

The present simulation approach throws some light by considering how pH-dependence of Q_{MAX} might interact with the CK-mediated effect of pH modelled in the foregoing. Simulations (not shown) reveal that, as expected, the greater the assumed (negative) slope of Q_{MAX} against pH (i.e. against pH throughout recovery), the greater τ_{PCr} at significantly subbasal pH_E, and that this effect adds to the τ_{PCr}-lengthening effects of acid pH_E modelled in Figure 5(c). A hypothetically pH-dependent Q_{MAX} has little effect on τ_{ADP} for near-resting pH_E, as one would expect, but actually rather small effects on τ_{ADP} even at larger changes in pH_E. It appears that although an independent pH-dependence of Q_{MAX} cannot be ruled out, it is not necessary to explain the pH-dependence in the dataset of (van den Broek *et al.* 2007). The broader point is that consensus on whether there are direct pH effects of this kind will have to await consensus on the correct mode of analysis (with the clear exceptions noted above).

Other implications for mitochondrial control

We now consider some more general effects of these interactions. The present approach takes V-[ADP] as causally fundamental in the feedback control of Q, yet PCr recovery kinetics depend on the shape of V-PCr (i.e. the relationship between the time-derivative and [PCr], or in this case the relative fall in [PCr]), in which each trajectory implies a PCr kinetics. Figure 7(a) shows relative oxidative ATP synthesis Q/Q_{MAX} (the primary relationship assumed here) as a function of [ADP] under various assumptions of Km and n. Assuming constant near-resting pH (which seems at first sight a reasonable approximation to recovery from near-resting pH_E), Figure 7(b) shows the Q/Q_{MAX} as a function of a function of [Cr], scaled to [TCr]. Figure 7(c) shows the similar plot of Q/Q_{MAX} against ΔG_{ATP}, a striking feature of which is that increases in Km for ADP translate into rightward shifts, while increases in n steepen the plot [given constant pH, the midpoint slope of Q/Q_{MAX} against ΔG_{ATP} is directly proportional to n (Kemp 2009)].

Figure 7(a–c) have in common that they plot a rate against something which may well be causally important in its regulation (Fig. 1). The relationship to [Cr] (Fig. 7b) has an additional significance, because the y-axis is related to the derivative of the x-axis, and thus the x-axis is related to the integral of the y-axis. This means that every trajectory through this space implies a shape of PCr kinetics: if it is linear the kinetics are exponential, with τ_{PCr} inversely proportional to its slope: this is case for Km = 50 μM (case 1). It can be seen that the other cases in Figure 7 (i.e. lower or higher Km values in cases 2 and 3, and the sigmoid relationship in case 4) will not correspond to monoexponential kinetics under the constant-pH assumption. This is a difficulty: we have seen that some cooperativity is essential for a single V-[ADP] relationship to cover the dynamic range, and this leads to a sigmoidal V-[PCr] (Fig. 7b). Yet, monoexponential kinetics are routinely seen unless pH is appreciably more acid than assumed here. Figure 7(d) shows that part of the answer lies in the fact that pH is (of course) not exactly constant, even when there has been little

 © 2014 Scandinavian Physiological Society. Published by John Wiley & Sons Ltd, doi: 10.1111/apha.12307

acidification during exercise. It shows the three pH-grouped end-exercise states and the curves corresponding to their simulated recovery, superimposed on the full-range curve implied by sigmoid ADP-dependent Q at hypothetical constant resting-pH, and for comparison a notional exponential-time-course recovery from full PCr depletion. For the low-pH data set, when the first 50% recovery of [PCr] has occurred, Q is smaller than 50% of its initial value, i.e. what it would be in the linear case; conversely, when Q has recovered to half its initial-recovery value, PCr has not yet recovered by 50%. We therefore expect the PCr halftime, and therefore also τ_{PCr}, to be longer than in the linear case with the same initial Q and $[PCr]_E$. This is, broadly, what we observe. The kinetic simulation, by accounting for small changes in pH that result from transient acidification in early recovery (due to H^+ production by PCr resynthesis) followed by pH recovery (driven by net H^+ efflux) 'flattens out' the trajectory from end-exercise back to the resting state, giving something closer to monoexponential kinetics.

Thus, a simple model of mitochondrial control and H^+ efflux explains much about post-exercise PCr and ADP recovery in relation to pH. It explains why between-individual variations in H^+ efflux dominate variation in τPCr with pH_E (van den Broek *et al.* 2007), but cautions that the slope of this relationship, and the effects on τ_{ADP} will depend on how $[PCr]_E$ (and therefore $[ADP]_E$) varies with pH_E. It also resolves an apparent paradox about the steady-state control relationships of ATP synthesis and the kinetics of PCr recovery. Simple modelling can thus avoid some ambiguities of verbal argument about an interacting system, and provides a bridge to more detailed mechanistic treatments of mitochondrial control (Jeneson *et al.* 2009, Schmitz *et al.* 2011).

Analysis of published data from ^{31}P MRS studies

Given the absence of definitive experiments, the paucity of large experiments able to examine detailed relationships between physiological and structural/biochemical/genetic measurements, and the difficulty of combining MR-based measurements with invasive physiological measurements (to be discussed below in Figs 10–12), much can be learned by collating published data in suitable analytical form; this approach has been applied to MR quantification of absolute concentrations (Kemp *et al.* 2007) and Pi-ATP exchange as a measure of mitochondrial function (Kemp 2008a, Kemp & Brindle 2012). To minimize the effects of minor variations in quantification of resting metabolites etc., a common approach will be used (described in the legend to Fig. 8).

^{31}P MRS studies of quadriceps muscle

Figure 8 shows results from quadriceps, the muscle which is the source of the example data in Figures 2–4, and the most used in the invasive experiments discussed below (in Figs 10–12). The results shown are largely single mean values from the normal-muscle studies cited in the figure legend. Two data sets are picked out (see legend) because they yield several data points at differing [ADP] values: although this was not the authors' original intention, these are particularly useful in showing that Q has a strong tendency to flatten off at high [ADP], as the standard model assumes. An apparent exception is one study (Jeneson & Bruggeman 2004), arrowed in Figure 8, to which we return in Figure 12. With this exception, there is reasonable consistency around the Q-[ADP] line in Figure 8(a) (cf Fig. 4b), and around the Q-ΔG_{ATP} line (not shown). The collected Q-PCr data in Figure 8(b) show the effects of the relationship between the k_{PCr} and pH_E which is shown in Figure 8(d). The relationship between k_{PCr} and the end-exercise fall in [PCr] shown in Figure 8(c) contains the mathematical relationship between those variables and initial V_{PCr}.

Comparison between muscles

Figure 9 shows in addition data obtained from three other muscles much studied by ^{31}P MRS: calf muscle (soleus and/or gastrocnemius), tibialis anterior and finger flexor muscles (usually flexor digitorum superficialis). Figure 9(a) shows the relationship of oxidative ATP synthesis rate to $[ADP]_E$, and Figure 9(b) the relationship of k_{PCr} to ΔpH_E. The collected apparent maximal rates in Figure 9(c) shows no obvious overall direct effect of pH. Directly comparing the apparent maximal rates in Figure 9(d) suggests no overall differences between the four muscles, despite such differences as the generally larger pH change in studies of finger flexors and calf muscle (which can be seen in Fig. 9c). This conclusion is reinforced by Figure 9(e), which summarizes the results of the few published comparisons between muscles in a single study.

The possible influence of the mode of exercise

Figures 8 and 9 do not distinguish between modes of exercise (isometric, shortening and lengthening), mechanical output (force or power), or ramp vs. incremental design, length of exercise, or duty cycle (contraction vs. relaxation in repeated exercise). There are many ways in which these might influence muscle

© 2014 Scandinavian Physiological Society. Published by John Wiley & Sons Ltd, doi: 10.1111/apha.12307

ATP turnover, but they have rarely been systematically studied by ^{31}P MRS. Inspection at least reveals no major effects on the Q-ADP relationship, which is consistent with a simple feedback control model, at least within this dynamic range. It would be premature to take occasional reports of differences between exercise modes (Crowther & Gronka 2002) as firm evidence of altered parallel activation. In this context, a major area of uncertainty is the possible effect of different patterns of muscle fibre recruitment on post-exercise PCr recovery. One case where recruitment patterns are certainly different is direct electrical stimulation. Figure 9 shows separately (grey symbols), data from electrically stimulated muscle. There appears to be a tendency for these to have lower values of Q (Fig. 9a) and Q_{MAX} (Fig. 9c,d) than voluntary exercise studies, which might be expected on the basis that electrical stimulation activates more glycolytic fibres than voluntary exercise. Alternatively, vascular perfusion might be lower. If these possibilities could be excluded one might speculate that the difference reflects reduced parallel activation in the absence of voluntary activation. However, the one reported direct comparison (Vanderthommen *et al.* 2003) shows no such difference.

Taken together, the published data thus give no obvious support to the uses of any particular mode of exercise in the ^{31}P MRS assessment of PCr recovery kinetics.

Directly measured oxygen consumption in exercising quadriceps

Another approach has been the invasive measurement of muscle V_{O2} by AVD methods, most of which has been done in quadriceps. Again, a common approach to the data will be used (Fig. 10).

Published V_{O2} data from in vivo *studies*

Using AVD methods, (Mortensen *et al.* 2008) directly compared one-legged knee extension (KE) and two-legged cycle exercise (CE), and found that V_{O2} (l min^{-1}) as a function of power output is essentially the same in both: the data are redrawn in the inset in Figure 10(a), while the main panel shows also data from many published studies of either KE or CE, in which the same relationship can be seen. Because of the different mass of exercising muscles involved, the relationship between V_{O2} per l muscle and power output is strikingly different (Mortensen *et al.* 2008): Figure 10(b) shows this for estimated oxidative ATP synthesis rate (calculated from V_{O2}), again with direct comparison data from (Mortensen *et al.* 2008) in the inset, and data from a variety of studies in the main panel. Considering only maximal-exercise data points from these studies, the implication is a much higher Q_{MAX} in KE than CE (Fig. 10c): this difference (usually expressed in terms of V_{O2}) is usually explained in terms of 'system' factors such as vascular limitations (Mortensen *et al.* 2008) although detailed mechanisms are not clear. Results for arm CE (see legend to Fig. 10) are rather similar to leg CE.

Extrapolations from ex vivo *data*

Figure 10(d) summarizes data from *ex vivo* studies of isolated mitochondria estimating maximum rates of O_2 consumption or ATP synthesis (here expressed as ATP synthesis), back-calculated as far as possible to the *in vivo* situation. Again, the striking difference between these rates and those obtained in maximal KE is attributed broadly to system factors, sometimes summarized by the idea of 'parallel' activation, although detailed mechanisms are unknown (Tonkonogi & Sahlin 1997, Rasmussen & Rasmussen 2000).

Comparing ^{31}P MRS and AVD data

Model-based extrapolations from AVD data

Comparing extrapolated ^{31}P MRS rates from submaximal exercise (Fig. 4) to actual AVD-derived rates from maximal exercise (Fig. 10c) is probably not valid, because in general the maximally exercising muscle is (as we shall see) not metabolically 'flat out' – maximal exercise does not mean complete PCr depletion. Instead, we should probably extrapolate V_{O2} the same way in the maximal exercise case, to answer for AVD studies the '^{31}P MRS' question: how fast would oxidative ATP synthesis be if the presumed driving signals were at maximal values? It is obvious that this makes assumptions about other aspects of the physiology: notably, that O_2 is not limiting (or rather, not more limiting in the maximal-exercise case than in the submaximal; Kemp *et al.* 2002b, Kemp 2004). These issues may only be resolved when we have a computational framework which can account for the whole system, lung-to-respiratory-chain. Here, in Figure 11, we simply put the two kinds of measurements,^{31}P MRS and AVD, on the same pragmatic footing (Figs 11 and 12).

There are severe technical limitations. There is only one reported study combining ^{31}P MRS measurements of [PCr], pH and [ADP] with parallel AVD measurements of V_{O2} in KE (Richardson *et al.* 2002), but there are a few KE studies combining needle biopsy metabolite measurements with AVD. These are plotted in Figure 11(b,e) together with the one study in which needle biopsy and AVD have

 © 2014 Scandinavian Physiological Society. Published by John Wiley & Sons Ltd, doi: 10.1111/apha.12307

been combined in CE (Stellingwerff *et al.* 2006). Assuming biopsy and ^{31}P MRS report technically comparable fractional changes, there is an even larger discrepancy between the various sets extrapolated values, whether this is done assuming the ADP-model (compare right-hand panels of Fig. 11a and b), the linear model (compare Fig. 11c and e) or the NET-model (not shown). The inset Figure 11(d) compares the Q_{MAX} estimates by the linear model with those of the ADP models: the former are larger except for severe exercise.

To sum up, the comparisons which have been made: in AVD studies, the absolute rates in maximal KE are considerably higher than in maximal CE (Fig. 10c); the rates in AVD maximal CE studies are, as it happens, quite close to the rates extrapolated to *in vivo* conditions from *ex vivo* studies (Fig. 10d), and so the rates in AVD maximum KE studies are much higher than those. The absolute rates in ^{31}P MRS studies (Figs 8a and 11a) are generally similar to those in AVD maximum CE studies (Fig. 10c), but much smaller than in AVD maximum KE studies (Fig. 10c). When the relationships between these rates and the changes in $[ADP]_E$ are compared on the same basis, the implied maximum rates are substantially higher for AVD KE studies (Fig. 11b) than for the ^{31}P MRS studies (Fig. 11a): the one AVD CE study for which biopsy data are available appears to resemble the ^{31}P MRS studies. Note that power output data, for comparison with Figure 10(b), are almost never available in MR experiments, which often use home-built ergometers and/or isometric exercise for which power outputs are not defined. One reason why these common-extrapolated values are so different is that the biopsy results in maximal KE do not show 'maximal' PCr depletion: this is not surprising, as this would bring problems of very high [ADP] (such as inhibition of ATPases), but here we draw attention to the implications for mitochondrial regulation. To a first approximation, what we see is rather similar results (in terms of absolute rates, size of [PCr] and [ADP] changes, and consequently implied maximum rates) between ^{31}P MRS studies (where exercise is usually limited approximately to the quadriceps), and CE (where the exercising muscle volume is the whole of one or two legs, depending on the set-up); both these data sets seem consistent with the *ex vivo* extrapolations. The results in AVD KE studies (where exercise is also limited to the quadriceps, but at a higher intensity than in the ^{31}P MRS experiments) are strikingly different, showing maximal rates which are substantially larger. We discuss some possible reasons for this below (in the section entitled 'Parallel activation revisited').

Possible kinetic implications of the comparison between ^{31}P MRS and AVD data

Even if the theory underpinning the traditional analyses is simplistic, consideration of Figure 11(e) suggests a prediction: if PCr recovery from maximal KE is exponential, its typical rate constant should be equal to the slopes of the notional straight lines connecting the data points to the origin in Figure 11(e); this should, further, be equal to the rate constant of V_{O2} recovery. This notional rate constant for the studies in Figure 11(e) is plotted on the left-hand side of Figure 12(a), and is very much higher than (on the right-hand side) the actual PCr recovery rate constants in the MRS studies analysed in Figure 11(e). This appears never to have been measured in AVD studies after exhaustive KE. AVD V_{O2} recovery kinetics appear only to have been measured once in high-intensity exercise (Krustrup *et al.* 2003), with the result shown (Fig. 12a: see key and legend). With appropriate caveats, whole-body V_{O2} should have similar recovery kinetics to PCr: this has been directly demonstrated for moderate- and high-intensity exercise (Rossiter *et al.* 2002b) in a study whose ^{31}P MRS data are analysed and presented in Figure 8, and as a pair of linked points in Figure 12(c). In published reports of whole-body V_{O2} off-kinetics k was 1.7–1.9 min^{-1} after high-intensity cycle exercise (Paterson & Whipp 1991, Cunningham *et al.* 2000) and 1.5 min^{-1} after high-intensity treadmill exercise, values much lower than Figure 12(a) predicts.

Figure 12(b) returns to the pH-dependence of recovery rate constants, which we have seen is readily explained if the primary relationship is between oxidative ATP synthesis rate and [ADP], as shown by the modelled lines in Figure 12(b): the ^{31}P MRS data show the effect clearly, and the AVD/biopsy data are not inconsistent with it, although the scatter is large. This all merits further investigation.

Figure 12(c) offers at least a suggestion that the value of Q_{MAX} that emerges from analysis of Q-[ADP] in exercise may be independently related to mechanical power output. Most of the MRS studies with reported power data cluster in the lower left-hand (low-power/low-Q_{MAX}) corner, the two exceptions being the only maximal-KE AVD and ^{31}P MRS study (Richardson *et al.* 2002) and the unusually high-power two-leg exercise ^{31}P MRS study (Jeneson & Bruggeman 2004) (arrowed here and in Figs 8 and 9); what looks like an anomalously high rate of ATP synthesis in Figures 8(a) and 9(a) seems less anomalous in Figure 12(c), compared to our calculation based on AVD-biopsy data from high-power exercise studies. Further studies to examine this point would

© 2014 Scandinavian Physiological Society. Published by John Wiley & Sons Ltd, doi: 10.1111/apha.12307

throw an interesting light on metabolic regulation in exercising skeletal muscle.

Parallel activation revisited

One possible explanation of the discrepancy noted in Figure 11 and related to power output in Figure 12(c) is the general category of parallel activation (Korzeniewski 1998), the postulated direct activation mechanism, standing outside closed-loop feedback control, shown schematically in Figure 1. As with the early discussion of possible direct pH effects, it is useful to consider more abstractly what might count as evidence of parallel activation. Again, assume we have reason to expect a (closed-loop feedback) relationship (Eqn 3) based on *in vivo* evidence of correlation, *ex vivo* evidence of direct effects, and perhaps also computational confirmation: this is, broadly, what we have for signals like [ADP] [perhaps taking account of specific effects of Pi (Schmitz *et al.* 2012, Wu *et al.* 2007), at least part of which may be captured by its incorporation into ΔG_{ATP} (Schmitz *et al.* 2012)]. Unless we are specifically interested in effects of pH (which are, if anything, negative), then we have putative evidence of parallel activation (in some form) whenever $Q \neq f(X)$. For example, what view we take of what one might call the 'dynamic range problem', i.e. the inability of hyperbolic Q-[ADP] relationships to encompass resting [ADP], depends on whether we accept that that relationship can be intrinsically sigmoid: in this review we have followed (Jeneson *et al.* 1996) in this, reinforced by the recent computational evidence (Jeneson *et al.* 2009), particularly when Pi is taken into account. If this is not accepted, then the basal data point is just such a $Q \neq f(X)$ anomaly: for resting [ADP] of ~14 μM (Kemp *et al.* 2007) and assuming the measured true resting rate (admittedly slightly method-dependent) of ~0.5 mM min^{-1} (Kemp & Brindle 2012) then for a Km value of ~50 μM (the value that gives near-linear relationship to PCr change (Kemp 1994)) the implied Q_{MAX} is ~2 mM min^{-1}, vastly too low to explain observed PCr recovery kinetics. Whether in this case our position would best be described as ignorance of some kind of parallel activation is debateable.

A more decisive case is when the same X occurs with very different Q: this may be the difference between KE and typical MR scanner exercise (Figs 11 and 12c), although as we have seen, directly comparable data are very scarce. At the very least this tells us that our understanding is incomplete, and that really Q is some more complicated function of other factors, say $Q = g(X,Y,Z\ldots)$. Whether these unknown factors amount to parallel activation depends on their relation to the contraction signal (Fig. 1) – this is a high-level functional description with considerable explanatory power. It does not of course necessarily mean that we can identify a family of $Q = f(X)$ curves scaled by some factor depending on ATP demand, although this is a useful way of conceptualizing it [Model 4 in (Wust *et al.* 2011)].

Other evidence is suggestive, but more indirect and implying more complicated mechanisms. For example, the observation in single Xenopus fibres that V_{O2} kinetics are biphasic at contraction onset, although monoexponential after cessation (i.e. during recovery, as defined here; Wust *et al.* 2013) certainly suggests things are more complicated than the simplest models assume. So too is the recent report that endurance training can accelerate V_{O2} on-kinetics before any change in muscle mitochondrial biogenesis or capillary density (Zoladz *et al.* 2013). Similarly, the occurrence of 'overshoot' in PCr (Kushmerick *et al.* 1992, Christ *et al.* 2001) recovery and undershoot in ADP recovery [(Arnold *et al.* 1984, Argov *et al.* 1996) defies simple explanation on any feedback-based model, but can be explained, at least in principle, in terms of the post-exercise decay kinetics of parallel activation (Korzeniewski & Zoladz 2005).

If parallel activation is active in exercise, PCr kinetics could be dominated by its intrinsic off-kinetics, slow once it settled back to the resting-state value (Kemp 2011) but potentially very fast as it is switching off (Korzeniewski & Zoladz 2013). We would not expect the 'track' in Q-ADP space (for example) of the recovering muscle to be the same as that achieved at the end of exercise; it is approximately so in Figure 4, but detailed studies remain to be done.

Another casualty of parallel activation is the assumption that the end-of exercise rate of oxidative ATP synthesis and the immediately-following initial-recovery rate are the same; in the extreme case where parallel activation switched off instantaneously the end-exercise (subscript E) and initial recovery (subscript I) rates might be two different functions of the same end-exercise state, say $Q_E = f_E(X_E)$ and $Q_I = f_I(X_I) = f_I(X_E)$ (Korzeniewski & Zoladz 2013). There is no clear evidence that this can be so, but this is perhaps not saying much.

And yet, as we have seen, MRS-based measures of 'mitochondrial capacity' correlate well with other measures like whole-body V_{O2max} and muscle mitochondrial content, as one would expect given the nature of the system; this is not what one would expect if responses to exercise were dominated by parallel activation phenomena that do not themselves correlate closely with 'fixed' factors like mitochondrial content.

 © 2014 Scandinavian Physiological Society. Published by John Wiley & Sons Ltd, doi: 10.1111/apha.12307

Conclusions

The relation between V_{O2} (or oxidative ATP synthesis rate) and feedback 'signals' such as [ADP] is well known for typical ^{31}P MRS experiments and deducible for some published maximum knee extension experiments; it is very different in these two situations, in that rates are much higher in KE, and (as has already been noted (Rasmussen *et al.* 2003, Rasmussen & Rasmussen 2000, Tonkonogi & Sahlin 1997)), higher than can be explained on the basis of mitochondrial properties *in vitro*. Maximum CE, despite using more muscle then either KE or ^{31}P MRS experiments (and therefore being more sensitive to cardiopulmonary limitation), seems to resemble the ^{31}P MRS case, although data on metabolite changes in CE are very rare. The relationship of oxidative ATP synthesis to PCr change in maximal KE implies very rapid recovery kinetics; an experiment in which AVD V_{O2} data were collected with high time-resolution during recovery from maximal KE would be an interesting test of the analytical approach, standard in ^{31}P MRS experiments, applied here to KE data.

There is no doubt that MMMF derived from ^{31}P MRS post-exercise recovery data offer a robust, non-invasive way to detect impaired mitochondrial function and to monitor changes in mitochondrial function *in vivo*. In a large range of experiments and four muscles, ^{31}P MRS data are fairly consistent, and there is ample evidence that MMMF derived from them correlate as expected with other measures of mitochondrial properties and function and other aspects of aerobic physiology. The ADP-model approach to interpreting these data seem to agree roughly on the implied maximum rates of oxidative ATP synthesis with CE experiments. An approach based on extrapolating linearly to complete PCr depletion gives much higher values, and is contradicted by what actually happens to PCr recovery when exercise is intense enough for appreciable pH changes. In contrast, the 'ADP-control model' approach (or similar) can explain these effects at least semi-quantitatively (but leaving open, currently, the possibility of direct effects of pH on mitochondrial ATP synthesis). Simulation (Fig. 5) suggests that the recovery kinetics of [ADP] are indeed (Kemp *et al.* 1997) relatively independent of pH, but supports the traditional advice to avoid large changes in pH when using PCr kinetics to assess mitochondrial function.

One kind of explanation for the quantitative differences identified between KE and ^{31}P MRS experiments is parallel activation, i.e. activating ATP synthesis directly, independently of the feedback loop and its signal(s). Data are so far lacking to test this. We have suggested that V_{O2} recovery kinetics at these very high powers (i.e. extending the AVD collection into recovery) would be interesting. So would studies of true maximal knee extension in an MR scanner (to see whether PCr recovery is as fast as KE AVD measurements imply): but there are formidable practical obstacles. Also interesting would be biopsy measurements (as ^{31}P MRS would be very difficult) of PCr kinetics during maximal CE, and kinetics of AVD V_{O2} recovery: are these (like ^{31}P typical MRS data) consistent with a simple model without recourse to parallel activation? This would focus on exercise intensity (ATP turnover) itself as the relevant difference. Taking another approach, computational models which have been found to fit some MR data reasonably well (Wu *et al.* 2007, Jeneson *et al.* 2009, Schmitz *et al.* 2012) will clearly need adjustment for maximum KE, but how? Recent work suggests that calcium stimulation at a number of steps can upregulate oxidative ATP synthesis (Glancy & Balaban 2012), but the key question for computational modelling is how much, and in what relation to ATP turnover (and other possible signals possible not directly related to ATP turnover).

Conflict of interest

The authors declare that they have no conflicts of interest.

Financial support for the experiments described in Figs 2–4 was kindly provided by the Government of Malaysia as a PhD studentship to REA. GJK's work in this area has been supported by the Biotechnology and Biological Sciences Research Council UK (BB/I001174/1) and by the Medical Research Council UK and Arthritis Research UK (MR/K006312/1) as part of the MRC – Arthritis Research UK Centre for Integrated Research into Musculoskeletal Ageing (CIMA). JJP is supported by a VIDI grant from the Netherlands Organisation for Scientific Research (VIDI 700.58.421) and by the Netherlands Consortium for Systems Biology (NCSB), which is part of the Netherlands Genomics Initiative / Netherlands Organisation for Scientific Research. GJK is grateful to HB Rossiter (University of Leeds and University of California, Los Angeles) and J Fulford (University of Exeter) for some valuable discussions.

References

Adamopoulos, S., Coats, A.J., Brunotte, F., Arnolda, L., Meyer, T., Thompson, C.H., Dunn, J.F., Stratton, J., Kemp, G.J., Radda, G.K. *et al.* 1993. Physical training improves skeletal muscle metabolism in patients with chronic heart failure. *J Am Coll Cardiol* **21**, 1101–1106.

Adatia, I., Kemp, G.J., Taylor, D.J., Radda, G.K., Rajagopalan, B. & Haworth, S.G. 1993. Abnormalities in skeletal muscle metabolism in cyanotic patients with congenital heart disease: a ^{31}P nuclear magnetic resonance spectroscopy study. *Clin Sci (Lond)* **85**, 105–109.

Ahlborg, G. & Jensen-Urstad, M. 1991a. Arm blood flow at rest and during arm exercise. *J Appl Physiol* **70**, 928–933.

Ahlborg, G. & Jensen-Urstad, M. 1991b. Metabolism in exercising arm vs. leg muscle. *Clin Physiol* **11**, 459–468.

Ahmad, R.E. 2010. Magnetic resonance studies of skeletal muscle mitochondrial function *in vivo*: physiological implications of metabolic and oxygenation analysis in health and diseased states (PhD Thesis). Musculoskeletal Biology. University of Liverpool.

Ahmad, R., Bimson, W. & Kemp, G. 2010. Estimates of mitochondrial capacity derived from phosphocreatine recovery kinetics in human calf and thigh muscle differ systematically from published measurements using invasive methods.) Joint Ann Meeting, Int Soc Magn Reson Med and Eur Soc Magn Reson Med Biol. Stockholm, Sweden.

Amann, M., Runnels, S., Morgan, D.E., Trinity, J.D., Fjeldstad, A.S., Wray, D.W., Reese, V.R. & Richardson, R.S. 2011. On the contribution of group III and IV muscle afferents to the circulatory response to rhythmic exercise in humans. *J Physiol* **589**, 3855–3866.

Andersen, P. & Saltin, B. 1985. Maximal perfusion of skeletal muscle in man. *J Physiol* **366**, 233–249.

Andersen, P., Adams, R.P., Sjogaard, G., Thorboe, A. & Saltin, B. 1985. Dynamic knee extension as model for study of isolated exercising muscle in humans. *J Appl Physiol* **59**, 1647–1653.

Argov, Z., Renshaw, P.F., Boden, B., Winokur, A. & Bank, W.J. 1988. Effects of thyroid hormones on skeletal muscle bioenergetics. *In vivo* phosphorus-31 magnetic resonance spectroscopy study of humans and rats. *J Clin Invest* **81**, 1695–1701.

Argov, Z., De Stefano, N. & Arnold, D.L. 1996. ADP recovery after a brief ischemic exercise in normal and diseased human muscle – a ^{31}P MRS study. *NMR Biomed* **9**, 165–172.

Arnold, D.L., Matthews, P.M. & Radda, G.K. 1984. Metabolic recovery after exercise and the assessment of mitochondrial function *in vivo* in human skeletal muscle by means of P-31 NMR. *Magn Reson Med* **1**, 307–315.

Arnold, D.L., Taylor, D.J. & Radda, G.K. 1985. Investigations of human mitochondrial myopathies by phosphorus magnetic resonance spectroscopy. *Ann Neurol* **18**, 189–196.

Bajpeyi, S., Pasarica, M., Moro, C., Conley, K., Jubrias, S., Sereda, O., Burk, D.H., Zhang, Z., Gupta, A., Kjems, L. & Smith, S.R. 2011. Skeletal muscle mitochondrial capacity and insulin resistance in type 2 diabetes. *J Clin Endocrinol Metab* **96**, 1160–1168.

Bangsbo, J., Gollnick, P.D., Graham, T.E., Juel, C., Kiens, B., Mizuno, M. & Saltin, B. 1990. Anaerobic energy production and O_2 deficit-debt relationship during exhaustive exercise in humans. *J Physiol* **422**, 539–559.

Bangsbo, J., Graham, T., Johansen, L., Strange, S., Christensen, C. & Saltin, B. 1992a. Elevated muscle acidity and energy production during exhaustive exercise in humans. *Am J Physiol* **263**, R891–R899.

Bangsbo, J., Graham, T.E., Kiens, B. & Saltin, B. 1992b. Elevated muscle glycogen and anaerobic energy production during exhaustive exercise in man. *J Physiol* **451**, 205–227.

Bangsbo, J., Johansen, L., Graham, T. & Saltin, B. 1993. Lactate and H^+ effluxes from human skeletal muscles during intense, dynamic exercise. *J Physiol* **462**, 115–133.

Bangsbo, J., Krustrup, P., Gonzalez-Alonso, J. & Saltin, B. 2001. ATP production and efficiency of human skeletal muscle during intense exercise: effect of previous exercise. *Am J Physiol Endocrinol Metab* **280**, E956–E964.

Bangsbo, J., Gibala, M.J., Krustrup, P., Gonzalez-Alonso, J. & Saltin, B. 2002. Enhanced pyruvate dehydrogenase activity does not affect muscle O_2 uptake at onset of intense exercise in humans. *Am J Physiol Regul Integr Comp Physiol* **282**, R273–R280.

Barker, A.R., Welsman, J.R., Fulford, J., Welford, D. & Armstrong, N. 2008. Muscle phosphocreatine kinetics in children and adults at the onset and offset of moderate-intensity exercise. *J Appl Physiol* **105**, 446–456.

Barnes, P.R., Kemp, G.J., Taylor, D.J. & Radda, G.K. 1997. Skeletal muscle metabolism in myotonic dystrophy A ^{31}P magnetic resonance spectroscopy study. *Brain* **120**, 1699–1711.

Barrett-O'Keefe, Z., Helgerud, J., Wagner, P.D. & Richardson, R.S. 2012. Maximal strength training and increased work efficiency: contribution from the trained muscle bed. *J Appl Physiol* **113**, 1846–1851.

Befroy, D.E., Petersen, K.F., Dufour, S., Mason, G.F., de Graaf, R.A., Rothman, D.L. & Shulman, G.I. 2007. Impaired mitochondrial substrate oxidation in muscle of insulin-resistant offspring of type 2 diabetic patients. *Diabetes* **56**, 1376–1381.

Befroy, D.E., Petersen, K.F., Dufour, S., Mason, G.F., Rothman, D.L. & Shulman, G.I. 2008. Increased substrate oxidation and mitochondrial uncoupling in skeletal muscle of endurance-trained individuals. *Proc Natl Acad Sci USA* **105**, 16701–16706.

Befroy, D.E., Falk Petersen, K., Rothman, D.L. & Shulman, G.I. 2009. Assessment of *in vivo* mitochondrial metabolism by magnetic resonance spectroscopy. *Methods Enzymol* **457**, 373–393.

Bendahan, D., Confort-Gouny, S., Kozak-Reiss, G. & Cozzone, P.J. 1990. Heterogeneity of metabolic response to muscular exercise in humans. New criteria of invariance defined by in vivo phosphorus-31 NMR spectroscopy. *FEBS Lett* **272**, 155–158.

Bendahan, D., Kemp, G.J., Roussel, M., Fur, Y.L. & Cozzone, P.J. 2003. ATP synthesis and proton handling in muscle during short periods of exercise and subsequent recovery. *J Appl Physiol* **94**, 2391–2397.

Bender, P.R., Groves, B.M., McCullough, R.E., McCullough, R.G., Huang, S.Y., Hamilton, A.J., Wagner, P.D., Cymerman, A. & Reeves, J.T. 1988. Oxygen transport to exercising leg in chronic hypoxia. *J Appl Physiol* **65**, 2592–2597.

Blei, M.L., Conley, K.E. & Kushmerick, M.J. 1993. Separate measures of ATP utilization and recovery in human skeletal muscle. *J Physiol* **465**, 203–222.

Blomstrand, E., Radegran, G. & Saltin, B. 1997. Maximum rate of oxygen uptake by human skeletal muscle in relation

 © 2014 Scandinavian Physiological Society. Published by John Wiley & Sons Ltd, doi: 10.1111/apha.12307

to maximal activities of enzymes in the Krebs cycle. *J Physiol* **501**, 455–460.

Boska, M. 1994. ATP production rates as a function of force level in the human gastrocnemius/soleus using ^{31}P MRS. *Magn Reson Med* **32**, 1–10.

Boushel, R., Gnaiger, E., Calbet, J.A., Gonzalez-Alonso, J., Wright-Paradis, C., Sondergaard, H., Ara, I., Helge, J.W. & Saltin, B. 2011. Muscle mitochondrial capacity exceeds maximal oxygen delivery in humans. *Mitochondrion* **11**, 303–307.

Brand, M.D. 2005. The efficiency and plasticity of mitochondrial energy transduction. *Biochem Soc Trans* **33**, 897–904.

Brindle, K.M., Blackledge, M.J., Challiss, R.A. & Radda, G.K. 1989. ^{31}P NMR magnetization-transfer measurements of ATP turnover during steady-state isometric muscle contraction in the rat hind limb *in vivo*. *Biochemistry* **28**, 4887–4893.

Brizendine, J.T., Ryan, T.E., Larson, R.D. & McCully, K.K. 2013. Skeletal muscle metabolism in endurance athletes with near-infrared spectroscopy. *Med Sci Sports Exerc* **45**, 869–875.

van den Broek, N.M., De Feyter, H.M., de Graaf, L., Nicolay, K. & Prompers, J.J. 2007. Intersubject differences in the effect of acidosis on phosphocreatine recovery kinetics in muscle after exercise are due to differences in proton efflux rates. *Am J Physiol Cell Physiol* **293**, C228–C237.

van den Broek, N.M., Ciapaite, J., Nicolay, K. & Prompers, J.J. 2010. Comparison of *in vivo* postexercise phosphocreatine recovery and resting ATP synthesis flux for the assessment of skeletal muscle mitochondrial function. *Am J Physiol Cell Physiol* **299**, C1136–C1143.

Brons, C., Jensen, C.B., Storgaard, H., Alibegovic, A., Jacobsen, S., Nilsson, E., Astrup, A., Quistorff, B. & Vaag, A. 2008. Mitochondrial function in skeletal muscle is normal and unrelated to insulin action in young men born with low birth weight. *J Clin Endocrinol Metab* **93**, 3885–3892.

Cannon, D.T., Howe, F.A., Whipp, B.J., Ward, S.A., McIntyre, D.J., Ladroue, C., Griffiths, J.R., Kemp, G.J. & Rossiter, H.B. 2013. Muscle metabolism and activation heterogeneity by combined ^{31}P chemical shift and T_2 imaging, and pulmonary O_2 uptake during incremental knee-extensor exercise. *J Appl Physiol* **115**, 839–849.

Carlier, P.G., Bertoldi, D., Baligand, C., Wary, C. & Fromes, Y. 2006. Muscle blood flow and oxygenation measured by NMR imaging and spectroscopy. *NMR Biomed* **19**, 954–967.

Chance, B. & Williams, G.R. 1955. Respiratory enzymes in oxidative phosphorylation. III. The steady state. *J Biol Chem* **217**, 409–427.

Chance, B., Leigh, J.S. Jr, Clark, B.J., Maris, J., Kent, J., Nioka, S. & Smith, D. 1985. Control of oxidative metabolism and oxygen delivery in human skeletal muscle: a steady-state analysis of the work/energy cost transfer function. *Proc Natl Acad Sci USA* **82**, 8384–8388.

Chen, J.T., Taivassalo, T., Argov, Z. & Arnold, D.L. 2001. Modeling *in vivo* recovery of intracellular pH in muscle to provide a novel index of proton handling: application to the diagnosis of mitochondrial myopathy. *Magn Reson Med* **46**, 870–878.

Chidnok, W., Fulford, J., Bailey, S.J., Dimenna, F.J., Skiba, P.F., Vanhatalo, A. & Jones, A.M. 2013. Muscle metabolic determinants of exercise tolerance following exhaustion: relationship to the "critical power". *J Appl Physiol* **115**, 243–250.

Christ, M., Zange, J., Janson, C.P., Muller, K., Kuklinski, P., Schmidt, B.M., Tillmann, H.C., Gerzer, R. & Wehling, M. 2001. Hypoxia modulates rapid effects of aldosterone on oxidative metabolism in human calf muscle. *J Endocrinol Invest* **24**, 587–597.

Cieslar, J.H. & Dobson, G.P. 2000. Free [ADP] and aerobic muscle work follow at least second order kinetics in rat gastrocnemius in vivo. *J Biol Chem* **275**, 6129–6134.

Cloutier, M. & Wellstead, P. 2010. The control systems structures of energy metabolism. *J R Soc Interface* **7**, 651–665.

Coen, P.M. & Goodpaster, B.H. 2012. Role of intramyocelluar lipids in human health. *Trends Endocrinol Metab* **23**, 391–398.

Combs, C.A., Aletras, A.H. & Balaban, R.S. 1999. Effect of muscle action and metabolic strain on oxidative metabolic responses in human skeletal muscle. *J Appl Physiol* **87**, 1768–1775.

Conley, K.E., Esselman, P.C., Jubrias, S.A., Cress, M.E., Inglin, B., Mogadam, C. & Schoene, R.B. 2000a. Ageing, muscle properties and maximal O_2 uptake rate in humans. *J Physiol* **526**, 211–217.

Conley, K.E., Jubrias, S.A. & Esselman, P.C. 2000b. Oxidative capacity and ageing in human muscle. *J Physiol* **526**, 203–210.

Connett, R.J. 1988. Analysis of metabolic control: new insights using scaled creatine kinase model. *Am J Physiol* **254**, R949–R959.

Cooke, S.R., Petersen, S.R. & Quinney, H.A. 1997. The influence of maximal aerobic power on recovery of skeletal muscle following anaerobic exercise. *Eur J Appl Physiol Occup Physiol* **75**, 512–519.

Cordina, R.L., O'Meagher, S., Karmali, A., Rae, C.L., Liess, C., Kemp, G.J., Puranik, R., Singh, N. & Celermajer, D.S. 2013. Resistance training improves cardiac output, exercise capacity and tolerance to positive airway pressure in Fontan physiology. *Int J Cardiol* **168**, 780–788.

Crowther, G.J. & Gronka, R.K. 2002. Fiber recruitment affects oxidative recovery measurements of human muscle *in vivo*. *Med Sci Sports Exerc* **34**, 1733–1737.

Crowther, G.J., Kemper, W.F., Carey, M.F. & Conley, K.E. 2002. Control of glycolysis in contracting skeletal muscle. II. Turning it off. *Am J Physiol Endocrinol Metab* **282**, E74–E79.

Crowther, G.J., Milstein, J.M., Jubrias, S.A., Kushmerick, M.J., Gronka, R.K. & Conley, K.E. 2003. Altered energetic properties in skeletal muscle of men with well-controlled insulin-dependent (type 1) diabetes. *Am J Physiol Endocrinol Metab* **284**, E655–E662.

Cunningham, D.A., Croix, C.M., Paterson, D.H., Ozyener, F. & Whipp, B.J. 2000. The off-transient pulmonary oxy-

© 2014 Scandinavian Physiological Society. Published by John Wiley & Sons Ltd, doi: 10.1111/apha.12307

gen uptake (VO_2) kinetics following attainment of a particular VO_2 during heavy-intensity exercise in humans. *Exp Physiol* **85**, 339–347.

Dawson, M.J., Gadian, D.G. & Wilkie, D.R. 1980. Studies of the biochemistry of contracting and relaxing muscle by the use of ^{31}P n.m.r. in conjunction with other techniques. *Philos Trans R Soc Lond B Biol Sci* **289**, 445–455.

De Feyter, H.M., van den Broek, N.M., Praet, S.F., Nicolay, K., van Loon, L.J. & Prompers, J.J. 2008. Early or advanced stage type 2 diabetes is not accompanied by *in vivo* skeletal muscle mitochondrial dysfunction. *Eur J Endocrinol* **158**, 643–653.

De Stefano, N., Argov, Z., Matthews, P.M., Karpati, G. & Arnold, D.L. 1996. Impairment of muscle mitochondrial oxidative metabolism in McArdles's disease. *Muscle Nerve* **19**, 764–769.

Dudley, C.R., Taylor, D.J., Ng, L.L., Kemp, G.J., Ratcliffe, P.J., Radda, G.K. & Ledingham, J.G. 1990. Evidence for abnormal Na^+/H^+ antiport activity detected by phosphorus nuclear magnetic resonance spectroscopy in exercising skeletal muscle of patients with essential hypertension. *Clin Sci (Lond)* **79**, 491–497.

Duteil, S., Bourrilhon, C., Raynaud, J.S., Wary, C., Richardson, R.S., Leroy-Willig, A., Jouanin, J.C., Guezennec, C.Y. & Carlier, P.G. 2004. Metabolic and vascular support for the role of myoglobin in humans: a multiparametric NMR study. *Am J Physiol Regul Integr Comp Physiol* **287**, R1441–R1449.

Edwards, L.M., Tyler, D.J., Kemp, G.J., Dwyer, R.M., Johnson, A., Holloway, C.J., Nevill, A.M. & Clarke, K. 2012. The reproducibility of 31-phosphorus MRS measures of muscle energetics at 3 Tesla in trained men. *PLoS ONE* **7**, e37237.

Edwards, L.M., Kemp, G.J., Dwyer, R.M., Walls, J.T., Fuller, H., Smith, S.R. & Earnest, C.P. 2013. Integrating muscle cell biochemistry and whole-body physiology in humans: ^{31}P-MRS data from the InSight trial. *Sci Rep*, **3**, 1182 (pp 7).

Esposito, F., Reese, V., Shabetai, R., Wagner, P.D. & Richardson, R.S. 2011. Isolated quadriceps training increases maximal exercise capacity in chronic heart failure: the role of skeletal muscle convective and diffusive oxygen transport. *J Am Coll Cardiol* **58**, 1353–1362.

Ferguson, R.A., Ball, D., Krustrup, P., Aagaard, P., Kjaer, M., Sargeant, A.J., Hellsten, Y. & Bangsbo, J. 2001. Muscle oxygen uptake and energy turnover during dynamic exercise at different contraction frequencies in humans. *J Physiol* **536**, 261–271.

Forbes, S.C., Kowalchuk, J.M., Thompson, R.T. & Marsh, G.D. 2007. Effects of hyperventilation on phosphocreatine kinetics and muscle deoxygenation during moderate-intensity plantar flexion exercise. *J Appl Physiol* **102**, 1565–1573.

Forbes, S.C., Slade, J.M. & Meyer, R.A. 2008. Short-term high-intensity interval training improves phosphocreatine recovery kinetics following moderate-intensity exercise in humans. *Appl Physiol Nutr Metab* **33**, 1124–1131.

Forbes, S.C., Paganini, A.T., Slade, J.M., Towse, T.F. & Meyer, R.A. 2009a. Phosphocreatine recovery kinetics following low- and high-intensity exercise in human triceps surae and rat posterior hindlimb muscles. *Am J Physiol Regul Integr Comp Physiol* **296**, R161–R170.

Forbes, S.C., Slade, J.M., Francis, R.M. & Meyer, R.A. 2009b. Comparison of oxidative capacity among leg muscles in humans using gated ^{31}P 2-D chemical shift imaging. *NMR Biomed* **22**, 1063–1071.

Funk, C.I., Clark, A. Jr & Connett, R.J. 1990. A simple model of aerobic metabolism: applications to work transitions in muscle. *Am J Physiol* **258**, C995–C1005.

Gam, C.M., Nielsen, H.B., Secher, N.H., Larsen, F.S., Ott, P. & Quistorff, B. 2011. In cirrhotic patients reduced muscle strength is unrelated to muscle capacity for ATP turnover suggesting a central limitation. *Clin Physiol Funct Imaging* **31**, 169–174.

Gibala, M.J., MacLean, D.A., Graham, T.E. & Saltin, B. 1998. Tricarboxylic acid cycle intermediate pool size and estimated cycle flux in human muscle during exercise. *Am J Physiol* **275**, E235–E242.

Glancy, B. & Balaban, R.S. 2012. Role of mitochondrial Ca^{2+} in the regulation of cellular energetics. *Biochemistry* **51**, 2959–2973.

Glancy, B., Barstow, T. & Willis, W.T. 2008. Linear relation between time constant of oxygen uptake kinetics, total creatine, and mitochondrial content *in vitro*. *Am J Physiol Cell Physiol* **294**, C79–C87.

Greiner, A., Esterhammer, R., Bammer, D., Messner, H., Kremser, C., Jaschke, W.R., Fraedrich, G. & Schocke, M.F. 2007. High-energy phosphate metabolism in the calf muscle of healthy humans during incremental calf exercise with and without moderate cuff stenosis. *Eur J Appl Physiol* **99**, 519–531.

Gussoni, M., Cremonini, M.A., Vezzoli, A., Greco, F. & Zetta, L. 2010. A quantitative method to assess muscle tissue oxygenation in vivo by monitoring ^{1}H nuclear magnetic resonance myoglobin resonances. *Anal Biochem* **400**, 33–45.

Hamaoka, T., McCully, K.K., Quaresima, V., Yamamoto, K. & Chance, B. 2007. Near-infrared spectroscopy/imaging for monitoring muscle oxygenation and oxidative metabolism in healthy and diseased humans. *J Biomed Opt*, **12**, 062105-1–062105-16.

Harkema, S.J. & Meyer, R.A. 1997. Effect of acidosis on control of respiration in skeletal muscle. *Am J Physiol* **272**, C491–C500.

Harris, R.C., Hultman, E., Kaijser, L. & Nordesjo, L.O. 1975. The effect of circulatory occlusion on isometric exercise capacity and energy metabolism of the quadriceps muscle in man. *Scand J Clin Lab Invest* **35**, 87–95.

Harris, R.C., Edwards, R.H., Hultman, E., Nordesjo, L.O., Nylind, B. & Sahlin, K. 1976. The time course of phosphorylcreatine resynthesis during recovery of the quadriceps muscle in man. *Pflugers Arch* **367**, 137–142.

Haseler, L.J., Hogan, M.C. & Richardson, R.S. 1999. Skeletal muscle phosphocreatine recovery in exercise-trained humans is dependent on O_2 availability. *J Appl Physiol* **86**, 2013–2018.

Haseler, L.J., Lin, A.P. & Richardson, R.S. 2004. Skeletal muscle oxidative metabolism in sedentary humans: ^{31}P-

 © 2014 Scandinavian Physiological Society. Published by John Wiley & Sons Ltd, doi: 10.1111/apha.12307

MRS assessment of O_2 supply and demand limitations. *J Appl Physiol* **97**, 1077–1081.

Haseler, L.J., Lin, A., Hoff, J. & Richardson, R.S. 2007. Oxygen availability and PCr recovery rate in untrained human calf muscle: evidence of metabolic limitation in normoxia. *Am J Physiol Regul Integr Comp Physiol* **293**, R2046–R2051.

Hou, X.Y., Green, S., Askew, C.D., Barker, G., Green, A. & Walker, P.J. 2002. Skeletal muscle mitochondrial ATP production rate and walking performance in peripheral arterial disease. *Clin Physiol Funct Imaging* **22**, 226–232.

Hunter, G.R., Newcomer, B.R., Larson-Meyer, D.E., Bamman, M.M. & Weinsier, R.L. 2001. Muscle metabolic economy is inversely related to exercise intensity and type II myofiber distribution. *Muscle Nerve* **24**, 654–661.

Hunter, G.R., Newcomer, B.R., Weinsier, R.L., Karapondo, D.L., Larson-Meyer, D.E., Joanisse, D.R. & Bamman, M.M. 2002. Age is independently related to muscle metabolic capacity in premenopausal women. *J Appl Physiol* **93**, 70–76.

Hunter, G.R., Bamman, M.M., Larson-Meyer, D.E., Joanisse, D.R., McCarthy, J.P., Blaudeau, T.E. & Newcomer, B.R. 2005. Inverse relationship between exercise economy and oxidative capacity in muscle. *Eur J Appl Physiol* **94**, 558–568.

Iotti, S., Lodi, R., Frassineti, C., Zaniol, P. & Barbiroli, B. 1993. *In vivo* assessment of mitochondrial functionality in human gastrocnemius muscle by ^{31}P MRS. The role of pH in the evaluation of phosphocreatine and inorganic phosphate recoveries from exercise. *NMR Biomed* **6**, 248–253.

Iotti, S., Frassineti, C., Sabatini, A., Vacca, A. & Barbiroli, B. 2005. Quantitative mathematical expressions for accurate in vivo assessment of cytosolic [ADP] and DeltaG of ATP hydrolysis in the human brain and skeletal muscle. *Biochim Biophys Acta* **1708**, 164–177.

Jeneson, J.A. & Bruggeman, F.J. 2004. Robust homeostatic control of quadriceps pH during natural locomotor activity in man. *FASEB J* **18**, 1010–1012.

Jeneson, J.A.L., Westerhoff, H.V., Brown, T.R., van Echteld, C.J.A. & Berger, R. 1995. Quasi-linear relationship between Gibbs free energy of ATP hydrolysis and power-output in human forearm muscle. *Am J Physiol* **268**, C1474–C1484.

Jeneson, J.A., Wiseman, R.W., Westerhoff, H.V. & Kushmerick, M.J. 1996. The signal transduction function for oxidative phosphorylation is at least second order in ADP. *J Biol Chem* **271**, 27995–27998.

Jeneson, J.A., Wiseman, R.W. & Kushmerick, M.J. 1997. Non-invasive quantitative ^{31}P MRS assay of mitochondrial function in skeletal muscle *in situ*. *Mol Cell Biochem* **174**, 17–22.

Jeneson, J.A., Westerhoff, H.V. & Kushmerick, M.J. 2000. A metabolic control analysis of kinetic controls in ATP free energy metabolism in contracting skeletal muscle. *Am J Physiol Cell Physiol* **279**, C813–C832.

Jeneson, J.A., Schmitz, J.P., van den Broek, N.M., van Riel, N.A., Hilbers, P.A., Nicolay, K. & Prompers, J.J. 2009. Magnitude and control of mitochondrial sensitivity to ADP. *Am J Physiol Endocrinol Metab* **297**, E774–E784.

Jensen-Urstad, M. & Ahlborg, G. 1992. Is the high lactate release during arm exercise due to a low training status? *Clin Physiol* **12**, 487–496.

Jensen-Urstad, M., Ahlborg, G. & Sahlin, K. 1993. High lactate and NH_3 release during arm vs. leg exercise is not due to beta-adrenoceptor stimulation. *J Appl Physiol* **74**, 2860–2867.

Johannsen, D.L., Conley, K.E., Bajpeyi, S., Punyanitya, M., Gallagher, D., Zhang, Z., Covington, J., Smith, S.R. & Ravussin, E. 2012. Ectopic lipid accumulation and reduced glucose tolerance in elderly adults are accompanied by altered skeletal muscle mitochondrial activity. *J Clin Endocrinol Metab* **97**, 242–250.

Jones, A.M., Wilkerson, D.P. & Fulford, J. 2009. Influence of dietary creatine supplementation on muscle phosphocreatine kinetics during knee-extensor exercise in humans. *Am J Physiol Regul Integr Comp Physiol* **296**, R1078–R1087.

Jones, A.M., Krustrup, P., Wilkerson, D.P., Berger, N.J., Calbet, J.A. & Bangsbo, J. 2012. Influence of exercise intensity on skeletal muscle blood flow, O_2 extraction and O_2 uptake on-kinetics. *J Physiol* **590**, 4363–4676.

Jubrias, S.A., Crowther, G.J., Shankland, E.G., Gronka, R.K. & Conley, K.E. 2003. Acidosis inhibits oxidative phosphorylation in contracting human skeletal muscle *in vivo*. *J Physiol* **553**, 589–599.

Jucker, B.M., Dufour, S., Ren, J., Cao, X., Previs, S.F., Underhill, B., Cadman, K.S. & Shulman, G.I. 2000. Assessment of mitochondrial energy coupling in vivo by ^{13}C/^{31}P NMR. *Proc Natl Acad Sci USA* **97**, 6880–6884.

Kemp, G.J. 1994. Interactions of mitochondrial ATP synthesis and the creatine kinase equilibrium in skeletal muscle. *J Theor Biol* **170**, 239–246.

Kemp, G.J. 2004. Mitochondrial dysfunction in chronic ischemia and peripheral vascular disease. *Mitochondrion* **4**, 629–640.

Kemp, G.J. 2005a. Kinetics of muscle oxygen use, oxygen content, and blood flow during exercise. *J Appl Physiol*, **99**, 2463–2468; author reply 2468-9.

Kemp, G.J. 2005b. Lactate accumulation, proton buffering, and pH change in ischemically exercising muscle. *Am J Physiol Regul Integr Comp Physiol*, **289**, R895–R901; author reply R904–R910.

Kemp, G.J. 2006a. Altered creatine dependence of muscle mitochondrial respiration *in vitro*: what are the likely effects *in vivo*? *J Appl Physiol* **101**, 1814–1815.

Kemp, G.J. 2006b. Mitochondrial respiration in creatine-loaded muscle: is there ^{31}P-MRS evidence of direct effects of phosphocreatine and creatine *in vivo*? *J Appl Physiol*, **100**, 1428–1429; author reply 1429–1430.

Kemp, G.J. 2008a. The interpretation of abnormal ^{31}P magnetic resonance saturation transfer measurements of Pi/ATP exchange in insulin-resistant skeletal muscle. *Am J Physiol Endocrinol Metab*, **294**, E640–E642; author reply E643–E644.

Kemp, G.J. 2008b. Physiological implications of linear kinetics of mitochondrial respiration *in vitro*. *Am J Physiol Cell Physiol* **295**, C844–C846.

© 2014 Scandinavian Physiological Society. Published by John Wiley & Sons Ltd, doi: 10.1111/apha.12307

Kemp, G.J. 2009. Interpreting the phosphocreatine time constant in aerobically exercising skeletal muscle. *J Appl Physiol*, **106**, 350; author reply 351.

Kemp, G.J. 2011. Implications of rapid early oxygen consumption in exercising skeletal muscle. *J Physiol*, **589**, 6243–6244; author reply 6245–6246.

Kemp, G.J. & Bevington, A. 1993. The regulation of intracellular orthophosphate concentration. *J Theor Biol* **161**, 77–94.

Kemp, G.J. & Brindle, K.M. 2012. What do magnetic resonance-based measurements of Pi–>ATP flux tell us about skeletal muscle metabolism? *Diabetes* **61**, 1927–1934.

Kemp, G.J. & Radda, G.K. 1994. Quantitative interpretation of bioenergetic data from ^{31}P and ^{1}H magnetic resonance spectroscopic studies of skeletal muscle: an analytical review. *Magn Reson Q* **10**, 43–63.

Kemp, G.J., Taylor, D.J. & Radda, G.K. 1993a. Control of phosphocreatine resynthesis during recovery from exercise in human skeletal muscle. *NMR Biomed* **6**, 66–72.

Kemp, G.J., Taylor, D.J., Thompson, C.H., Hands, L.J., Rajagopalan, B., Styles, P. & Radda, G.K. 1993b. Quantitative analysis by ^{31}P magnetic resonance spectroscopy of abnormal mitochondrial oxidation in skeletal muscle during recovery from exercise. *NMR Biomed* **6**, 302–310.

Kemp, G.J., Thompson, C.H., Barnes, P.R. & Radda, G.K. 1994a. Comparisons of ATP turnover in human muscle during ischemic and aerobic exercise using ^{31}P magnetic resonance spectroscopy. *Magn Reson Med* **31**, 248–258.

Kemp, G.J., Thompson, C.H., Sanderson, A.L. & Radda, G.K. 1994b. pH control in rat skeletal muscle during exercise, recovery from exercise, and acute respiratory acidosis. *Magn Reson Med* **31**, 103–109.

Kemp, G.J., Hands, L.J., Ramaswami, G., Taylor, D.J., Nicolaides, A., Amato, A. & Radda, G.K. 1995. Calf muscle mitochondrial and glycogenolytic ATP synthesis in patients with claudication due to peripheral vascular disease analysed using ^{31}P magnetic resonance spectroscopy. *Clin Sci (Lond)* **89**, 581–590.

Kemp, G.J., Thompson, C.H., Stratton, J.R., Brunotte, F., Conway, M., Adamopoulos, S., Arnolda, L., Radda, G.K. & Rajagopalan, B. 1996. Abnormalities in exercising skeletal muscle in congestive heart failure can be explained in terms of decreased mitochondrial ATP synthesis, reduced metabolic efficiency, and increased glycogenolysis. *Heart* **76**, 35–41.

Kemp, G.J., Thompson, C.H., Taylor, D.J. & Radda, G.K. 1997. Proton efflux in human skeletal muscle during recovery from exercise. *Eur J Appl Physiol* **76**, 462–471.

Kemp, G.J., Manners, D.N., Clark, J.F., Bastin, M.E. & Radda, G.K. 1998. Theoretical modelling of some spatial and temporal aspects of the mitochondrion/creatine kinase/myofibril system in muscle. *Mol Cell Biochem* **184**, 249–289.

Kemp, G.J., Roberts, N., Bimson, W.E., Bakran, A., Harris, P.L., Gilling-Smith, G.L., Brennan, J., Rankin, A. & Frostick, S.P. 2001a. Mitochondrial function and oxygen supply in normal and in chronically ischemic muscle: a combined ^{31}P magnetic resonance spectroscopy and near infrared spectroscopy study *in vivo*. *J Vasc Surg* **34**, 1103–1110.

Kemp, G.J., Roussel, M., Bendahan, D., Le Fur, Y. & Cozzone, P.J. 2001b. Interrelations of ATP synthesis and proton handling in ischaemically exercising human forearm muscle studied by ^{31}P magnetic resonance spectroscopy. *J Physiol* **535**, 901–928.

Kemp, G.J., Roberts, N., Bimson, W.E., Bakran, A. & Frostick, S.P. 2002a. Muscle oxygenation and ATP turnover when blood flow is impaired by vascular disease. *Mol Biol Rep* **29**, 187–191.

Kemp, G.J., Roberts, N., Bimson, W.E., Bakran, A. & Frostick, S.P. 2002b. Muscle oxygenation and ATP turnover when blood flow is impaired by vascular disease. *Spectroscopy* **16**, 317–334.

Kemp, G.J., Crowe, A.V., Anijeet, H.K., Gong, Q.Y., Bimson, W.E., Frostick, S.P., Bone, J.M., Bell, G.M. & Roberts, J.N. 2004. Abnormal mitochondrial function and muscle wasting, but normal contractile efficiency, in haemodialysed patients studied non-invasively *in vivo*. *Nephrol Dial Transplant* **19**, 1520–1527.

Kemp, G.J., Boning, D., Beneke, R. & Maassen, N. 2006. Explaining pH change in exercising muscle: lactic acid, proton consumption, and buffering vs. strong ion difference. *Am J Physiol Regul Integr Comp Physiol*, **291**, R235–R237; author reply R238–R239.

Kemp, G.J., Meyerspeer, M. & Moser, E. 2007. Absolute quantification of phosphorus metabolite concentrations in human muscle in vivo by ^{31}P MRS: a quantitative review. *NMR Biomed* **20**, 555–565.

Kemp, G.J., Tonon, C., Malucelli, E., Testa, C., Liava, A., Manners, D., Trevisi, E., Martinuzzi, A., Barbiroli, B. & Lodi, R. 2009. Cytosolic pH buffering during exercise and recovery in skeletal muscle of patients with McArdle's disease. *Eur J Appl Physiol* **105**, 687–694.

Kemp, G.J., van den Broek, N.M.A., Nicolay, K. & Prompers, J.J. 2010. The pH-dependence of post-exercise PCr and ADP recovery: a simple modelling approach reproduces important features of ^{31}P MRS data from skeletal muscle. Joint Ann Meeting, Int Soc Magn Reson Med and Eur Soc Magn Reson Med Biol. Stockholm, Sweden.

Kemps, H.M., Prompers, J.J., Wessels, B., De Vries, W.R., Zonderland, M.L., Thijssen, E.J., Nicolay, K., Schep, G. & Doevendans, P.A. 2010. Skeletal muscle metabolic recovery following submaximal exercise in chronic heart failure is limited more by O_2 delivery than O_2 utilization. *Clin Sci (Lond)* **118**, 203–210.

Kent-Braun, J.A. & Ng, A.V. 2000. Skeletal muscle oxidative capacity in young and older women and men. *J Appl Physiol* **89**, 1072–1078.

Khushu, S., Rana, P., Sekhri, T., Sripathy, G. & Tripathi, R.P. 2010. Bio-energetic impairment in human calf muscle in thyroid disorders: a ^{31}P MRS study. *Magn Reson Imaging* **28**, 683–689.

Knight, D.R., Poole, D.C., Schaffartzik, W., Guy, H.J., Prediletto, R., Hogan, M.C. & Wagner, P.D. 1992. Relationship between body and leg V_{O2} during maximal cycle ergometry. *J Appl Physiol* **73**, 1114–1121.

 © 2014 Scandinavian Physiological Society. Published by John Wiley & Sons Ltd, doi: 10.1111/apha.12307

Knight, D.R., Schaffartzik, W., Poole, D.C., Hogan, M.C., Bebout, D.E. & Wagner, P.D. 1993. Effects of hyperoxia on maximal leg O_2 supply and utilization in men. *J Appl Physiol* **75**, 2586–2594.

Ko, S.F., Huang, C.C., Hsieh, M.J., Ng, S.H., Lee, C.C., Lin, T.K., Chen, M.C. & Lee, L. 2008. ^{31}P MR spectroscopic assessment of muscle in patients with myasthenia gravis before and after thymectomy: initial experience. *Radiology* **247**, 162–169.

Kornblum, C., Schroder, R., Muller, K., Vorgerd, M., Eggers, J., Bogdanow, M., Papassotiropoulos, A., Fabian, K., Klockgether, T. & Zange, J. 2005. Creatine has no beneficial effect on skeletal muscle energy metabolism in patients with single mitochondrial DNA deletions: a placebo-controlled, double-blind ^{31}P-MRS crossover study. *Eur J Neurol* **12**, 300–309.

Korzeniewski, B. 1998. Regulation of ATP supply during muscle contraction: theoretical studies. *Biochem J* **330**, 1189–1195.

Korzeniewski, B. & Zoladz, J.A. 2005. Some factors determining the PCr recovery overshoot in skeletal muscle. *Biophys Chem* **116**, 129–136.

Korzeniewski, B. & Zoladz, J.A. 2013. Slow VO_2 off-kinetics in skeletal muscle is associated with fast PCr off-kinetics - and inversely. *J Appl Physiol* **115**, 605–612.

Krustrup, P., Gonzalez-Alonso, J., Quistorff, B. & Bangsbo, J. 2001. Muscle heat production and anaerobic energy turnover during repeated intense dynamic exercise in humans. *J Physiol* **536**, 947–956.

Krustrup, P., Ferguson, R.A., Kjaer, M. & Bangsbo, J. 2003. ATP and heat production in human skeletal muscle during dynamic exercise: higher efficiency of anaerobic than aerobic ATP resynthesis. *J Physiol* **549**, 255–269.

Krustrup, P., Hellsten, Y. & Bangsbo, J. 2004. Intense interval training enhances human skeletal muscle oxygen uptake in the initial phase of dynamic exercise at high but not at low intensities. *J Physiol* **559**, 335–345.

Krustrup, P., Jones, A.M., Wilkerson, D.P., Calbet, J.A. & Bangsbo, J. 2009. Muscular and pulmonary O_2 uptake kinetics during moderate- and high-intensity sub-maximal knee-extensor exercise in humans. *J Physiol* **587**, 1843–1856.

Kushmerick, M.J. 1997. Multiple equilibria of cations with metabolites in muscle bioenergetics. *Am J Physiol* **272**, C1739–C1747.

Kushmerick, M.J., Meyer, R.A. & Brown, T.R. 1992. Regulation of oxygen consumption in fast- and slow-twitch muscle. *Am J Physiol* **263**, C598–C606.

Lanza, I.R., Befroy, D.E. & Kent-Braun, J.A. 2005. Age-related changes in ATP-producing pathways in human skeletal muscle *in vivo*. *J Appl Physiol* **99**, 1736–1744.

Lanza, I.R., Wigmore, D.M., Befroy, D.E. & Kent-Braun, J.A. 2006. *In vivo* ATP production during free-flow and ischaemic muscle contractions in humans. *J Physiol* **577**, 353–367.

Lanza, I.R., Bhagra, S., Nair, K.S. & Port, J.D. 2011. Measurement of human skeletal muscle oxidative capacity by ^{31}P-MR spectroscopy: a cross-validation with *in vitro* measurements. *J Magn Reson Imaging* **34**, 1143–1150.

Larsen, R.G., Callahan, D.M., Foulis, S.A. & Kent-Braun, J.A. 2009. *In vivo* oxidative capacity varies with muscle and training status in young adults. *J Appl Physiol* **107**, 873–879.

Larsen, R.G., Callahan, D.M., Foulis, S.A. & Kent-Braun, J.A. 2012. Age-related changes in oxidative capacity differ between locomotory muscles and are associated with physical activity behavior. *Appl Physiol Nutr Metab* **37**, 88–99.

Larsen, R.G., Befroy, D.E. & Kent-Braun, J.A. 2013. High-intensity interval training increases in vivo oxidative capacity with no effect on Pi–>ATP rate in resting human muscle. *Am J Physiol Regul Integr Comp Physiol* **304**, R333–R342.

Larson-Meyer, D.E., Newcomer, B.R., Hunter, G.R., Hetherington, H.P. & Weinsier, R.L. 2000. ^{31}P MRS measurement of mitochondrial function in skeletal muscle: reliability, force-level sensitivity and relation to whole body maximal oxygen uptake. *NMR Biomed* **13**, 14–27.

Larson-Meyer, D.E., Newcomer, B.R., Hunter, G.R., Joanisse, D.R., Weinsier, R.L. & Bamman, M.M. 2001. Relation between *in vivo* and *in vitro* measurements of skeletal muscle oxidative metabolism. *Muscle Nerve* **24**, 1665–1676.

Lawrenson, L., Poole, J.G., Kim, J., Brown, C., Patel, P. & Richardson, R.S. 2003. Vascular and metabolic response to isolated small muscle mass exercise: effect of age. *Am J Physiol Heart Circ Physiol* **285**, H1023–H1031.

Lawson, J.W. & Veech, R.L. 1979. Effects of pH and free Mg^{2+} on the K_{eq} of the creatine kinase reaction and other phosphate hydrolyses and phosphate transfer reactions. *J Biol Chem* **254**, 6528–6537.

Layec, G., Bringard, A., Le Fur, Y., Vilmen, C., Micallef, J.P., Perrey, S., Cozzone, P.J. & Bendahan, D. 2009. Reproducibility assessment of metabolic variables characterizing muscle energetics in vivo: a ^{31}P-MRS study. *Magn Reson Med* **62**, 840–854.

Layec, G., Bringard, A., Le Fur, Y., Vilmen, C., Micallef, J.P., Perrey, S., Cozzone, P.J. & Bendahan, D. 2011. Comparative determination of energy production rates and mitochondrial function using different ^{31}P MRS quantitative methods in sedentary and trained subjects. *NMR Biomed* **24**, 425–438.

Layec, G., Haseler, L.J., Hoff, J., Hart, C.R., Liu, X., Le Fur, Y., Jeong, E.K. & Richardson, R.S. 2013a. Short-term training alters the control of mitochondrial respiration rate before maximal oxidative ATP synthesis. *Acta Physiol (Oxf)* **208**, 376–386.

Layec, G., Haseler, L.J. & Richardson, R.S. 2013b. Reduced muscle oxidative capacity is independent of O_2 availability in elderly people. *Age (Dordr)* **35**, 1183–1192.

Layec, G., Haseler, L.J., Trinity, J.D., Hart, C.R., Liu, X., Le Fur, Y., Jeong, E.K. & Richardson, R.S. 2013c. Mitochondrial function and increased convective O_2 transport: implications for the assessment of mitochondrial respiration *in vivo*. *J Appl Physiol* **115**, 803–811.

Layec, G., Malucelli, E., Le Fur, Y., Manners, D., Yashiro, K., Testa, C., Cozzone, P.J., Iotti, S. & Bendahan, D. 2013d. Effects of exercise-induced intracellular acidosis on the phosphocreatine recovery kinetics: a ^{31} P MRS study in

three muscle groups in humans. *NMR Biomed* **26**, 1403–1411.

Layec, G., Trinity, J.D., Hart, C.R., Kim, S.E., Groot, H.J., Le Fur, Y., Sorensen, J.R., Jeong, E.K. & Richardson, R.S. 2014. In vivo evidence of an age-related increase in ATP cost of contraction in the plantar flexor muscles. *Clin Sci (Lond)* **126**, 581–592.

Ljungberg, M., Sunnerhagen, K.S., Vikhoff-Baaz, B., Starck, G., Forssell-Aronsson, E., Hedberg, M., Ekholm, S. & Grimby, G. 2003. ^{31}P MRS evaluation of fatigue in anterior tibial muscle in postpoliomyelitis patients and healthy volunteers. *Clin Physiol Funct Imaging* **23**, 190–198.

Lodi, R., Kemp, G.J., Iotti, S., Radda, G.K. & Barbiroli, B. 1997a. Influence of cytosolic pH on in vivo assessment of human muscle mitochondrial respiration by phosphorus magnetic resonance spectroscopy. *MAGMA* **5**, 165–171.

Lodi, R., Kemp, G.J., Montagna, P., Pierangeli, G., Cortelli, P., Iotti, S., Radda, G.K. & Barbiroli, B. 1997b. Quantitative analysis of skeletal muscle bioenergetics and proton efflux in migraine and cluster headache. *J Neurol Sci* **146**, 73–80.

Lodi, R., Kemp, G.J., Muntoni, F., Thompson, C.H., Rae, C., Taylor, J., Styles, P. & Taylor, D.J. 1999. Reduced cytosolic acidification during exercise suggests defective glycolytic activity in skeletal muscle of patients with Becker muscular dystrophy. An in vivo ^{31}P magnetic resonance spectroscopy study. *Brain* **122**, 121–130.

Mahler, M. 1985. First-order kinetics of muscle oxygen consumption, and an equivalent proportionality between QO_2 and phosphorylcreatine level. Implications for the control of respiration. *J Gen Physiol* **86**, 135–165.

Makimura, H., Stanley, T.L., Sun, N., Connelly, J.M., Hemphill, L.C., Hrovat, M.I., Systrom, D.M. & Grinspoon, S.K. 2011a. Increased skeletal muscle phosphocreatine recovery after sub-maximal exercise is associated with increased carotid intima-media thickness. *Atherosclerosis* **215**, 214–217.

Makimura, H., Stanley, T.L., Sun, N., Hrovat, M.I., Systrom, D.M. & Grinspoon, S.K. 2011b. The association of growth hormone parameters with skeletal muscle phosphocreatine recovery in adult men. *J Clin Endocrinol Metab* **96**, 817–823.

Mancini, B., Coyle, E., Coggin, A., Beltz, J., Ferraro, N., Montain, S. & Wilson, J.R. 1989. Contribution of intrinsic skeletal muscle changes to ^{31}P NMR skeletal muscle metabolic abnormalities in patients with chronic heart failure. *Circulation* **80**, 1338–1346.

Mancini, D.M., Walter, G., Reichek, N., Lenkinski, R., McCully, K.K., Mullen, J.L. & Wilson, J.R. 1992. Contribution of skeletal muscle atrophy to exercise intolerance and altered muscle metabolism in heart failure. *Circulation* **85**, 1364–1373.

Mannix, E.T., Boska, M.D., Galassetti, P., Burton, G., Manfredi, F. & Farber, M.O. 1995. Modulation of ATP production by oxygen in obstructive lung disease as assessed by ^{31}P-MRS. *J Appl Physiol* **78**, 2218–2227.

Marcinek, D.J., Ciesielski, W.A., Conley, K.E. & Schenkman, K.A. 2003. Oxygen regulation and limitation to cellular respiration in mouse skeletal muscle *in vivo*. *Am J Physiol Heart Circ Physiol* **285**, H1900–H1908.

Marcinek, D.J., Schenkman, K.A., Ciesielski, W.A. & Conley, K.E. 2004. Mitochondrial coupling *in vivo* in mouse skeletal muscle. *Am J Physiol Cell Physiol* **286**, C457–C463.

Marrades, R.M., Alonso, J., Roca, J., Gonzalez de Suso, J.M., Campistol, J.M., Barbera, J.A., Diaz, O., Torregrosa, J.V., Masclans, J.R., Rodriguez-Roisin, R. & Wagner, P.D. 1996. Cellular bioenergetics after erythropoietin therapy in chronic renal failure. *J Clin Invest* **97**, 2101–2110.

Martinuzzi, A., Liava, A., Trevisi, E., Frare, M., Tonon, C., Malucelli, E., Manners, D., Kemp, G.J., Testa, C., Barbiroli, B. & Lodi, R. 2007. Randomized, placebo-controlled, double-blind pilot trial of ramipril in McArdle's disease. *Muscle Nerve* **37**, 350–357.

McCully, K.K., Fielding, R.A., Evans, W.J., Leigh, J.S.J. & Posner, J.D. 1993. Relationships between *in vivo* and *in vitro* measurements of metabolism in young and old human calf muscles. *J Appl Physiol* **75**, 813–819.

McCully, K.K., Iotti, S., Kendrick, K., Wang, Z., Posner, J.D., Leigh, J. Jr & Chance, B. 1994. Simultaneous *in vivo* measurements of HbO_2 saturation and PCr kinetics after exercise in normal humans. *J Appl Physiol* **77**, 5–10.

McCully, K.K., Turner, T.N., Langley, J. & Zhao, Q. 2009. The reproducibility of measurements of intramuscular magnesium concentrations and muscle oxidative capacity using ^{31}P MRS. *Dyn Med* **8**, 5.

McCully, K.K., Mulcahy, T.K., Ryan, T.E. & Zhao, Q. 2011. Skeletal muscle metabolism in individuals with spinal cord injury. *J Appl Physiol (1985)*, **111**, 143–148.

Meex, R.C., Schrauwen-Hinderling, V.B., Moonen-Kornips, E., Schaart, G., Mensink, M., Phielix, E., van de Weijer, T., Sels, J.P., Schrauwen, P. & Hesselink, M.K. 2010. Restoration of muscle mitochondrial function and metabolic flexibility in type 2 diabetes by exercise training is paralleled by increased myocellular fat storage and improved insulin sensitivity. *Diabetes* **59**, 572–579.

Meyer, R.A. 1988. A linear model of muscle respiration explains monoexponential phosphocreatine changes. *Am J Physiol* **254**, C548–C553.

Meyer, R.A. 1989. Linear dependence of muscle phosphocreatine kinetics on total creatine content. *Am J Physiol* **257**, C1149–C1157.

Meyer, R.A., Sweeney, H.L. & Kushmerick, M.J. 1984. A simple analysis of the "phosphocreatine shuttle". *Am J Physiol* **246**, C365–C377.

Meyerspeer, M., Scheenen, T., Schmid, A.I., Mandl, T., Unger, E. & Moser, E. 2011. Semi-LASER localized dynamic ^{31}P magnetic resonance spectroscopy in exercising muscle at ultra-high magnetic field. *Magn Reson Med* **65**, 1207–1215.

Meyerspeer, M., Robinson, S., Nabuurs, C.I., Scheenen, T., Schoisengeier, A., Unger, E., Kemp, G.J. & Moser, E. 2012. Comparing localized and nonlocalized dynamic ^{31}P magnetic resonance spectroscopy in exercising muscle at 7 T. *Magn Reson Med* **68**, 1713–1723.

 © 2014 Scandinavian Physiological Society. Published by John Wiley & Sons Ltd, doi: 10.1111/apha.12307

Mitchell, C.S., Savage, D.B., Dufour, S., Schoenmakers, N., Murgatroyd, P., Befroy, D., Halsall, D., Northcott, S., Raymond-Barker, P., Curran, S. *et al.* 2010. Resistance to thyroid hormone is associated with raised energy expenditure, muscle mitochondrial uncoupling, and hyperphagia. *J Clin Invest* **120**, 1345–1354.

Mortensen, S.P., Damsgaard, R., Dawson, E.A., Secher, N.H. & Gonzalez-Alonso, J. 2008. Restrictions in systemic and locomotor skeletal muscle perfusion, oxygen supply and VO_2 during high-intensity whole-body exercise in humans. *J Physiol* **586**, 2621–2635.

Mourtzakis, M., Gonzalez-Alonso, J., Graham, T.E. & Saltin, B. 2004. Hemodynamics and O_2 uptake during maximal knee extensor exercise in untrained and trained human quadriceps muscle: effects of hyperoxia. *J Appl Physiol* **97**, 1796–1802.

Nachbauer, W., Boesch, S., Schneider, R., Eigentler, A., Wanschitz, J., Poewe, W. & Schocke, M. 2013. Bioenergetics of the calf muscle in Friedreich ataxia patients measured by ^{31}P-MRS before and after treatment with recombinant human erythropoietin. *PLoS ONE* **8**, e69229.

Odoom, J.E., Kemp, G.J. & Radda, G.K. 1996. The regulation of total creatine content in a myoblast cell line. *Mol Cell Biochem* **158**, 179–188.

van Oorschot, J.W., Schmitz, J.P., Webb, A., Nicolay, K., Jeneson, J.A. & Kan, H.E. 2013. ^{31}P MR spectroscopy and computational modeling identify a direct relation between Pi content of an alkaline compartment in resting muscle and phosphocreatine resynthesis kinetics in active muscle in humans. *PLoS ONE* **8**, e76628.

Paganini, A.T., Foley, J.M. & Meyer, R.A. 1997. Linear dependence of muscle phosphocreatine kinetics on oxidative capacity. *Am J Physiol* **272**, C501–C510.

Parasoglou, P., Xia, D., Chang, G. & Regatte, R.R. 2013. Dynamic three-dimensional imaging of phosphocreatine recovery kinetics in the human lower leg muscles at 3T and 7T: a preliminary study. *NMR Biomed* **26**, 348–356.

Paterson, D.H. & Whipp, B.J. 1991. Asymmetries of oxygen uptake transients at the on- and offset of heavy exercise in humans. *J Physiol* **443**, 575–586.

Pedersen, P.K., Kiens, B. & Saltin, B. 1999. Hyperoxia does not increase peak muscle oxygen uptake in small muscle group exercise. *Acta Physiol Scand* **166**, 309–318.

Perry, C.G., Kane, D.A., Herbst, E.A., Mukai, K., Lark, D.S., Wright, D.C., Heigenhauser, G.J., Neufer, P.D., Spriet, L.L. & Holloway, G.P. 2012. Mitochondrial creatine kinase activity and phosphate shuttling are acutely regulated by exercise in human skeletal muscle. *J Physiol* **590**, 5475–5486.

Persson, P.B. 2013. Good publication practice in physiology 2013 guidelines for Acta Physiologica. *Acta Physiol (Oxf)* **209**, 250–253.

Pesta, D., Paschke, V., Hoppel, F., Kobel, C., Kremser, C., Esterhammer, R., Burtscher, M., Kemp, G.J. & Schocke, M. 2013. Different metabolic responses during incremental exercise assessed by localized 31P MRS in sprint and endurance athletes and untrained individuals. *Int J Sports Med* **34**, 669–675.

Petersen, K.F., Befroy, D., Dufour, S., Dziura, J., Ariyan, C., Rothman, D.L., DiPietro, L., Cline, G.W. & Shulman, G.I. 2003. Mitochondrial dysfunction in the elderly: possible role in insulin resistance. *Science* **300**, 1140–1142.

Pipinos, I.I., Shepard, A.D., Anagnostopoulos, P.V., Katsamouris, A. & Boska, M.D. 2000. Phosphorus 31 nuclear magnetic resonance spectroscopy suggests a mitochondrial defect in claudicating skeletal muscle. *J Vasc Surg* **31**, 944–952.

Polgreen, K.E., Kemp, G.J., Leighton, B. & Radda, G.K. 1994. Modulation of Pi transport in skeletal muscle by insulin and IGF-1. *Biochim Biophys Acta* **1223**, 279–284.

Poole, D.C., Schaffartzik, W., Knight, D.R., Derion, T., Kennedy, B., Guy, H.J., Prediletto, R. & Wagner, P.D. 1991. Contribution of exercising legs to the slow component of oxygen uptake kinetics in humans. *J Appl Physiol* **71**, 1245–1260.

Poole, D.C., Gaesser, G.A., Hogan, M.C., Knight, D.R. & Wagner, P.D. 1992. Pulmonary and leg VO_2 during submaximal exercise: implications for muscular efficiency. *J Appl Physiol* **72**, 805–810.

Praet, S.F., De Feyter, H.M., Jonkers, R.A., Nicolay, K., van Pul, C., Kuipers, H., van Loon, L.J. & Prompers, J.J. 2006. ^{31}P MR spectroscopy and *in vitro* markers of oxidative capacity in type 2 diabetes patients. *MAGMA* **19**, 321–331.

Quistorff, B., Johansen, L. & Sahlin, K. 1993. Absence of phosphocreatine resynthesis in human calf muscle during ischaemic recovery. *Biochem J* **291**, 681–686.

Radegran, G. & Saltin, B. 2000. Human femoral artery diameter in relation to knee extensor muscle mass, peak blood flow, and oxygen uptake. *Am J Physiol Heart Circ Physiol* **278**, H162–H167.

Rasmussen, U.F. & Rasmussen, H.N. 2000. Human skeletal muscle mitochondrial capacity. *Acta Physiol Scand* **168**, 473–480.

Rasmussen, U.F., Rasmussen, H.N., Krustrup, P., Quistorff, B., Saltin, B. & Bangsbo, J. 2001. Aerobic metabolism of human quadriceps muscle: *in vivo* data parallel measurements on isolated mitochondria. *Am J Physiol Endocrinol Metab* **280**, E301–E307.

Rasmussen, U.F., Krustrup, P., Kjaer, M. & Rasmussen, H.N. 2003. Human skeletal muscle mitochondrial metabolism in youth and senescence: no signs of functional changes in ATP formation and mitochondrial oxidative capacity. *Pflugers Arch* **446**, 270–278.

Rasmussen, U.F., Vielwerth, S.E. & Rasmussen, H.N. 2004. Skeletal muscle bioenergetics: a comparative study of mitochondria isolated from pigeon pectoralis, rat soleus, rat biceps brachii, pig biceps femoris and human quadriceps. *Comp Biochem Physiol A Mol Integr Physiol* **137**, 435–446.

Richardson, R.S., Noyszewski, E.A., Kendrick, K.F., Leigh, J.S. & Wagner, P.D. 1995. Myoglobin O2 desaturation during exercise. Evidence of limited O_2 transport. *J Clin Invest* **96**, 1916–1926.

Richardson, R.S., Leigh, J.S., Wagner, P.D. & Noyszewski, E.A. 1999. Cellular PO_2 as a determinant of maximal

mitochondrial O_2 consumption in trained human skeletal muscle. *J Appl Physiol* **87**, 325–331.

Richardson, R.S., Noyszewski, E.A., Saltin, B. & Gonzalez-Alonso, J. 2002. Effect of mild carboxy-hemoglobin on exercising skeletal muscle: intravascular and intracellular evidence. *Am J Physiol Regul Integr Comp Physiol* **283**, R1131–R1139.

Roca, J., Agusti, A.G., Alonso, A., Poole, D.C., Viegas, C., Barbera, J.A., Rodriguez-Roisin, R., Ferrer, A. & Wagner, P.D. 1992. Effects of training on muscle O_2 transport at VO_{2max}. *J Appl Physiol* **73**, 1067–1076.

Rossiter, H.B. 2011. Exercise: kinetic considerations for gas exchange. *Compr Physiol* **1**, 203–244.

Rossiter, H.B., Ward, S.A., Howe, F.A., Kowalchuk, J.M., Griffiths, J.R. & Whipp, B.J. 2002a. Dynamics of intramuscular ^{31}P-MRS Pi peak splitting and the slow components of PCr and O_2 uptake during exercise. *J Appl Physiol* **93**, 2059–2069.

Rossiter, H.B., Ward, S.A., Kowalchuk, J.M., Howe, F.A., Griffiths, J.R. & Whipp, B.J. 2002b. Dynamic asymmetry of phosphocreatine concentration and O_2 uptake between the on- and off-transients of moderate- and high-intensity exercise in humans. *J Physiol* **541**, 991–1002.

Roussel, M., Bendahan, D., Mattei, J.P., Le Fur, Y. & Cozzone, P.J. 2000. ^{31}P magnetic resonance spectroscopy study of phosphocreatine recovery kinetics in skeletal muscle: the issue of intersubject variability. *Biochim Biophys Acta* **1457**, 18–26.

Rud, B., Foss, O., Krustrup, P., Secher, N.H. & Hallen, J. 2012. One-legged endurance training: leg blood flow and oxygen extraction during cycling exercise. *Acta Physiol (Oxf)* **205**, 177–185.

Ryan, T.E., Southern, W.M., Reynolds, M.A. & McCully, K.K. 2013. A cross-validation of near-infrared spectroscopy measurements of skeletal muscle oxidative capacity with phosphorus magnetic resonance spectroscopy. *J Appl Physiol* **115**, 1757–1766.

Ryschon, T.W., Fowler, M.D., Wysong, R.E., Anthony, A. & Balaban, R.S. 1997. Efficiency of human skeletal muscle in vivo: comparison of isometric, concentric, and eccentric muscle action. *J Appl Physiol* **83**, 867–874.

Sahlin, K., Harris, R.C. & Hultman, E. 1979. Resynthesis of creatine phosphate in human muscle after exercise in relation to intramuscular pH and availability of oxygen. *Scand J Clin Lab Invest* **39**, 551–558.

Saks, V., Guzun, R., Timohhina, N., Tepp, K., Varikmaa, M., Monge, C., Beraud, N., Kaambre, T., Kuznetsov, A., Kadaja, L., Eimre, M. & Seppet, E. 2010. Structure-function relationships in feedback regulation of energy fluxes *in vivo* in health and disease: mitochondrial interactosome. *Biochim Biophys Acta* **1797**, 678–697.

Sala, E., Roca, J., Marrades, R.M., Alonso, J., Gonzalez De Suso, J.M., Moreno, A., Barbera, J.A., Nadal, J., de Jover, L., Rodriguez-Roisin, R. & Wagner, P.D. 1999. Effects of endurance training on skeletal muscle bioenergetics in chronic obstructive pulmonary disease. *Am J Respir Crit Care Med* **159**, 1726–1734.

Schaffartzik, W., Barton, E.D., Poole, D.C., Tsukimoto, K., Hogan, M.C., Bebout, D.E. & Wagner, P.D. 1993. Effect of reduced hemoglobin concentration on leg oxygen uptake during maximal exercise in humans. *J Appl Physiol*, **75**, 491–498; discussion 489-490.

Scheuermann-Freestone, M., Madsen, P.L., Manners, D., Blamire, A.M., Buckingham, R.E., Styles, P., Radda, G.K., Neubauer, S. & Clarke, K. 2003. Abnormal cardiac and skeletal muscle energy metabolism in patients with type 2 diabetes. *Circulation* **107**, 3040–3046.

Schmid, A.I., Schrauwen-Hinderling, V.B., Andreas, M., Wolzt, M., Moser, E. & Roden, M. 2012. Comparison of measuring energy metabolism by different ^{31}P-magnetic resonance spectroscopy techniques in resting, ischemic, and exercising muscle. *Magn Reson Med* **67**, 898–905.

Schmitz, J.P., van Riel, N.A., Nicolay, K., Hilbers, P.A. & Jeneson, J.A. 2010. Silencing of glycolysis in muscle: experimental observation and numerical analysis. *Exp Physiol* **95**, 380–397.

Schmitz, J.P., Vanlier, J., van Riel, N.A. & Jeneson, J.A. 2011. Computational modeling of mitochondrial energy transduction. *Crit Rev Biomed Eng* **39**, 363–377.

Schmitz, J.P., Jeneson, J.A., van Oorschot, J.W., Prompers, J.J., Nicolay, K., Hilbers, P.A. & van Riel, N.A. 2012. Prediction of muscle energy states at low metabolic rates requires feedback control of mitochondrial respiratory chain activity by inorganic phosphate. *PLoS ONE* **7**, e34118.

Schmitz, J.P., Groenendaal, W., Wessels, B., Wiseman, R.W., Hilbers, P.A., Nicolay, K., Prompers, J.J., Jeneson, J.A. & van Riel, N.A. 2013. Combined *in vivo* and *in silico* investigations of activation of glycolysis in contracting skeletal muscle. *Am J Physiol Cell Physiol* **304**, C180–C193.

Schrauwen-Hinderling, V.B., Kooi, M.E., Hesselink, M.K., Jeneson, J.A., Backes, W.H., van Echteld, C.J., van Engelshoven, J.M., Mensink, M. & Schrauwen, P. 2007. Impaired *in vivo* mitochondrial function but similar intramyocellular lipid content in patients with type 2 diabetes mellitus and BMI-matched control subjects. *Diabetologia* **50**, 113–120.

Schrauwen-Hinderling, V.B., Mensink, M., Hesselink, M.K., Sels, J.P., Kooi, M.E. & Schrauwen, P. 2008. The insulin-sensitizing effect of rosiglitazone in type 2 diabetes mellitus patients does not require improved *in vivo* muscle mitochondrial function. *J Clin Endocrinol Metab* **93**, 2917–2921.

Sinha, A., Hollingsworth, K.G., Ball, S. & Cheetham, T. 2013. Improving the vitamin D status of vitamin D deficient adults is associated with improved mitochondrial oxidative function in skeletal muscle. *J Clin Endocrinol Metab* **98**, E509–E513.

Sinha, A., Hollingsworth, K.G., Ball, S. & Cheetham, T. 2014. Impaired quality of life in growth hormone-deficient adults is independent of the altered skeletal muscle oxidative metabolism found in conditions with peripheral fatigue. *Clin Endocrinol (Oxf)* **80**, 107–114.

Slade, J.M., Towse, T.F., Delano, M.C., Wiseman, R.W. & Meyer, R.A. 2006. A gated ^{31}P NMR method for the estimation of phosphocreatine recovery time and contractile ATP cost in human muscle. *NMR Biomed* **19**, 573–580.

 © 2014 Scandinavian Physiological Society. Published by John Wiley & Sons Ltd, doi: 10.1111/apha.12307

Slattery, M.J., Bredella, M.A., Thakur, H., Torriani, M. & Misra, M. 2014. Insulin resistance and impaired mitochondrial function in obese adolescent girls. *Metab Syndr Relat Disord* **12**, 56–61.

Sleigh, A., Raymond-Barker, P., Thackray, K., Porter, D., Hatunic, M., Vottero, A., Burren, C., Mitchell, C., McIntyre, M., Brage, S. *et al.* 2011. Mitochondrial dysfunction in patients with primary congenital insulin resistance. *J Clin Invest* **121**, 2457–2461.

Sleigh, A., Stears, A., Thackray, K., Watson, L., Gambineri, A., Nag, S., Campi, V.I., Schoenmakers, N., Brage, S., Carpenter, T.A., Murgatroyd, P.R., O'Rahilly, S., Kemp, G.J. & Savage, D.B. 2012. Mitochondrial oxidative phosphorylation is impaired in patients with congenital lipodystrophy. *J Clin Endocrinol Metab* **97**, E438–E442.

Smith, S.A., Montain, S.J., Zientara, G.P. & Fielding, R.A. 2004. Use of phosphocreatine kinetics to determine the influence of creatine on muscle mitochondrial respiration: an *in vivo* ^{31}P-MRS study of oral creatine ingestion. *J Appl Physiol* **96**, 2288–2292.

Spriet, L.L., Soderlund, K., Bergstrom, M. & Hultman, E. 1987a. Anaerobic energy release in skeletal muscle during electrical stimulation in men. *J Appl Physiol* **62**, 611–615.

Spriet, L.L., Soderlund, K., Bergstrom, M. & Hultman, E. 1987b. Skeletal muscle glycogenolysis, glycolysis, and pH during electrical stimulation in men. *J Appl Physiol* **62**, 616–621.

Starritt, E.C., Angus, D. & Hargreaves, M. 1999. Effect of short-term training on mitochondrial ATP production rate in human skeletal muscle. *J Appl Physiol* **86**, 450–454.

Stellingwerff, T., Leblanc, P.J., Hollidge, M.G., Heigenhauser, G.J. & Spriet, L.L. 2006. Hyperoxia decreases muscle glycogenolysis, lactate production, and lactate efflux during steady-state exercise. *Am J Physiol Endocrinol Metab* **290**, E1180–E1190.

Stratton, J.R., Dunn, J.F., Adamopoulos, S., Kemp, G.J., Coats, A.J. & Rajagopalan, B. 1994. Training partially reverses skeletal muscle metabolic abnormalities during exercise in heart failure. *J Appl Physiol* **76**, 1575–1582.

Styles, P., Kemp, G.J. & Radda, G.K. 1992. A model for metabolic control which reproduces the main features of recovery from exercise which are observed by ^{31}P MRS. 11th Ann Meeting Soc Magn Reson Med. Berlin, Germany.

Styles, P., Kemp, G.J. & Radda, G.K. 1993. Modelling ^{31}P MRS observations in patients with mitochondrial dysfunction. Proc 12th Ann Meeting Soc Magn Reson Med. New York, U.S.A.

Taivassalo, T., Shoubridge, E.A., Chen, J., Kennaway, N.G., DiMauro, S., Arnold, D.L. & Haller, R.G. 2001. Aerobic conditioning in patients with mitochondrial myopathies: physiological, biochemical, and genetic effects. *Ann Neurol* **50**, 133–141.

Takahashi, H., Inaki, M., Fujimoto, K., Katsuta, S., Anno, I., Niitsu, M. & Itai, Y. 1995. Control of the rate of phosphocreatine resynthesis after exercise in trained and untrained human quadriceps muscles. *Eur J Appl Physiol* **71**, 396–404.

Tartaglia, M.C., Chen, J.T., Caramanos, Z., Taivassalo, T., Arnold, D.L. & Argov, Z. 2000. Muscle phosphorus magnetic resonance spectroscopy oxidative indices correlate with physical activity. *Muscle Nerve* **23**, 175–181.

Taylor, D.J., Bore, P.J., Styles, P., Gadian, D.G. & Radda, G.K. 1983. Bioenergetics of intact human muscle. A 31P nuclear magnetic resonance study. *Mol Biol Med* **1**, 77–94.

Taylor, D.J., Rajagopalan, B. & Radda, G.K. 1992. Cellular energetics in hypothyroid muscle. *Eur J Clin Invest* **22**, 358–365.

Taylor, D.J., Kemp, G.J. & Radda, G.K. 1994. Bioenergetics of skeletal muscle in mitochondrial myopathy. *J Neurol Sci* **127**, 198–206.

Taylor, D.J., Kemp, G.J., Thompson, C.H. & Radda, G.K. 1997. Ageing: effects on oxidative function of skeletal muscle in vivo. *Mol Cell Biochem* **174**, 321–324.

Thompson, C.H., Kemp, G.J., Taylor, D.J., Ledingham, J.G., Radda, G.K. & Rajagopalan, B. 1993. Effect of chronic uraemia on skeletal muscle metabolism in man. *Nephrol Dial Transplant* **8**, 218–222.

Thompson, C.H., Kemp, G.J., Sanderson, A.L. & Radda, G.K. 1995. Skeletal muscle mitochondrial function studied by kinetic analysis of postexercise phosphocreatine resynthesis. *J Appl Physiol* **78**, 2131–2139.

van Tienen, F.H., Praet, S.F., de Feyter, H.M., van den Broek, N.M., Lindsey, P.J., Schoonderwoerd, K.G., de Coo, I.F., Nicolay, K., Prompers, J.J., Smeets, H.J. & van Loon, L.J. 2012. Physical activity is the key determinant of skeletal muscle mitochondrial function in type 2 diabetes. *J Clin Endocrinol Metab* **97**, 3261–3269.

Tonkonogi, M. & Sahlin, K. 1997. Rate of oxidative phosphorylation in isolated mitochondria from human skeletal muscle: effect of training status. *Acta Physiol Scand* **161**, 345–353.

Tonkonogi, M., Walsh, B., Tiivel, T., Saks, V. & Sahlin, K. 1999. Mitochondrial function in human skeletal muscle is not impaired by high intensity exercise. *European Journal of Physiology* **437**, 562–568.

Tonson, A., Ratel, S., Le Fur, Y., Vilmen, C., Cozzone, P.J. & Bendahan, D. 2010. Muscle energetics changes throughout maturation: a quantitative ^{31}P-MRS analysis. *J Appl Physiol* **109**, 1769–1778.

Tran, T.K., Sailasuta, N., Kreutzer, U., Hurd, R., Chung, Y., Mole, P., Kuno, S. & Jue, T. 1999. Comparative analysis of NMR and NIRS measurements of intracellular PO2 in human skeletal muscle. *Am J Physiol* **276**, R1682–R1690.

Trenell, M.I., Sue, C.M., Kemp, G.J., Sachinwalla, T. & Thompson, C.H. 2006. Aerobic exercise and muscle metabolism in patients with mitochondrial myopathy. *Muscle Nerve* **33**, 524–531.

Trenell, M.I., Sue, C.M., Thompson, C.H. & Kemp, G.J. 2007. Supplemental oxygen and muscle metabolism in mitochondrial myopathy patients. *Eur J Appl Physiol* **99**, 541–547.

Trenell, M.I., Hollingsworth, K.G., Lim, E.L. & Taylor, R. 2008. Increased daily walking improves lipid oxidation

© 2014 Scandinavian Physiological Society. Published by John Wiley & Sons Ltd, doi: 10.1111/apha.12307

without changes in mitochondrial function in type 2 diabetes. *Diabetes Care* **31**, 1644–1649.

Valkovic, L., Ukropcova, B., Chmelik, M., Balaz, M., Bogner, W., Schmid, A.I., Frollo, I., Zemkova, E., Klimes, I., Ukropec, J., Trattnig, S. & Krssak, M. 2013. Interrelation of ^{31}P-MRS metabolism measurements in resting and exercised quadriceps muscle of overweight-to-obese sedentary individuals. *NMR Biomed* **26**, 1714–1722.

Van der Meer, R., Westeroff, H.V. & Van Dam, K. 1980. Linear relation between rate and thermodynamic force in enzyme-catalyzed reactions. *Biochim Biophys Acta* **591**, 488–493.

Vandenberghe, K., Van Hecke, P., Van Leemputte, M., Vanstapel, F. & Hespel, P. 1999. Phosphocreatine resynthesis is not affected by creatine loading. *Med Sci Sports Exerc* **31**, 236–242.

Vanderthommen, M., Duteil, S., Wary, C., Raynaud, J.S., Leroy-Willig, A., Crielaard, J.M. & Carlier, P.G. 2003. A comparison of voluntary and electrically induced contractions by interleaved ^{1}H- and ^{31}P-NMRS in humans. *J Appl Physiol* **94**, 1012–1024.

Vinnakota, K., Kemp, M.L. & Kushmerick, M.J. 2006. Dynamics of muscle glycogenolysis modeled with pH time course computation and pH-dependent reaction equilibria and enzyme kinetics. *Biophys J* **91**, 1264–1287.

Vinnakota, K.C., Wu, F., Kushmerick, M.J. & Beard, D.A. 2009. Multiple ion binding equilibria, reaction kinetics, and thermodynamics in dynamic models of biochemical pathways. *Methods Enzymol* **454**, 29–68.

Volianitis, S. & Secher, N.H. 2002. Arm blood flow and metabolism during arm and combined arm and leg exercise in humans. *J Physiol* **544**, 977–984.

Volianitis, S., Yoshiga, C.C., Nissen, P. & Secher, N.H. 2004. Effect of fitness on arm vascular and metabolic responses to upper body exercise. *Am J Physiol Heart Circ Physiol* **286**, H1736–H1741.

Wackerhage, H., Hoffmann, U., Essfeld, D., Leyk, D., Mueller, K. & Zange, J. 1998. Recovery of free ADP, Pi, and free energy of ATP hydrolysis in human skeletal muscle. *J Appl Physiol* **85**, 2140–2145.

Walsh, B., Tiivel, T., Tonkonogi, M. & Sahlin, K. 2002. Increased concentrations of Pi and lactic acid reduce creatine-stimulated respiration in muscle fibers. *J Appl Physiol* **92**, 2273–2276.

Walsh, B., Hooks, R.B., Hornyak, J.E., Koch, L.G., Britton, S.L. & Hogan, M.C. 2006. Enhanced mitochondrial sensitivity to creatine in rats bred for high aerobic capacity. *J Appl Physiol* **100**, 1765–1769.

Walter, G., Vandenborne, K., McCully, K.K. & Leigh, J.S. 1997. Noninvasive measurement of phosphocreatine recovery kinetics in single human muscles. *Am J Physiol* **272**, C525–C534.

Walter, G., Vandenborne, K., Elliott, M. & Leigh, J.S. 1999. *In vivo* ATP synthesis rates in single human muscles during high intensity exercise. *J Physiol* **519**, 901–910.

Watt, M.J. & Hoy, A.J. 2012. Lipid metabolism in skeletal muscle: generation of adaptive and maladaptive intracellular signals for cellular function. *Am J Physiol Endocrinol Metab* **302**, E1315–E1328.

Welch, H.G., Bonde-Petersen, F., Graham, T., Klausen, K. & Secher, N. 1977. Effects of hyperoxia on leg blood flow and metabolism during exercise. *J Appl Physiol Respir Environ Exerc Physiol* **42**, 385–390.

Westerhoff, H.V. & van Dam, K. 1987. *Thermodynamics and Control of Biological Free-Energy Transduction*. Elsevier, Amsterdam.

Westerhoff, H.V., van Echteld, C.J. & Jeneson, J.A. 1995. On the expected relationship between Gibbs energy of ATP hydrolysis and muscle performance. *Biophys Chem* **54**, 137–142.

Willcocks, R.J., Williams, C.A., Barker, A.R., Fulford, J. & Armstrong, N. 2010. Age- and sex-related differences in muscle phosphocreatine and oxygenation kinetics during high-intensity exercise in adolescents and adults. *NMR Biomed* **23**, 569–577.

Williams, A.D., Selig, S., Hare, D.L., Hayes, A., Krum, H., Patterson, J., Geerling, R.H., Toia, D. & Carey, M.F. 2004. Reduced exercise tolerance in CHF may be related to factors other than impaired skeletal muscle oxidative capacity. *J Card Fail* **10**, 141–148.

Wray, D.W., Nishiyama, S.K., Monnet, A., Wary, C., Duteil, S., Carlier, P.G. & Richardson, R.S. 2009. Multiparametric NMR-based assessment of skeletal muscle perfusion and metabolism during exercise in elderly persons: preliminary findings. *J Gerontol A Biol Sci Med Sci* **64**, 968–974.

Wu, F., Jeneson, J.A. & Beard, D.A. 2007. Oxidative ATP synthesis in skeletal muscle is controlled by substrate feedback. *Am J Physiol Cell Physiol* **292**, C115–C124.

Wust, R.C., Grassi, B., Hogan, M.C., Howlett, R.A., Gladden, L.B. & Rossiter, H.B. 2011. Kinetic control of oxygen consumption during contractions in self-perfused skeletal muscle. *J Physiol* **589**, 3995–4009.

Wust, R.C., van der Laarse, W.J. & Rossiter, H.B. 2013. On-off asymmetries in oxygen consumption kinetics of single Xenopus laevis skeletal muscle fibres suggest higher-order control. *J Physiol* **591**, 731–744.

Yoshida, T. 2002. The rate of phosphocreatine hydrolysis and resynthesis in exercising muscle in humans using 31P-MRS. *J Physiol Anthropol Appl Human Sci* **21**, 247–255.

Yoshida, T. & Watari, H. 1993. 31P-nuclear magnetic resonance spectroscopy study of the time course of energy metabolism during exercise and recovery. *Eur J Appl Physiol Occup Physiol* **66**, 494–499.

Yoshida, T., Abe, D. & Fukuoka, Y. 2013. Phosphocreatine resynthesis during recovery in different muscles of the exercising leg by ^{31}P-MRS. *Scand J Med Sci Sports* **23**, e313–e319.

Yquel, R.J., Arsac, L.M., Thiaudiere, E., Canioni, P. & Manier, G. 2002. Effect of creatine supplementation on phosphocreatine resynthesis, inorganic phosphate accumulation and pH during intermittent maximal exercise. *J Sports Sci* **20**, 427–437.

Zoladz, J.A., Grassi, B., Majerczak, J., Szkutnik, Z., Korostynski, M., Karasinski, J., Kilarski, W. & Korzeniewski, B. 2013. Training-induced acceleration of O_2 uptake on-kinetics precedes muscle mitochondrial biogenesis in humans. *Exp Physiol* **98**, 883–898.

 © 2014 Scandinavian Physiological Society. Published by John Wiley & Sons Ltd, doi: 10.1111/apha.12307